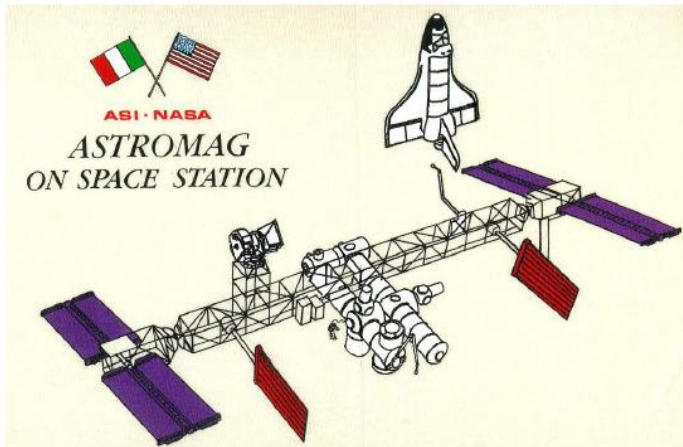


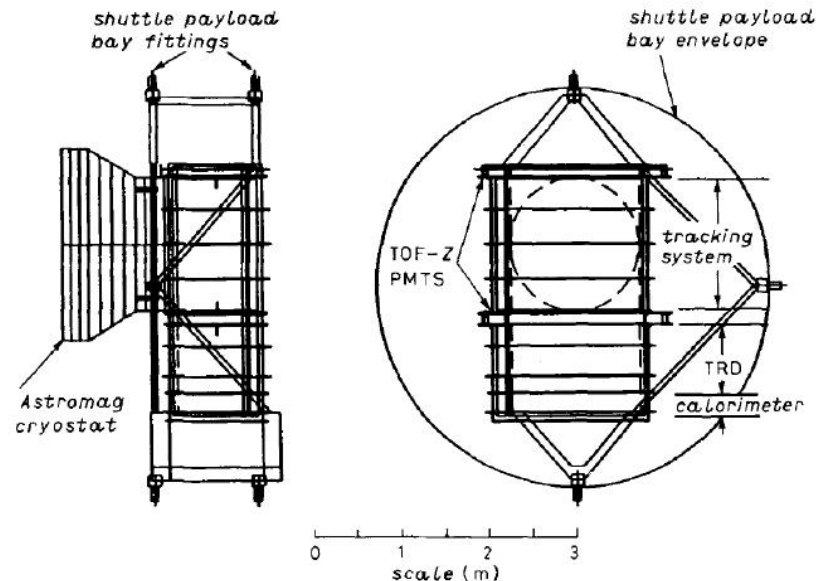
Risultati scientifici dell'esperimento Wizard/PAMELA

Vannuccini Elena

Astromag/WiZard



- ▶ Extensive R&D in the '80s aiming to optimize **superconducting magnet facility** to be flown as a U.S.-Italy project on Space Station Freedom in the late '90s
 - ▶ **WiZard** experiment dedicated to search for primordial antimatter



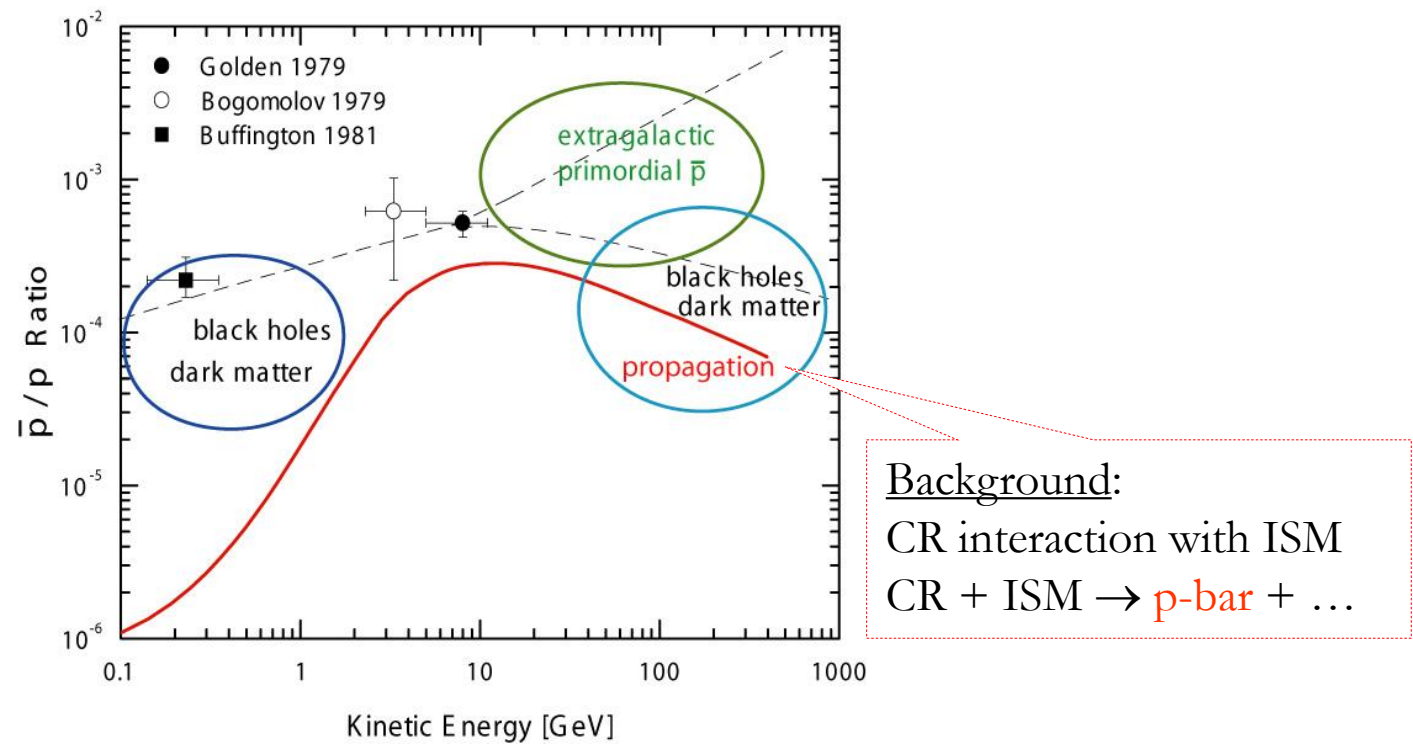
Golden et al N.Cim. 105 (1990) 191

Project canceled!

Antimatter in CRs



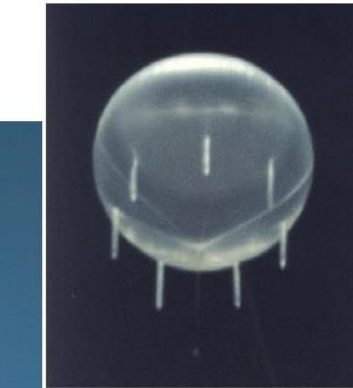
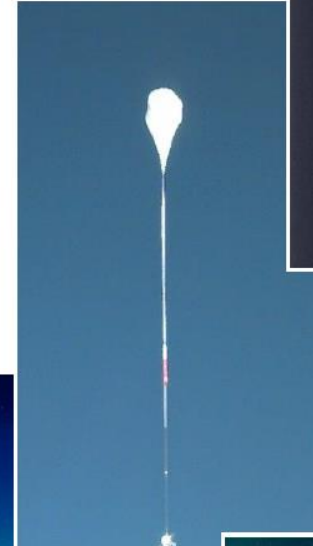
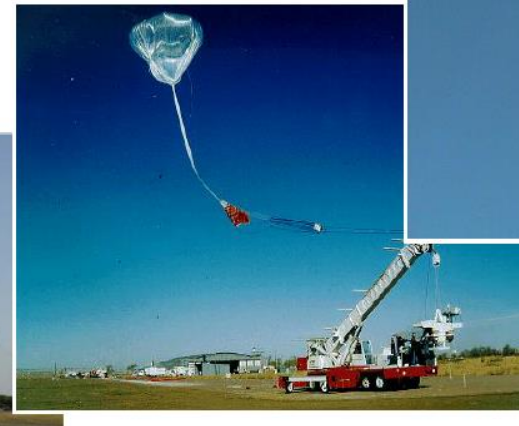
The first historical measurements of the \bar{p}/p - ratio and various Ideas of theoretical Interpretations



CR-antimatter measurements in the '90s



- ▶ Extensive campaign of **daily balloon flights** operated by several groups
 - ▶ Wizard (MASS, TS, CAPRICE)
 - ▶ BESS
 - ▶ Others (HEAT, IMAX...)
- ▶ Main instrument characteristics
 - ▶ Superconducting magnets ($\sim 1T$ field)
 - ▶ MWPC & drift chamber tracking systems ($O(100\mu m)$ resolution)
 - ▶ MDR $\sim 100 \div 300$ GV

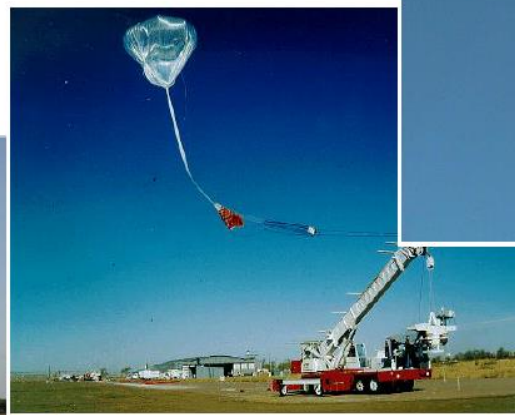
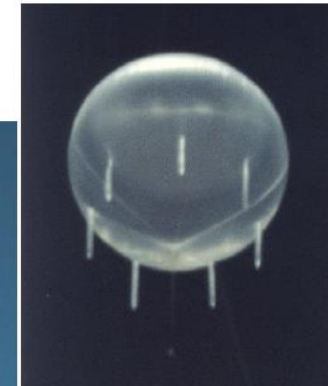
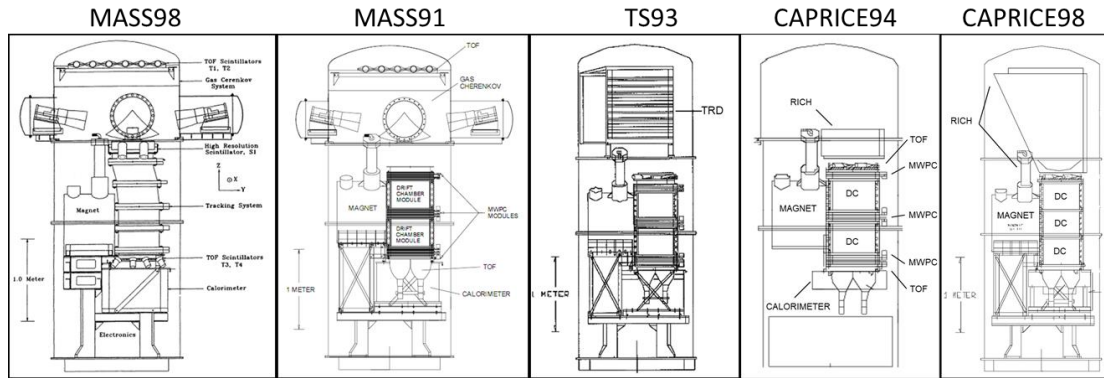


CR-antimatter measurements in the '90s

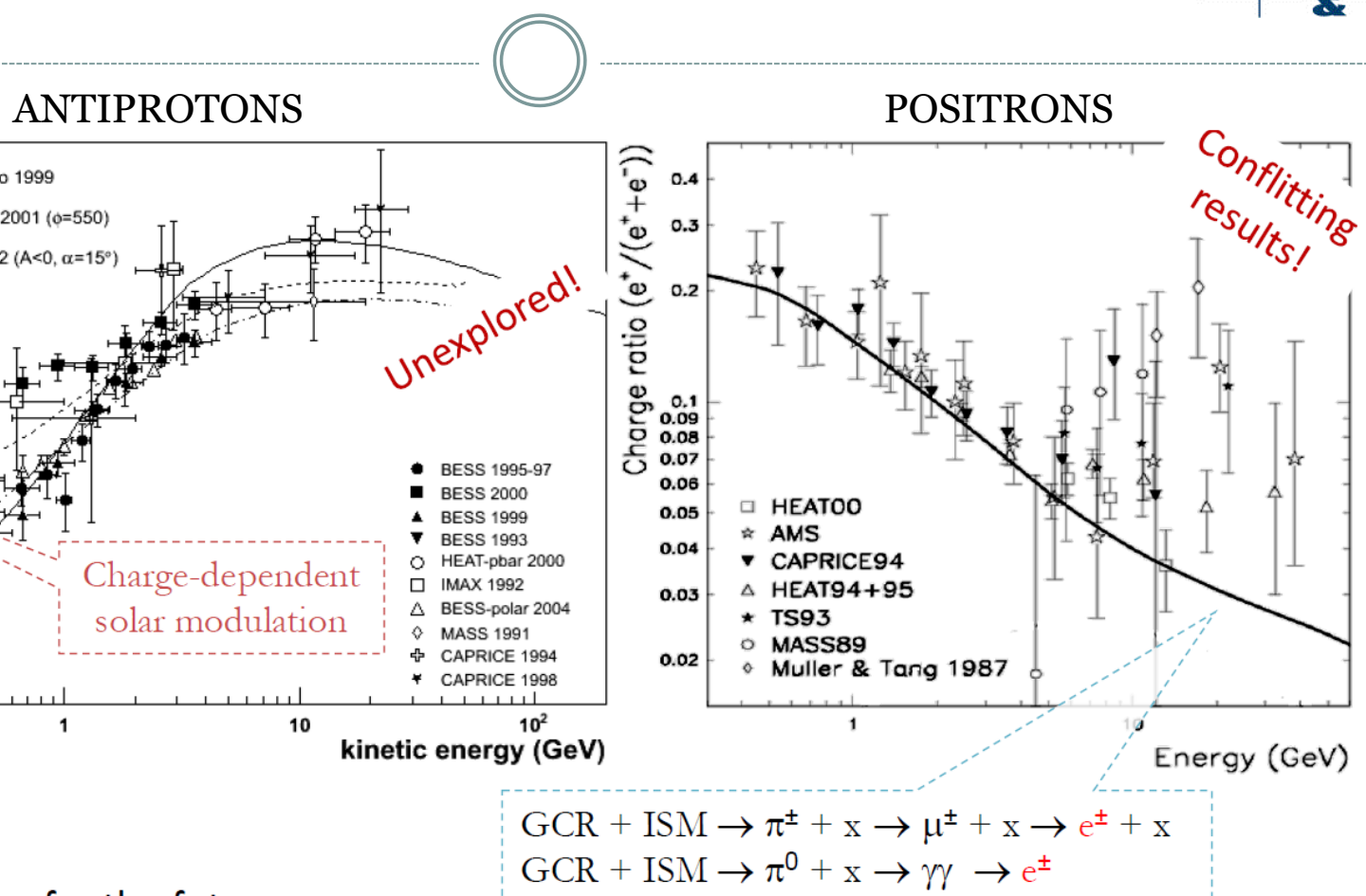


- Extensive campaign of **daily balloon flights** operated by several groups

- Wizard (MASS, TS, CAPRICE)**



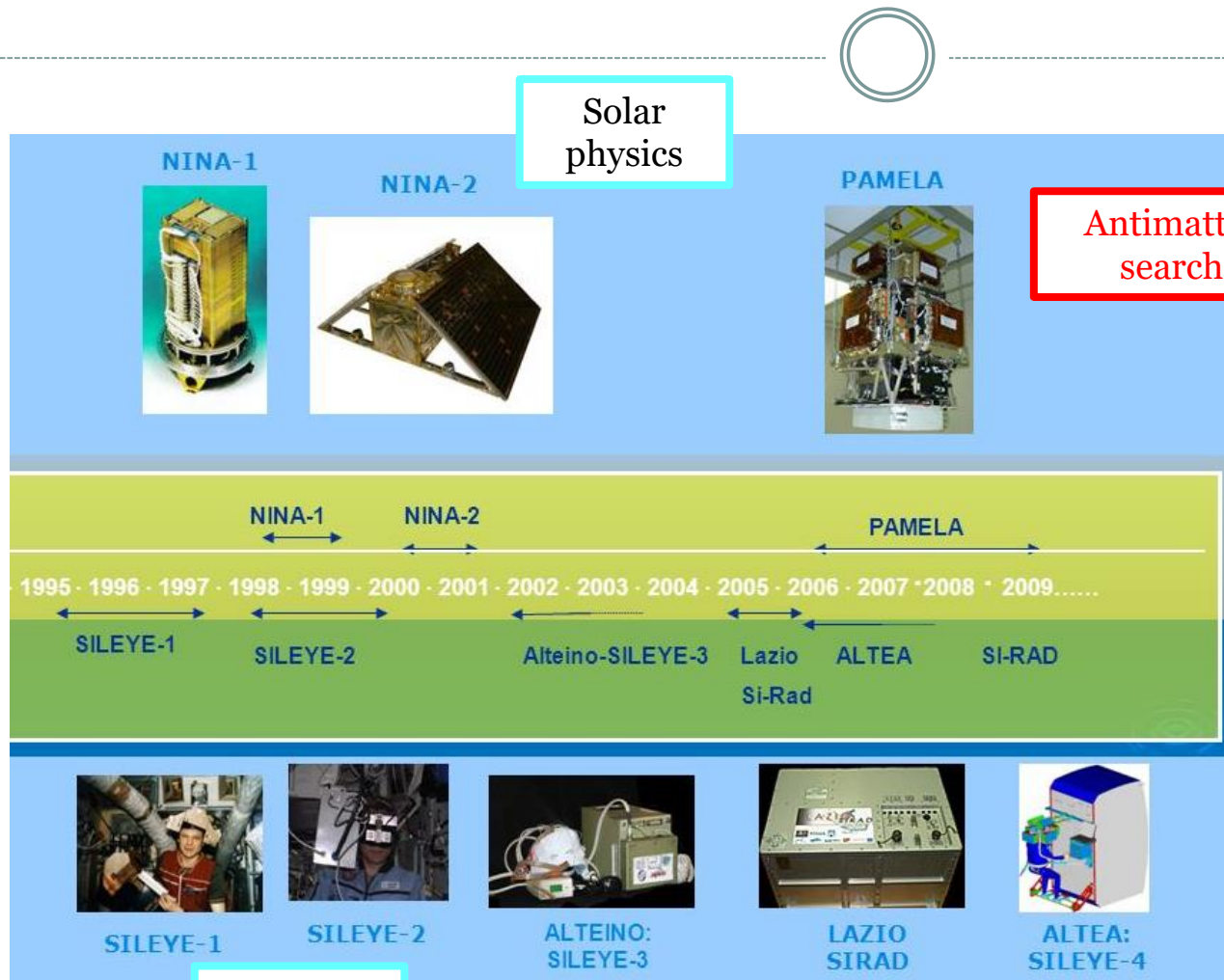
Status at the beginning of 2000s



Two directions for the future:

- ▶ High-statistics measurement of \bar{p} @ low energy → BESS-Polar
- ▶ \bar{p} and e^+ measurement @ high energy → PAMELA & AMS02

The Russian-Italian Mission

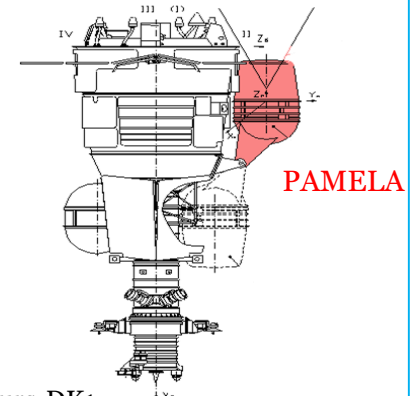


PAMELA timeline

1998 → MoU between INFN and Russian Space Agency

2006 → June 15, Launch!

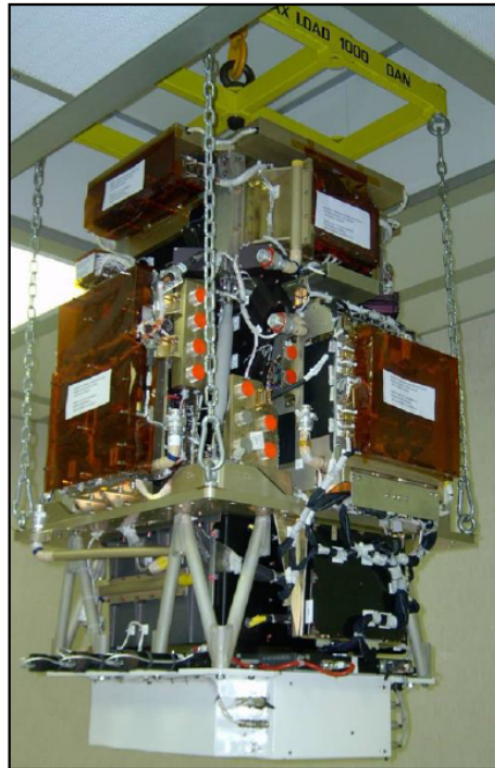
2016 → January, downlink operation were terminated



Resurs-DK1
Mass: 6.7 tonnes
Height: 7.4 m
Solar array area: 36 m²

Life science

The PAMELA apparatus



GF: $21.5 \text{ cm}^2 \text{ sr}$
 Mass: 470 kg
 Size: $130 \times 70 \times 70 \text{ cm}^3$
 Power Budget: 360W

Time-Of-Flight

plastic scintillators + PMT:

- Trigger
- Albedo rejection;
- Mass identification up to 1 GeV;
- Charge identification from dE/dX

Electromagnetic calorimeter

W/Si sampling ($16.3 X_0, 0.6 \lambda l$)

- Discrimination e^+ / p , $\text{anti-}p / e^-$ (shower topology)
- Direct E measurement for e^-

Neutron detector

plastic scintillators + PMT:

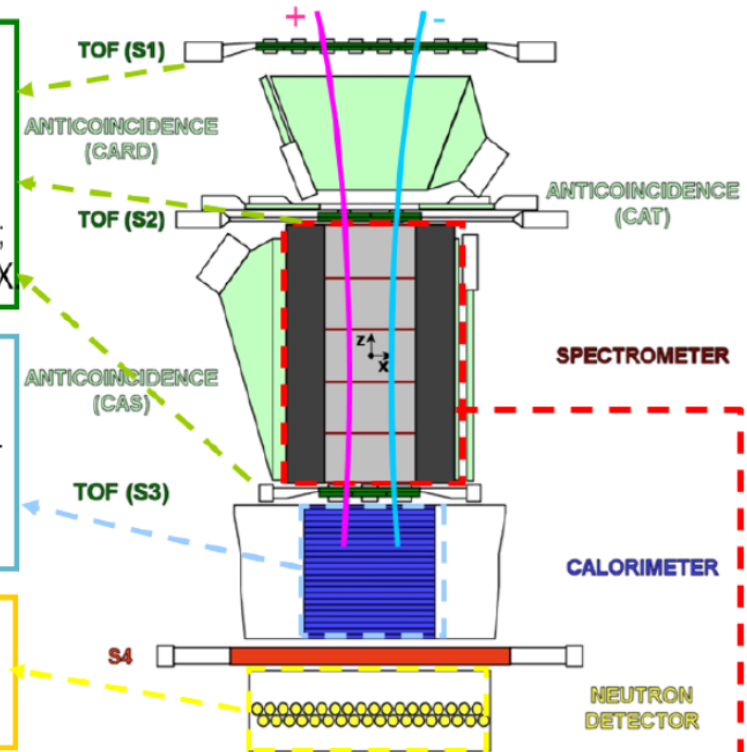
- High-energy e/h discrimination

Spectrometer

microstrip silicon tracking system + permanent magnet

It provides:

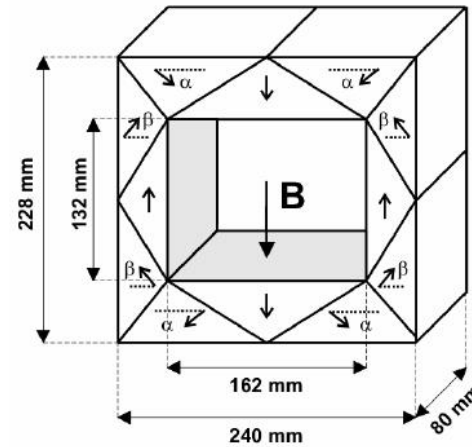
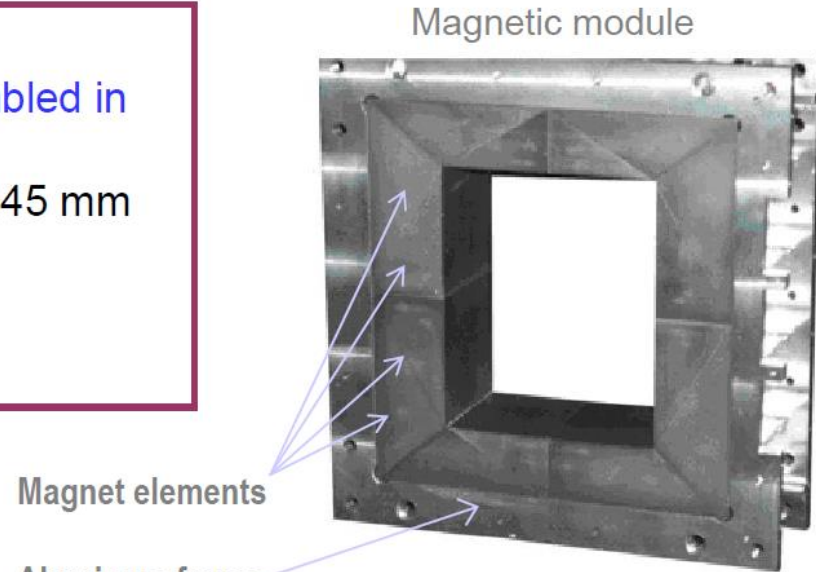
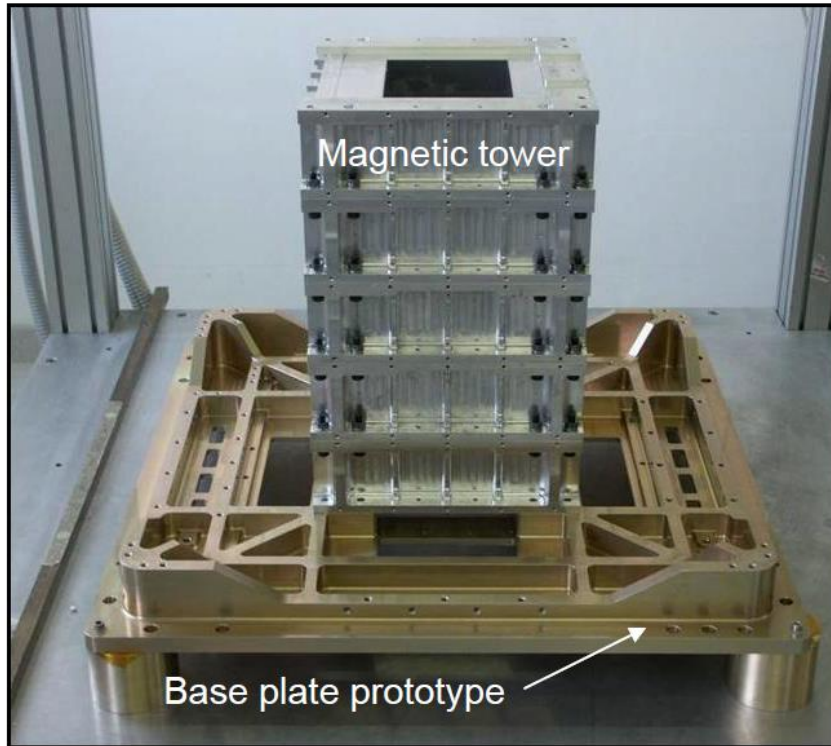
- Magnetic rigidity $\rightarrow R = pc/Ze$
- Charge sign
- Charge value from dE/dx



MDR ~1TV

The magnet

- 5 magnetic modules
- Permanent magnet (Nd-Fe-B alloy) assembled in an aluminum mechanics
- Magnetic cavity sizes (132 x 162) mm² x 445 mm
- Geometric Factor: 20.5 cm²sr
- Black IR absorbing painting
- Magnetic shields



- 0.48 T @ center
- Average field along the axis: 0.43 T

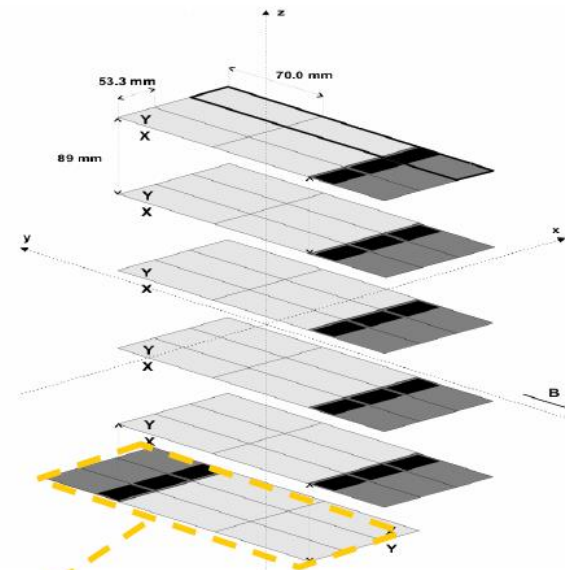


The tracking system

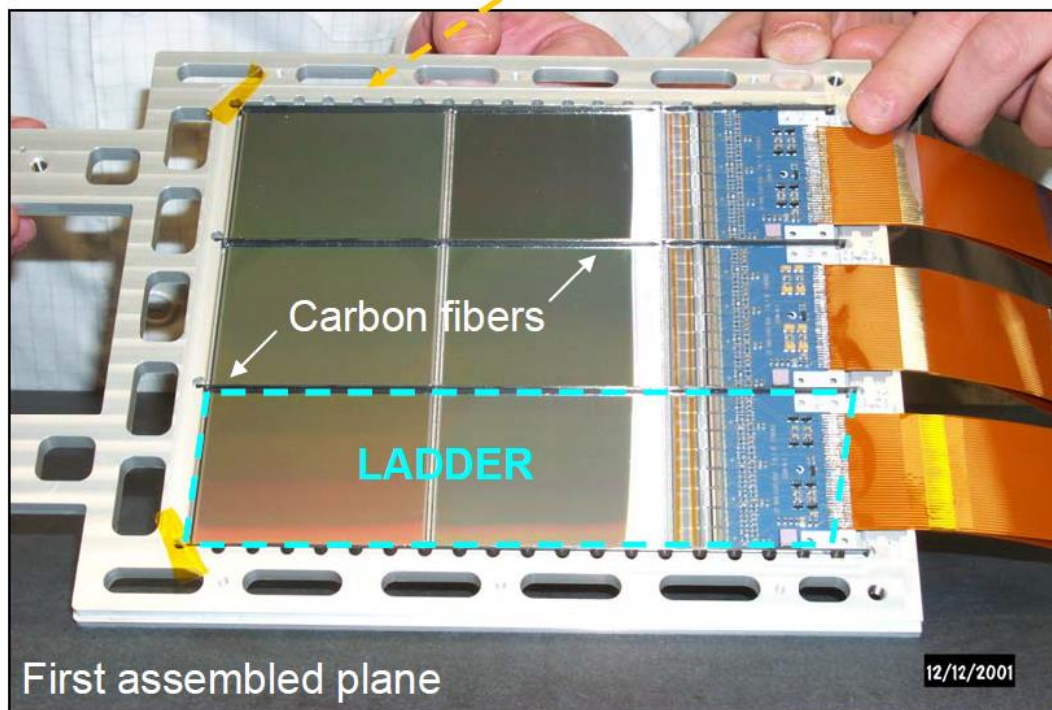
6 detector planes, each composed by 3 ladders

Mechanical assembly

- aluminum frames
- carbon fibers stiffeners glued laterally to the ladders
- no material above/below the plane
 1 plane = **0.3% X_0** → reduced multiple scattering
- elastic + rigid gluing



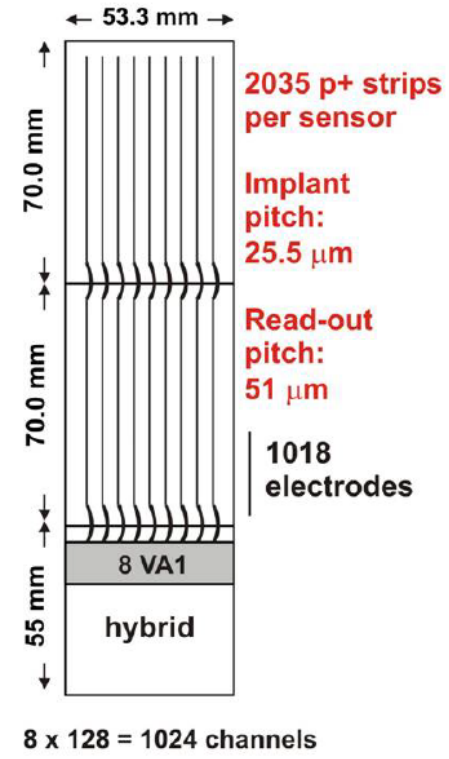
Test of plane lodging inside the magnet



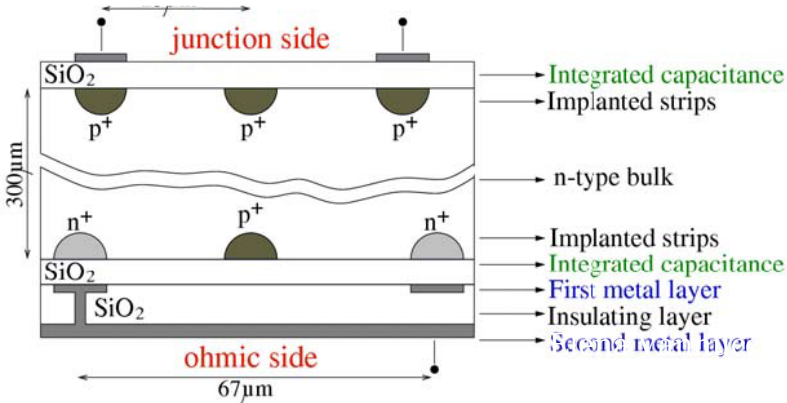
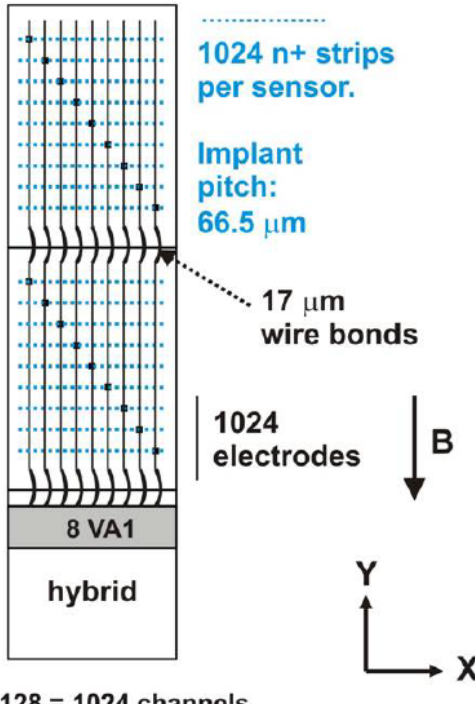
First assembled plane

Silicon detector ladders

**X view
(junction)**



**Y view
(ohmic)**



- 2 microstrip silicon sensors
- 1 “hybrid” with front-end electronics

Silicon sensors (Hamamatsu):

- 300 μm , double sided - x & y view
- AC coupled (no external chips)
- double metal (no kapton fanout)
- 1024 read-out channels per view
 - strip/electrode coupling $\sim 20 \text{ pF/cm}$;
 - channel capacitance to ground:
 - junction: $< 10 \text{ pF}$
 - ohmic: $< 20 \text{ pF}$

Bias:

- VY -VX = + 80 V fed through guard ring surrounding the strips
- Bias resistor:
 - junction: punch-through, $> 50 \text{ M}\Omega$;
 - ohmic: polysilicon, $> 10 \text{ M}\Omega$.
- Leakage current $< 1 \mu\text{A}/\text{sensor}$.

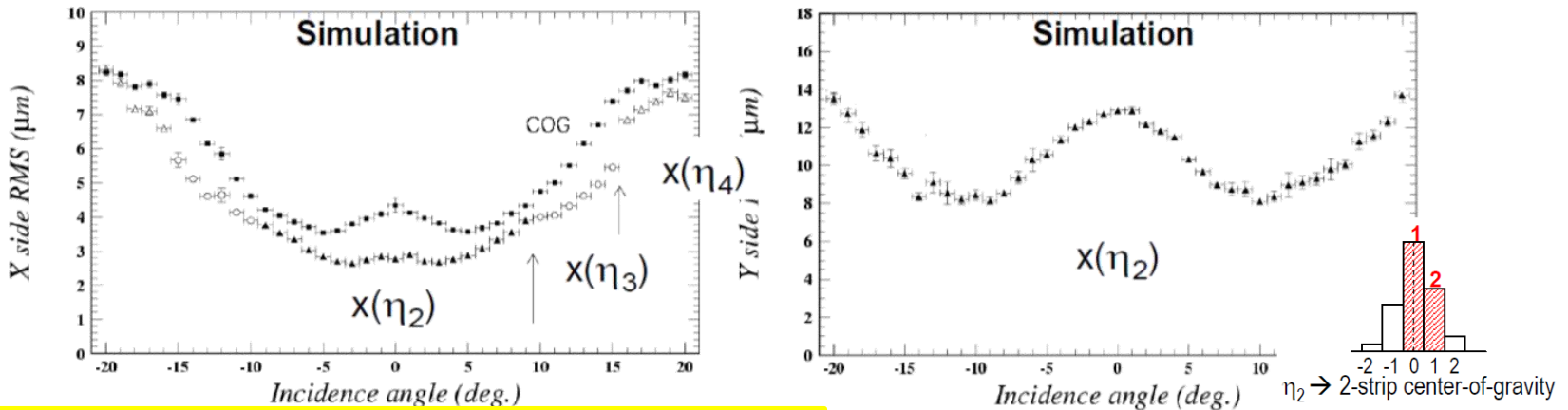


Spatial resolution



Sensor intrinsic resolution

Spatial resolution studied by means of beam-test of silicon detectors and simulation



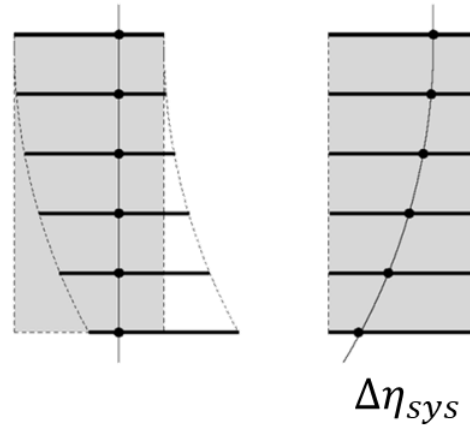
- junction side (X): $3 \mu\text{m}$ @ 0° , $< 4 \mu\text{m}$ up to 10° (\rightarrow determines momentum resolution)
- ohmic side (Y): $8 \div 13 \mu\text{m}$
- Position finding algorithm accounts for non-linear charge collection, asymmetric signal distribution, discretization effects \rightarrow Landi NIMA 554 (2005)

Sensor alignment

Track-based alignment: minimization of spatial residuals as a function of the roto-traslational parameters of each sensor

- Proton beam (@CERN-SPS 2003) and atmospheric muons (cross-check) $\rightarrow \sim 100 \pm 1 \mu\text{m}$
- In-flight corrections with protons $\rightarrow \sim 10 \mu\text{m}$

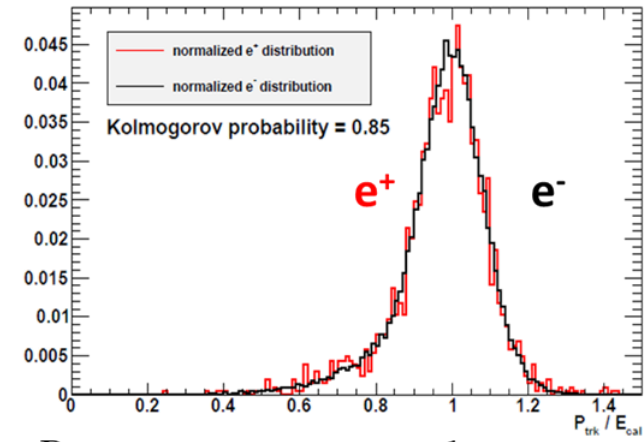
Spectrometer systematics



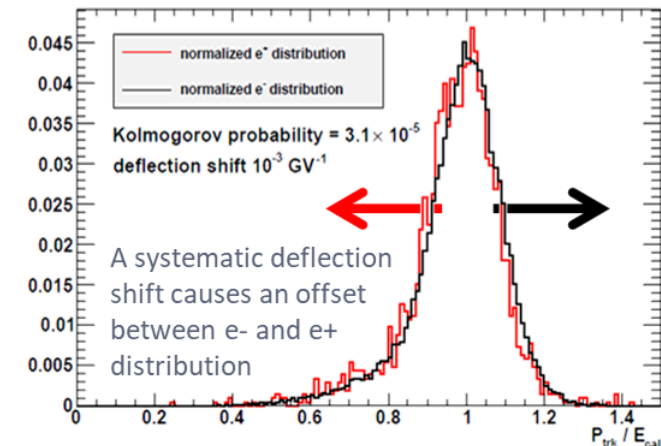
- Due to possible residual distortion of the tracking system
- Evaluated from electron/positron data by comparing the spectrometer momentum with the calorimeter energy
- Upper limit set by positron statistics:

$$\Delta\eta_{sys} \sim 10^{-4} \text{ GV}^{-1}$$

(MDR_{max} ~ 1200 GV)

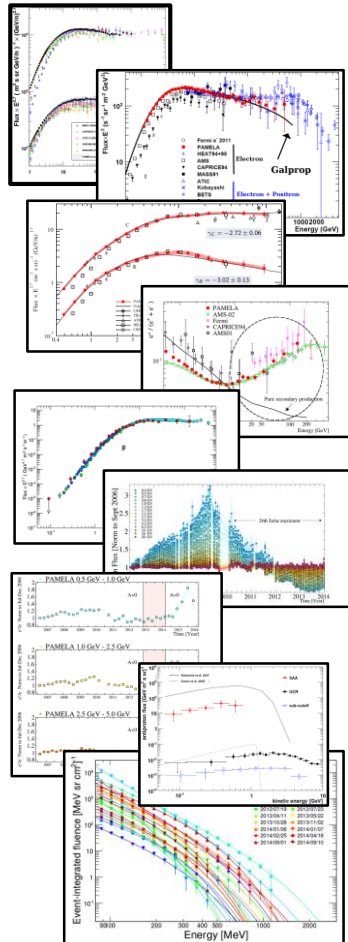


$$\frac{P_{trk}}{E_{cal}} \xrightarrow{\text{sys}} \frac{1}{E_{cal}(1 + \varepsilon_{sys}) \cdot |\eta_{trk} + \Delta\eta_{sys}|}$$





Ten years of PAMELA data



The PAMELA Mission: Heraldng a new era in precision cosmic ray physics

O. Adriani ^{a,b}, G.C. Barbarino^{c,d}, G.A. Bazilevskaya^e, R. Bellotti^{f,g}, M. Boezio^b, E.A. Bogomolov^b, M. Bongi^h, V. Bonvicini^b, S. Bottai^b, A. Bruno^{f,g}, F. Cafagna^g, D. Campana^d, R. Carbone^{h,i}, P. Carlson^k, M. Casolino^l, G. Castellini^m, M.P. De Pascale^{j,n}, C. De Santis^{l,o}, N. De Simone^l, V. Di Felice^l, V. Formaro^{h,p}, M.G. Galper^p, U. Giacconi^d, A.V. Kareljin^p, M.D. Kheyman^p, S.V. Koldashov^b, S. Koldobskiy^p, S.YU. Krurkovⁱ, A.N. Kvashnin^d, A. Leonov^b, V. Malakhov^p, L. Marcelliⁿ, M. Martucci^{h,q}, A.G. Mayorov^p, W. Menn^b, V.V. Mikhailov^p, E. Mocchiutti^b, A. Monaco^b, N. Mori^o, R. Munini^{b,k,p}, N. Nikonorov^{l,p}, G. Osteria^d, P. Papini^b, M. Pearce^h, P. Picozza^{l,p}, C. Pizzolotto^{h,f}, M. Ricci^q, S.B. Ricciarini^{b,m}, L. Rossetto^h, R. Sarkar^b, M. Simon^r, R. Sparvoli^{h,p}, P. Spillantini^{h,b}, Y.I. Stozhkov^b, A. Vacchi^b, E. Vannuccini^b, G.I. Vasilyevⁱ, S.A. Voronov^p, J. Wu^l, Y.T. Yurkin^b, G. Zampa^b, N. Zampa^b, V.G. Zverev^p

^aUniversity of Florence, Department of Physics, I-50019 Sesto Fiorentino, Florence, Italy

^bINFN, Sezione di Firenze, I-50019 Sesto Fiorentino, Florence, Italy

^cUniversity of Naples "Federico II", Department of Physics, I-80126 Naples, Italy

^dINFN, Sezione di Napoli, I-80126 Naples, Italy

^eLobachevsky Institute, 60-730454 Moscow, Russia

^fINFN, Sezione di Roma, I-00133 Rome, Italy

^gINFN, Sezione di Trieste, I-34147 Trieste, Italy

^hRJF Physical Technical Institute, 611-94021 St. Petersburg, Russia

ⁱKTH Royal Institute of Technology, Department of Physics, AlbaNova University Center, SE-10691 Stockholm, Sweden

^jThe Order-Kicks Center for Cosmic-ray Physics, AlbaNova University Center, SE-10691 Stockholm, Sweden

^kINFN, Sezione di Roma "Tor Vergata", I-00133 Rome, Italy

^lFATC, I-50019 Sesto Fiorentino, Florence, Italy

^mUniversity of Trieste, Department of Physics, I-34147 Trieste, Italy

ⁿNational Research Nuclear University MEPhI Moscow Physics Engineering Institute, 115409 Moscow, Russia

^oINFN, Sezione di Padova, I-35131 Padova, Italy

^pUniversita Siegen, Department of Physics, D-57068 Siegen, Germany

^qINFN, Sezione di Perugia, I-06123 Perugia, Italy

^rINFN Sezione di Perugia, I-06123 Perugia, Italy

^sINFN Sezione di Perugia, I-06123 Perugia, Italy

^tINFN Sezione di Perugia, I-06123 Perugia, Italy

^uSchool of Mathematics and Physics, China University of Geosciences, CH-430074 Wuhan, China

■ LA RIVISTA DEL NUOVO CIMENTO

YEAR 2017 - ISSUE 10 - OCTOBER

Ten years of PAMELA in space

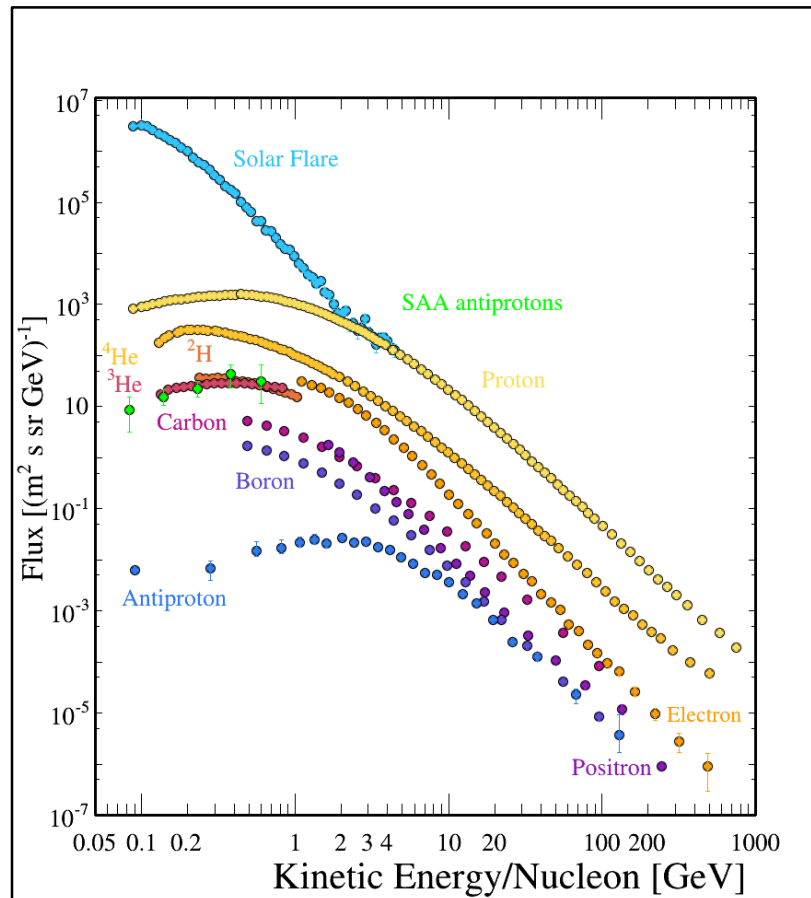
Authors: PAMELA Collaboration - O. Adriani, G. C. Barbarino, G. A. Bazilevskaya, R. Bellotti, M. Boezio, E. A. Bogomolov, M. Bongi, V. Bonvicini, S. Bottai, A. Bruno, F. Campana, P. Carlson, M. Casolino, G. Castellini, C. De Santis, V. Di Felice, A. M. Galper, A. V. Kareljin, S. V. Koldashov, S. Y. Krurkov, A. N. Kvashnin, A. Leonov, V. Malakhov, L. Marcelli, M. Martucci, A. G. Mayorov, W. Menn, M. Mergé, V. V. Mikhailov, E. Mocchiutti, A. Monaco, R. Munini, N. Mori, G. Osteria, B. Panico, P. Papini, M. Pearce, P. Picozza, M. Ricci, S. B. Ricciarini, M. Simon, R. Sparvoli, P. Spillantini, Y. I. Stozhkov, A. Vacchi, E. Vannuccini, G. Vasilyev, S. A. Voronov, Y. T. Yurkin, G. Zampa, N. Zampa

DOI: 10.1393/ncr/2017-10140-x

pp. 473-522

Published online 27 September 2017

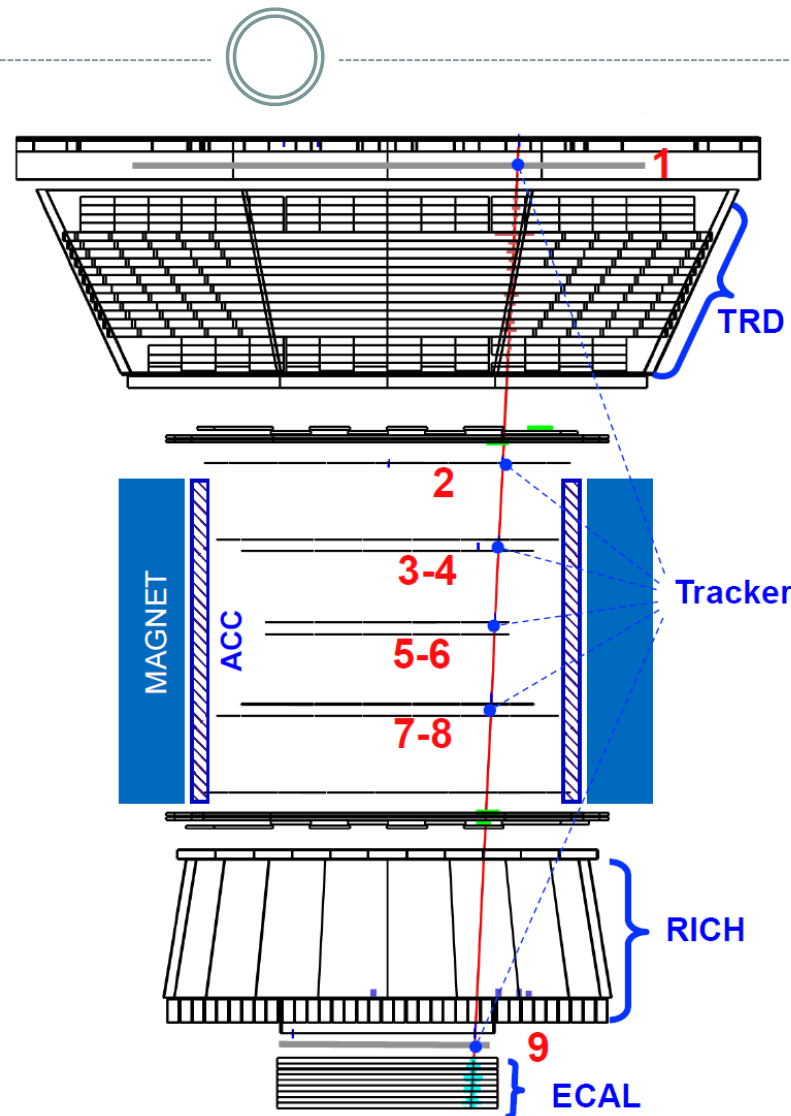
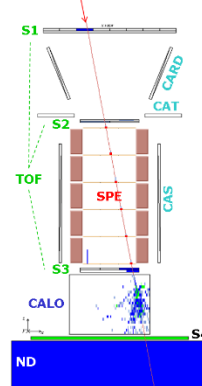
Download fulltext



PAMELA & AMS-02



2006-2016
GF $21.5 \text{ cm}^2\text{sr}$
MDR $\sim 1.2 \text{ TV}$



2011
GF $0.5 \text{ m}^2\text{sr}$
MDR $\sim 2 \text{ TV}$

Antiparticles &co.

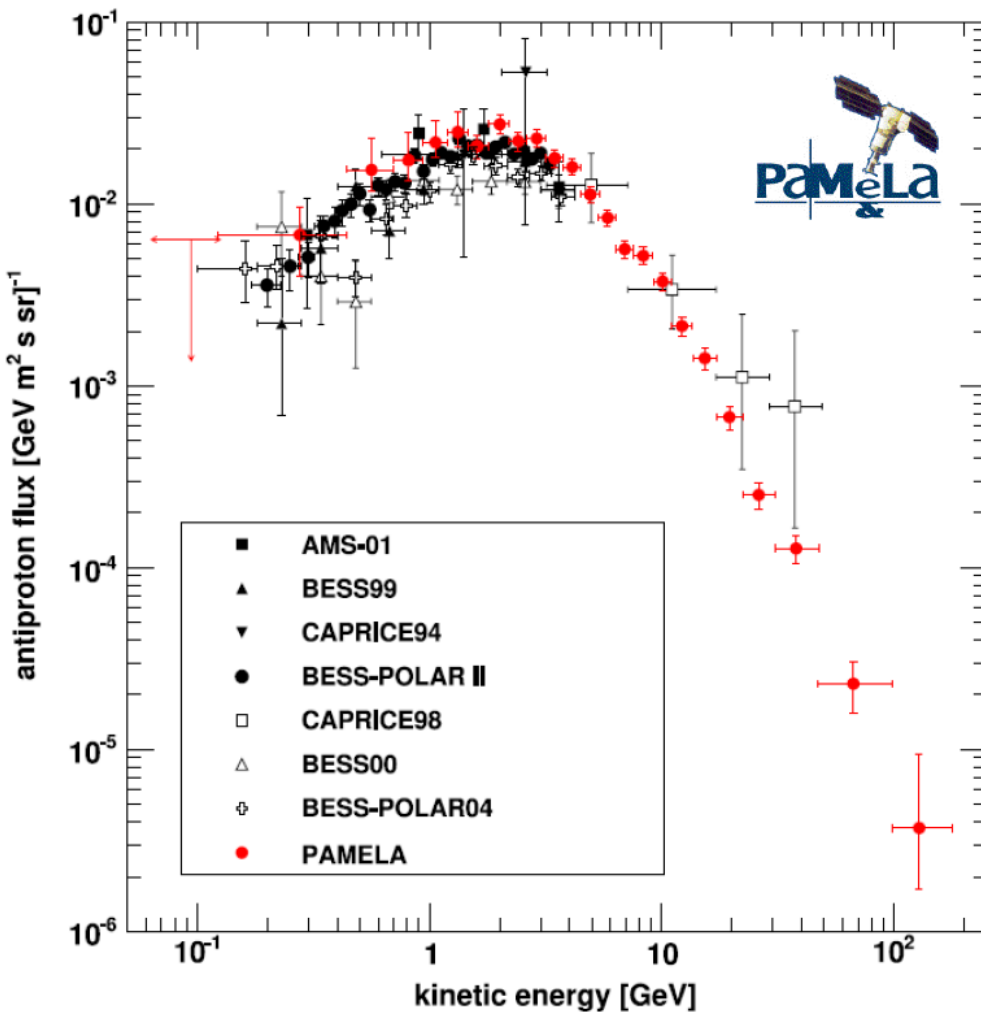


- Antiproton abundance
- Positron & electron abundance, upper limity on anysotropy
- Upper limits on Anti-Helium and SQM





Antiprotons



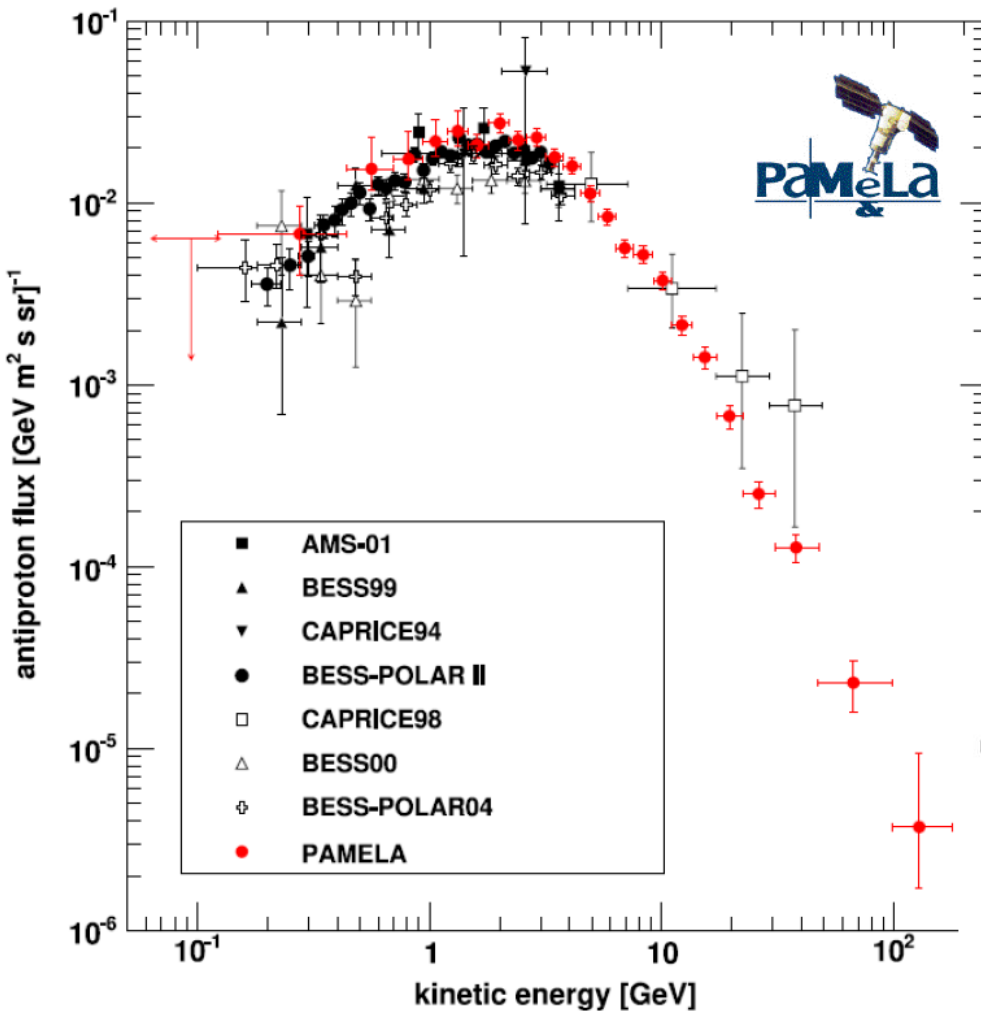
Adriani et al. - PRL 102 (2009) 051101
Adriani et al. - PRL 105 (2010) 121101
Adriani et al. - PR 544 (2014) 323

First measurement
extending up to 200 GV

Largest energy range
covered up to then

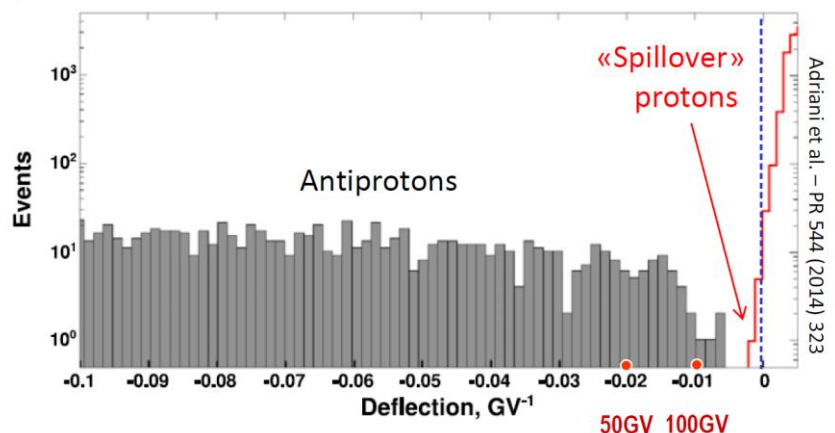


Antiprotons



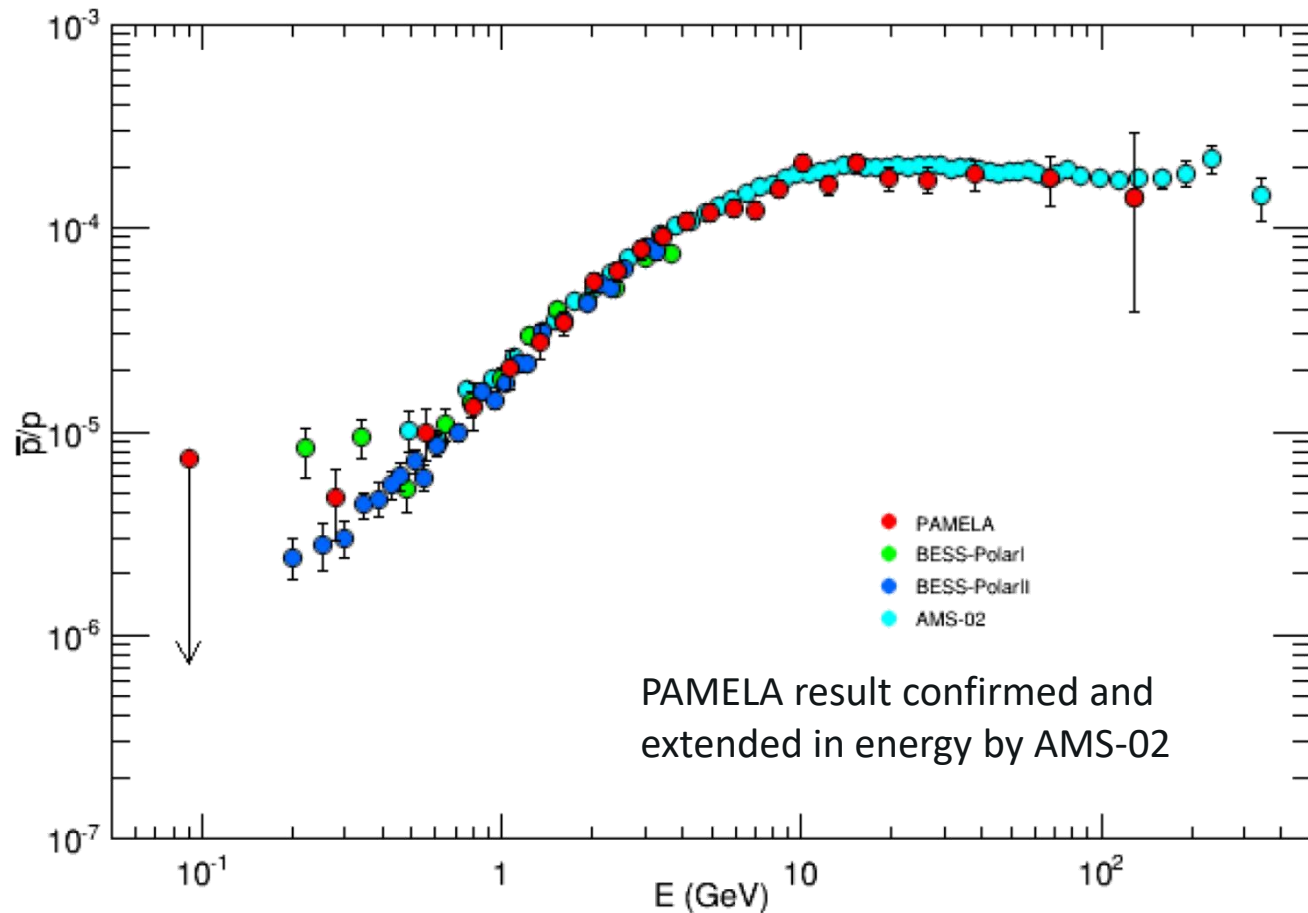
Adriani et al. - PRL 102 (2009) 051101
Adriani et al. - PRL 105 (2010) 121101
Adriani et al. - PR 544 (2014) 323

First measurement
extending up to 200 GV



Selected particles with h-like pattern in the calorimeter

Antiprotons



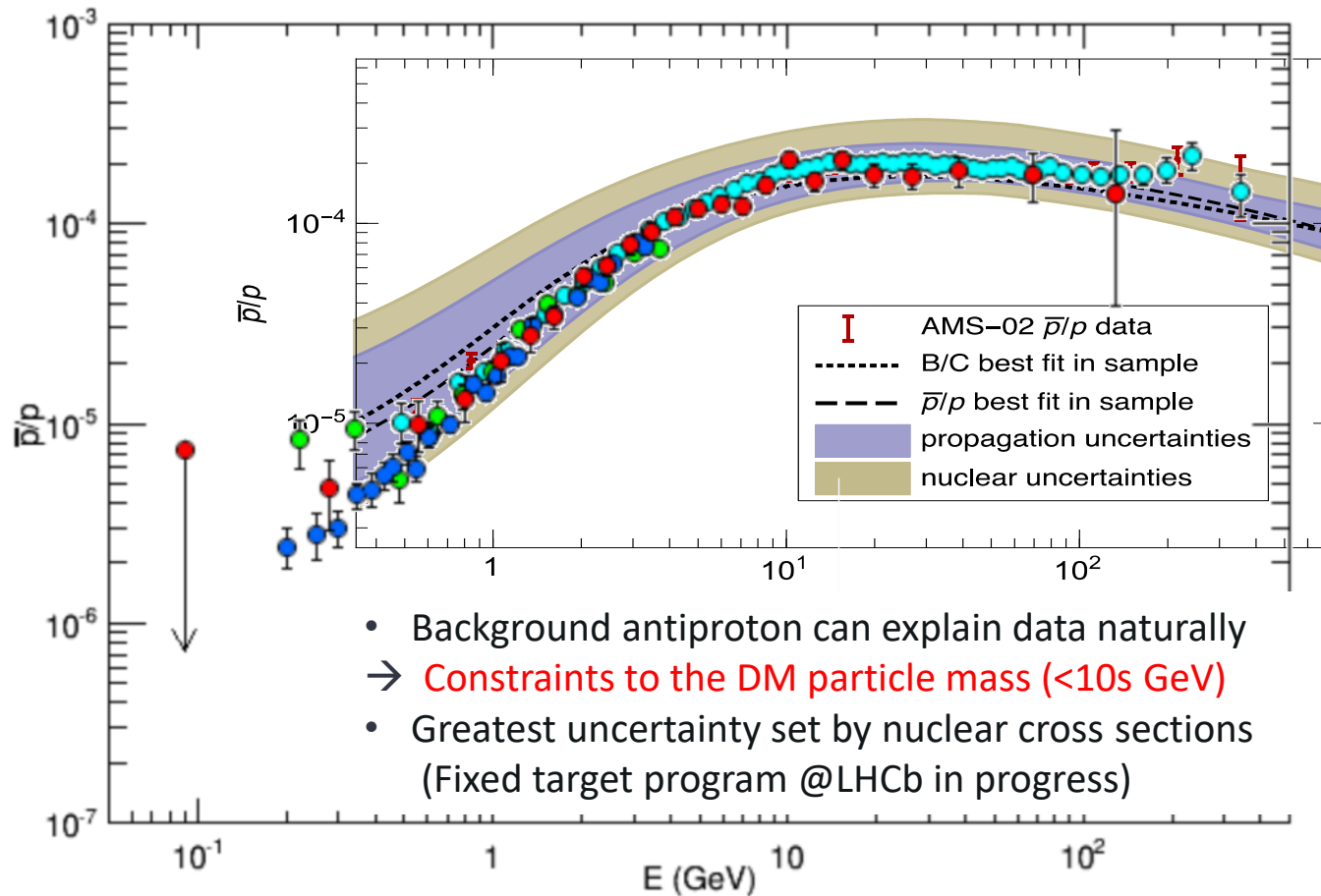
Adriani et al., Riv. N.Cim., 10, 473-522, 2017



Antiprotons



Kappl, Reinert, Winkler JCAP 2015
Adriani et al., Riv. N.Cim., 10, 473-522, 2017



The positron excess

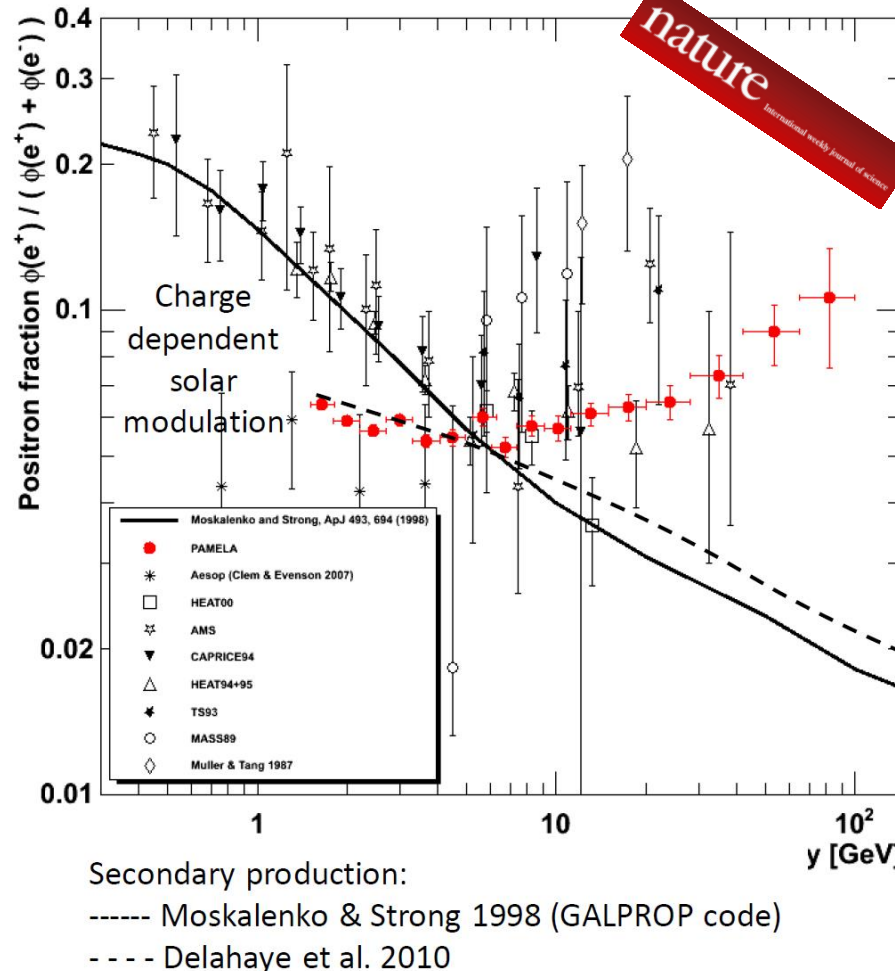


@high energy:

- First measurement extending up to 200 GV
- **Clear evidence of increasing positron fraction above 10 GeV with respect to pure secondary production**

@low-energy

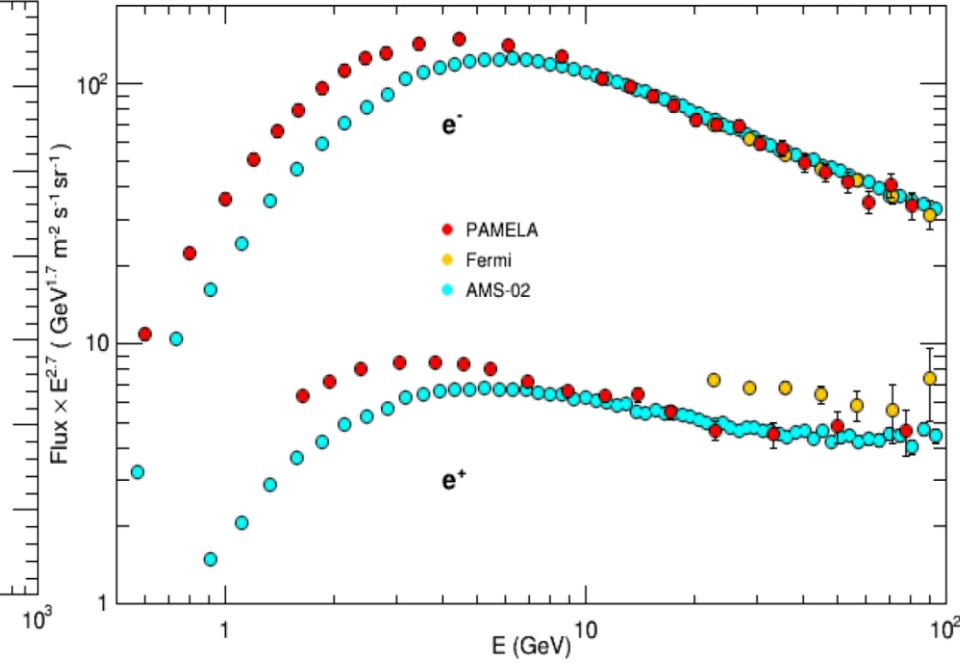
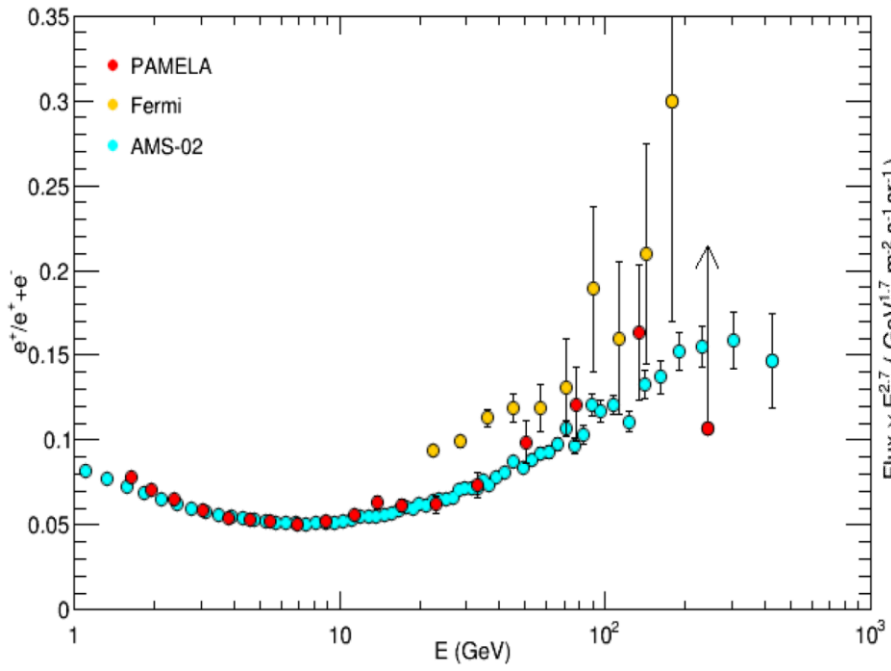
- Deviation from previous measurements → charge-dependent solar modulation



Adriani et al, Nature 458 (2009) 607;
Adriani et al. Astropart. Phys. 34 (2010) 1

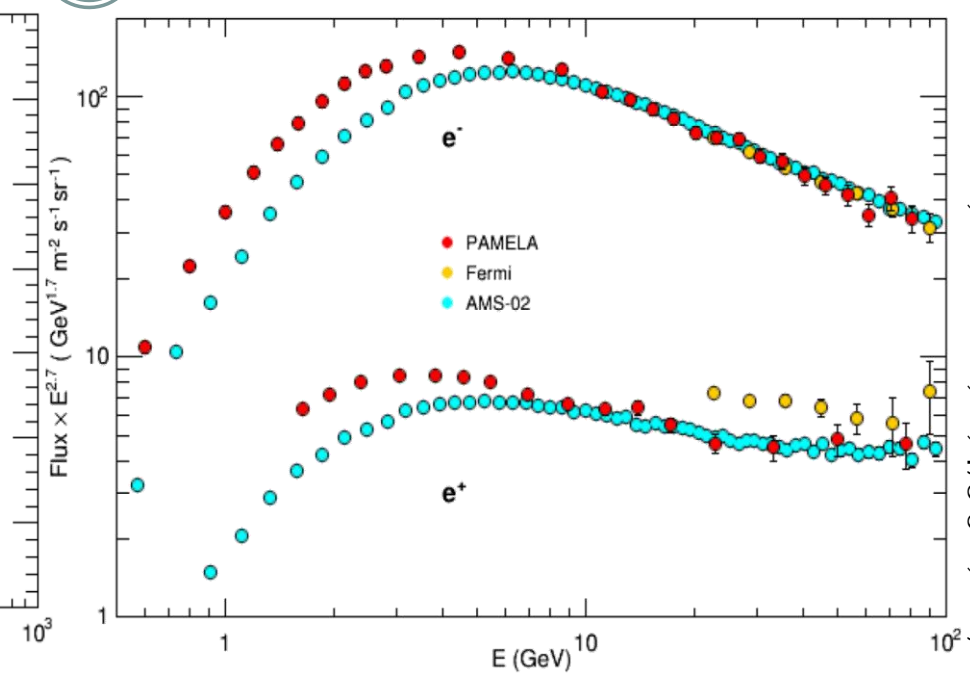
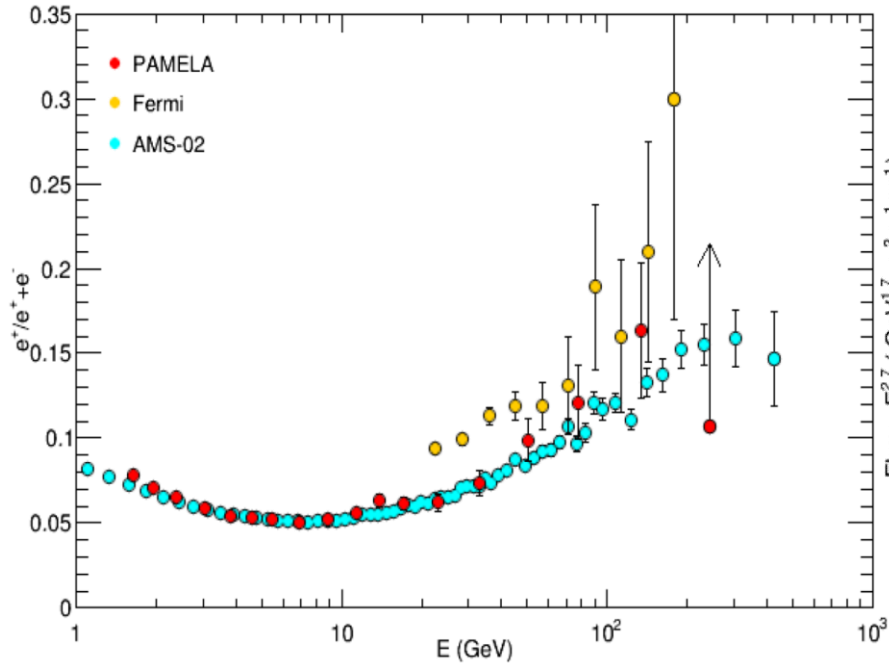
CR leptons

Adriani et al., Riv. N.Cim., 10, 473-522, 2017



PAMELA result confirmed by AMS-02 and extended in energy.
 (Indication for a decreasing trend above 300 GV...)

CR leptons



Adriani et al., Riv. N.Cim., 10, 473-522, 2017

Measurement of individual spectra confirms the presence of an additional positron component

Possible interpretations:

Dark matter → lepton vs hadron yield must be consistent with \bar{p} observations

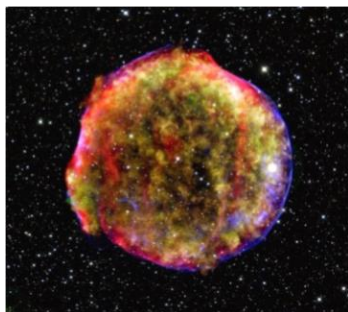
Astrophysical processes → known processes (eg. pulsars, dense SNR), but large uncertainties on environmental parameters

Propagation → diffusion coefficient with weird energy dependency or other subtleties, disfavored

The nuclear component of GCRs



- H&He primary nuclei
- Secondary nuclei from GCR interactions with the ISM:
 - B-to-C abundance
 - H and He isotopes
 - Li, Be, B isotopes



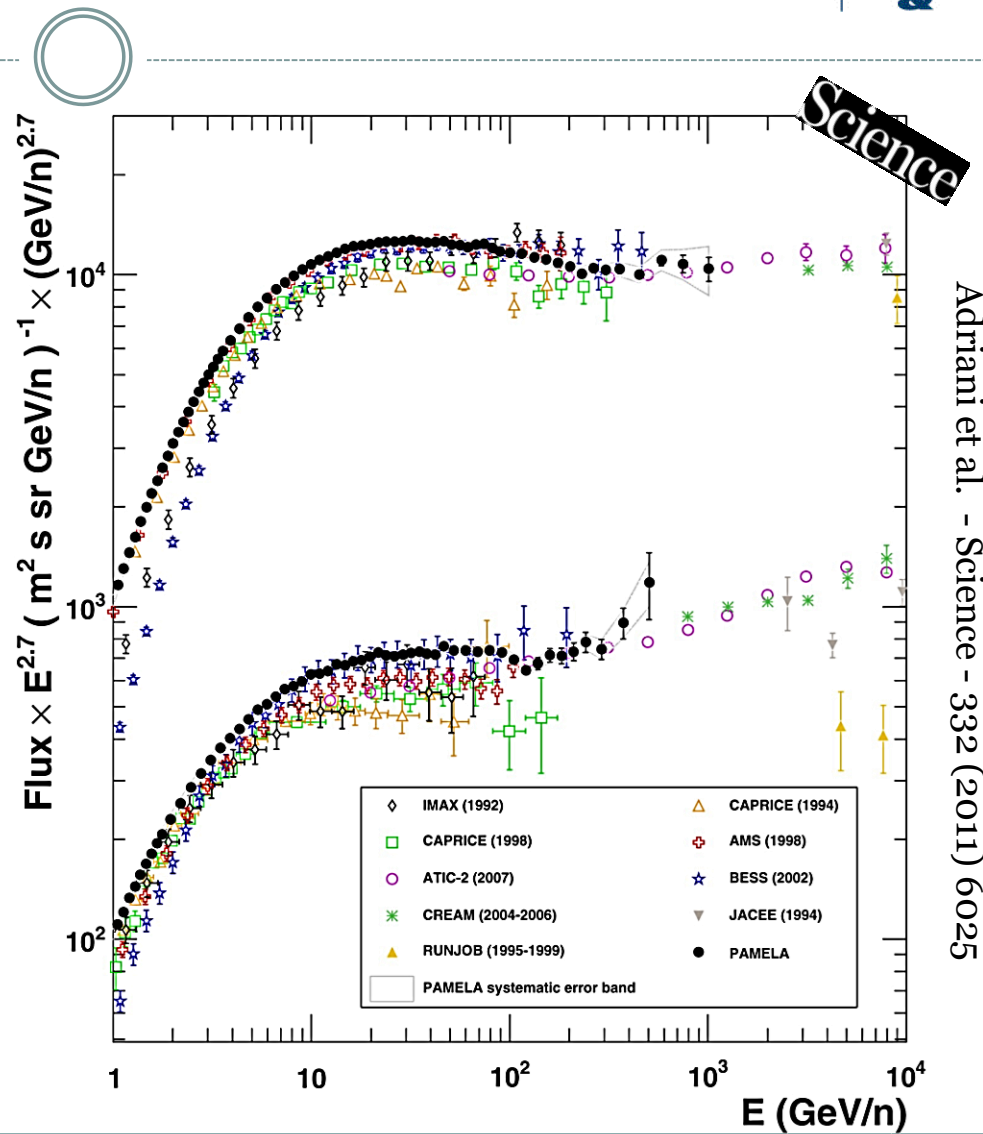
H&He absolute fluxes



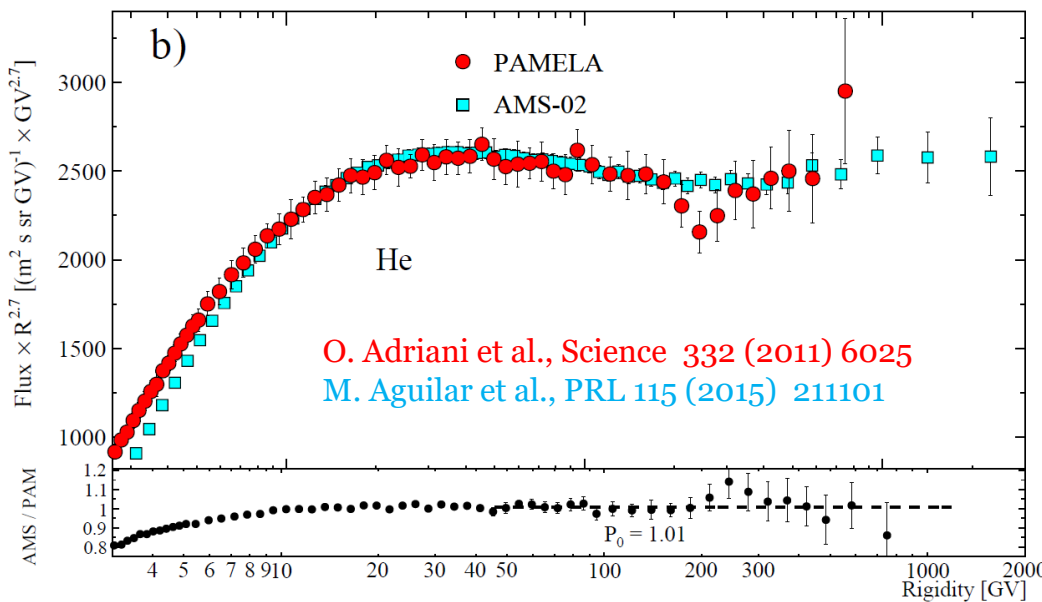
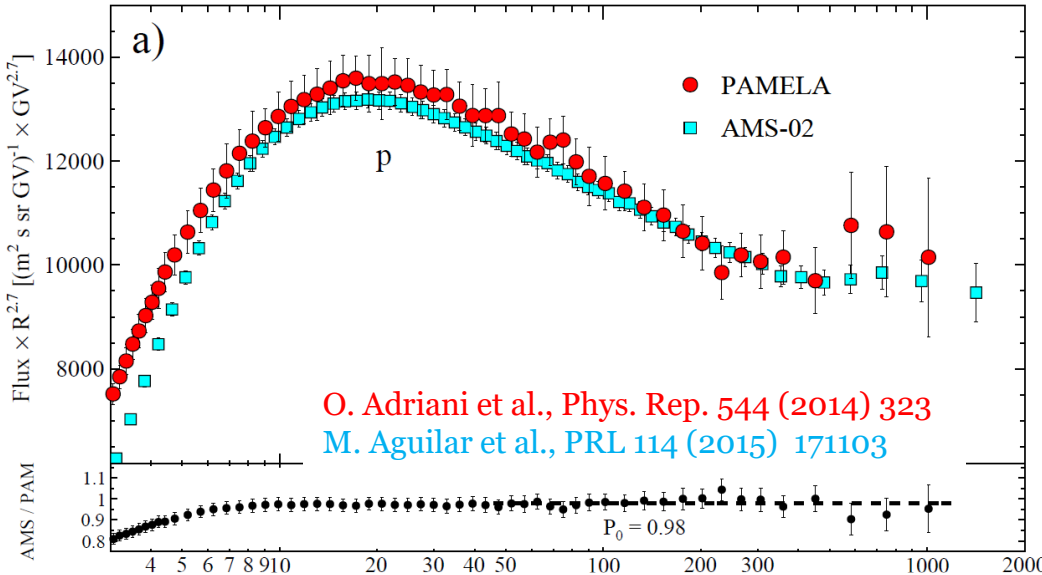
First high-statistics and high-precision measurement over three decades in energy

@ Low energy → minimum solar activity ($\phi = 450 \div 550$ GV)

@ High-energy → Significant hardening above 230 GV for both H and He.



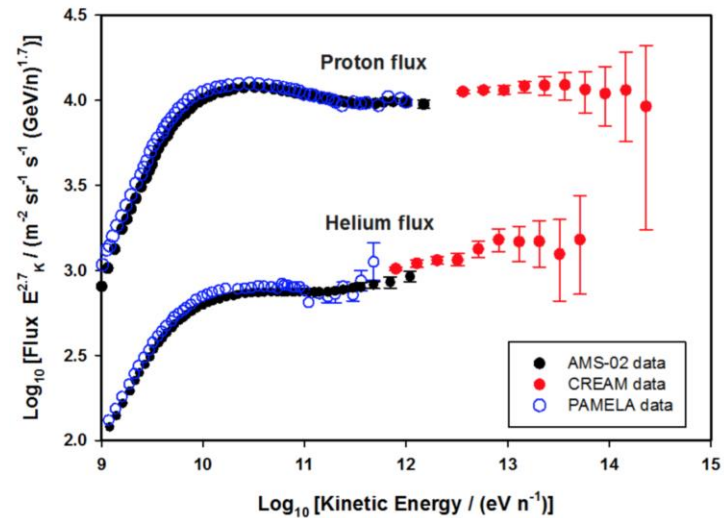
PAMELA data → Jul 2006 ÷ Mar 2008
 AMS02 data → May 2011 ÷ Nov 2013



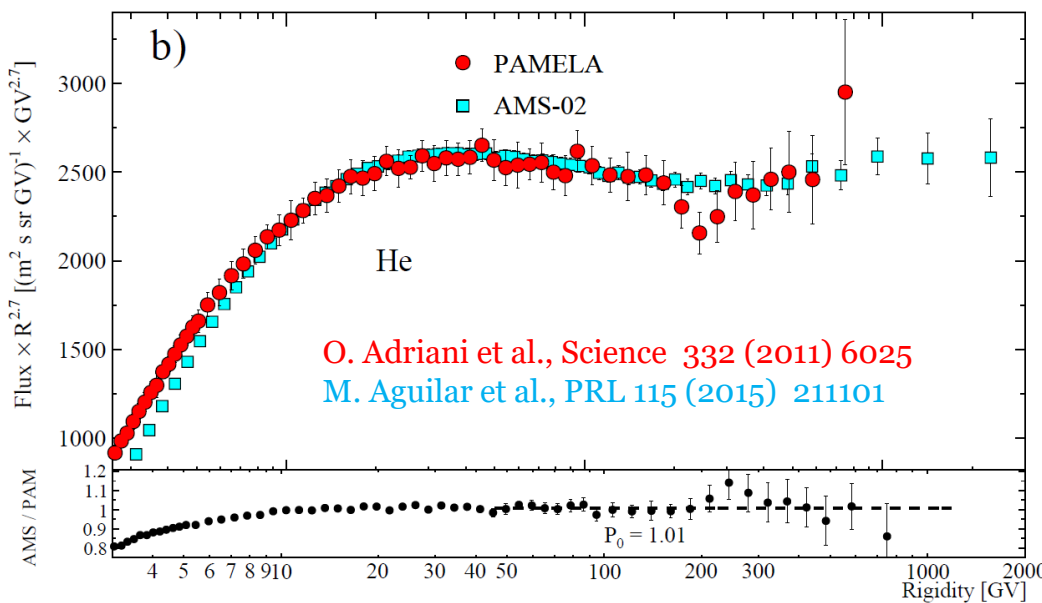
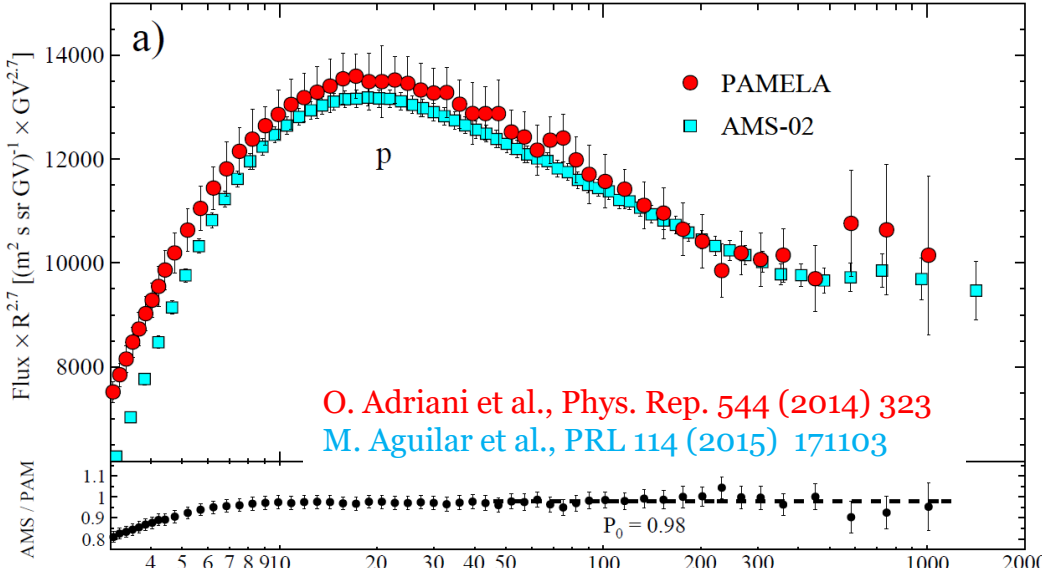
H & He



- Excellent agreement between PAMELA and AMS-02 results, within 2%
- Significant hardening above 230 GV for both H and He.
- Consistent with high-energy calorimetric measurements



PAMELA data → Jul 2006 ÷ Mar 2008
 AMS02 data → May 2011 ÷ Nov 2013



H & He

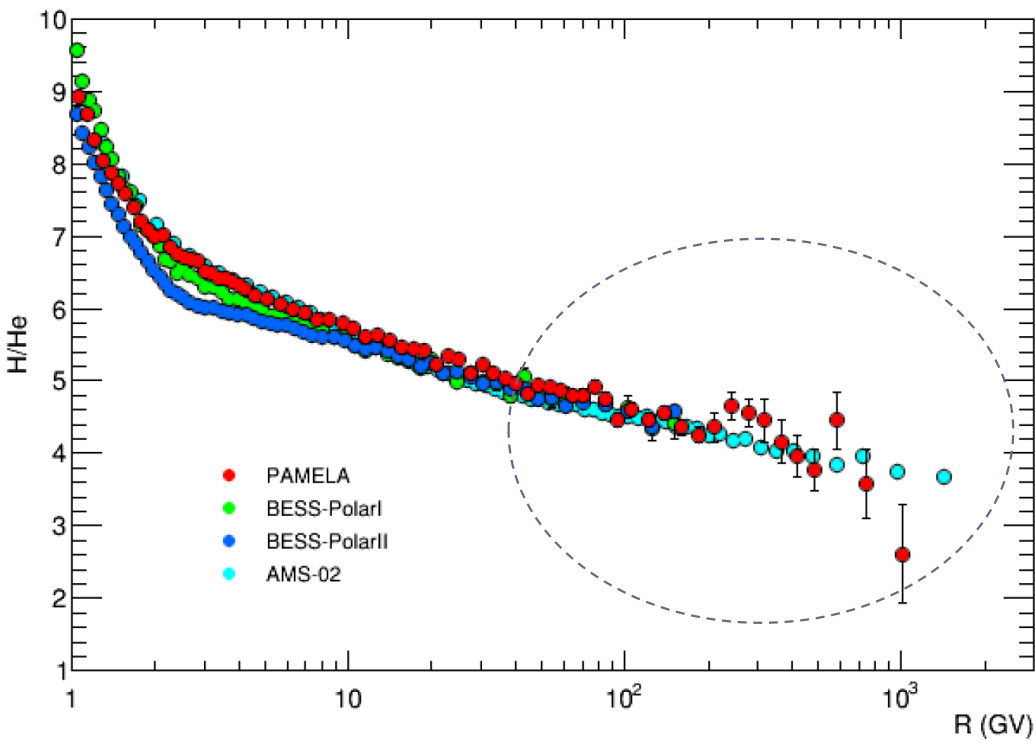


- Excellent agreement between PAMELA and AMS-02 results, within 2%
- Significant hardening above 230 GV for both H and He.
- Consistent with high-energy calorimetric measurements

Possible interpretations:

- Source effect (multi-population, spectral features at injection)
- Propagation effect

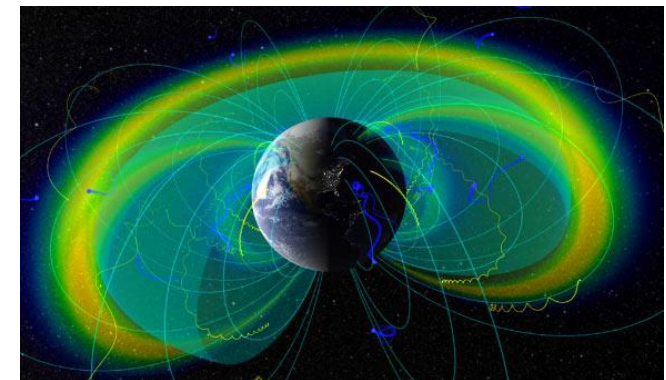
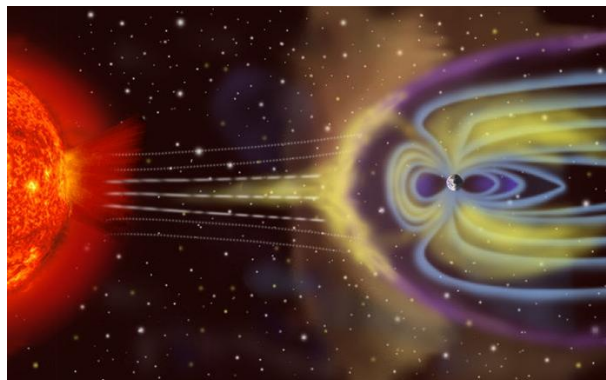
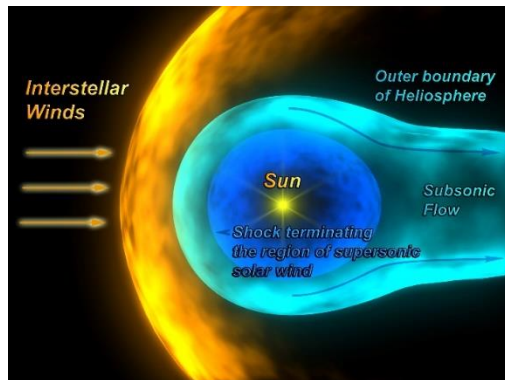
H-to-He ratio



Systematic uncertainties partly cancel out at high energy

- Propagation effects small above $\sim 100\text{GV}$
→ information about source spectra
- Different slope for H and He
- No indication of spectral features above 10 GV

Heliosphere end Magnetosphere



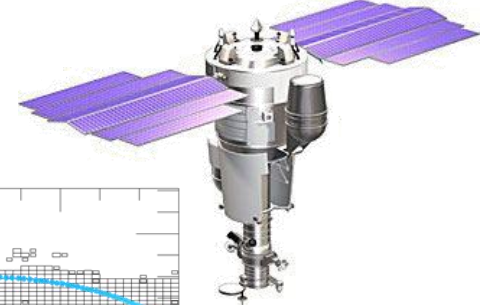
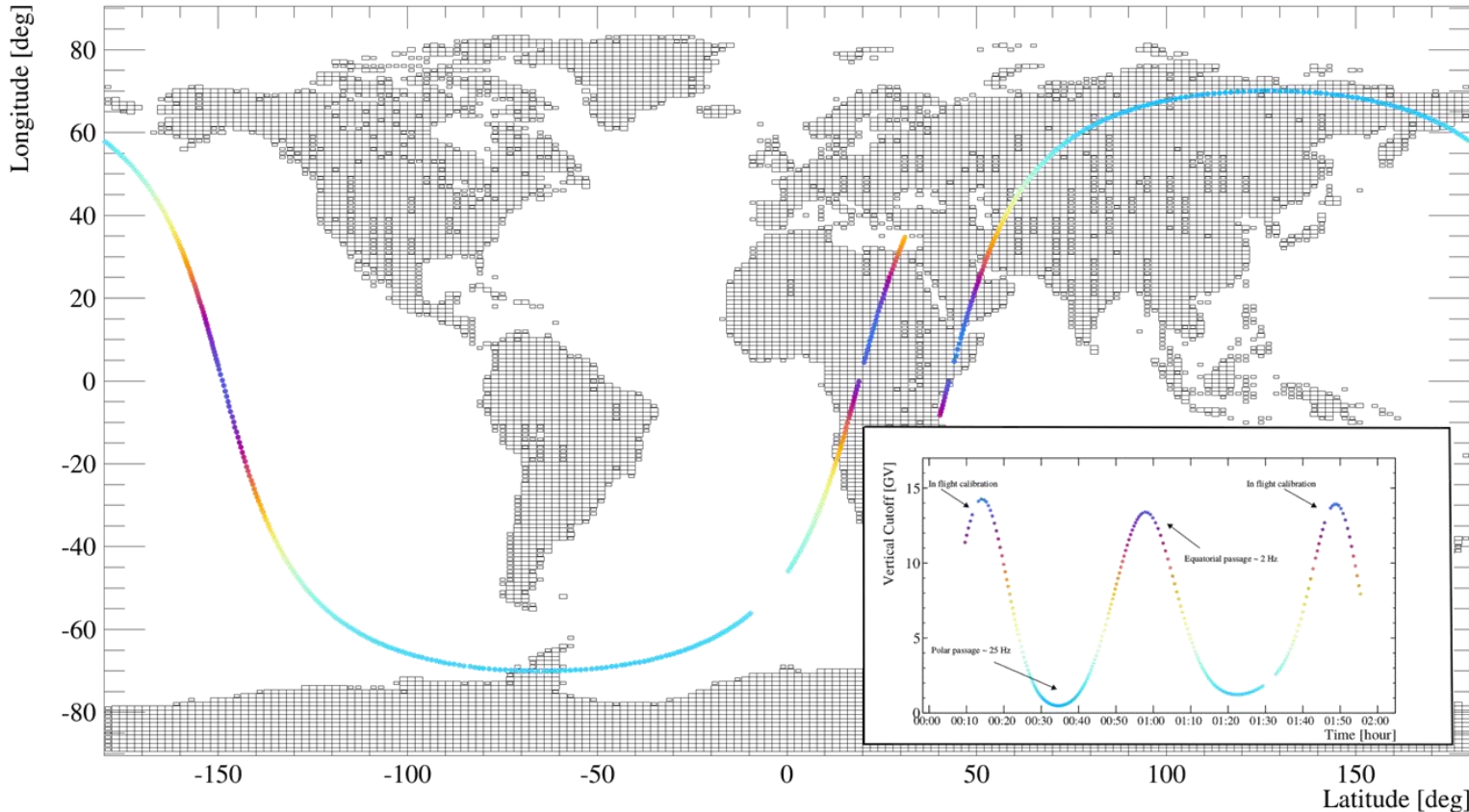
Resurs-DK1 orbit



Quasi-polar elliptical orbit (circular from 2010)

Inclination $\sim 70^\circ$

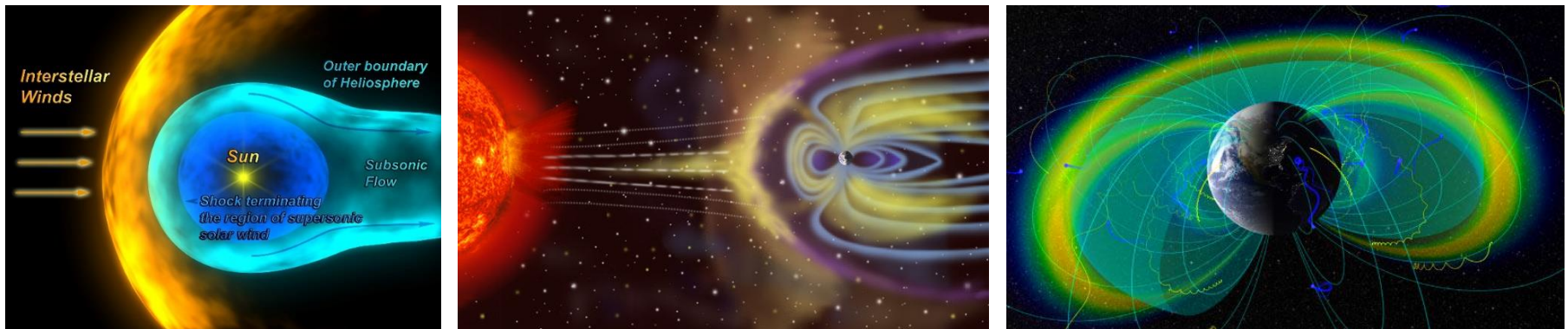
Altitude $\sim 300 \div 600$ km



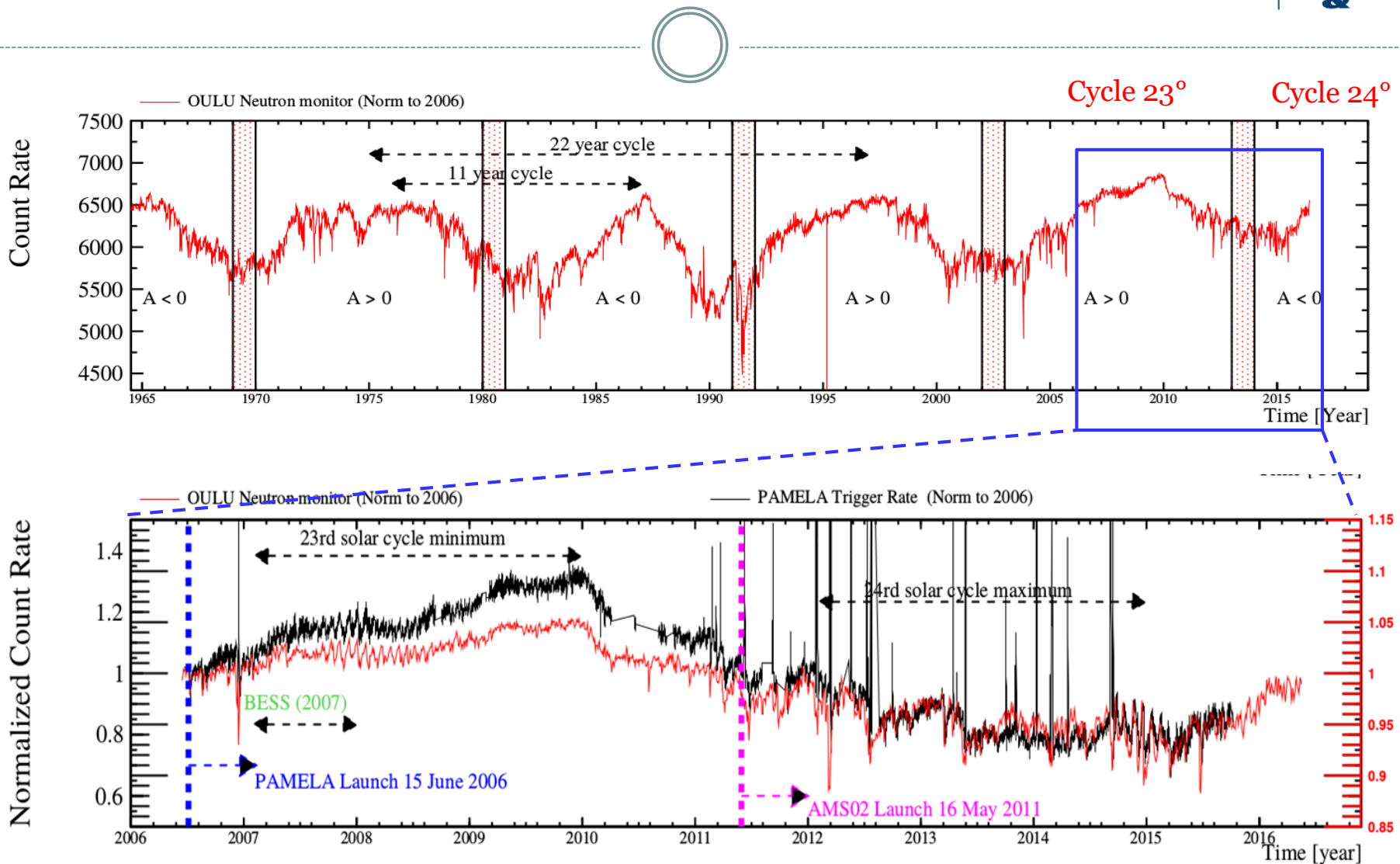
Heliosphere end Magnetosphere



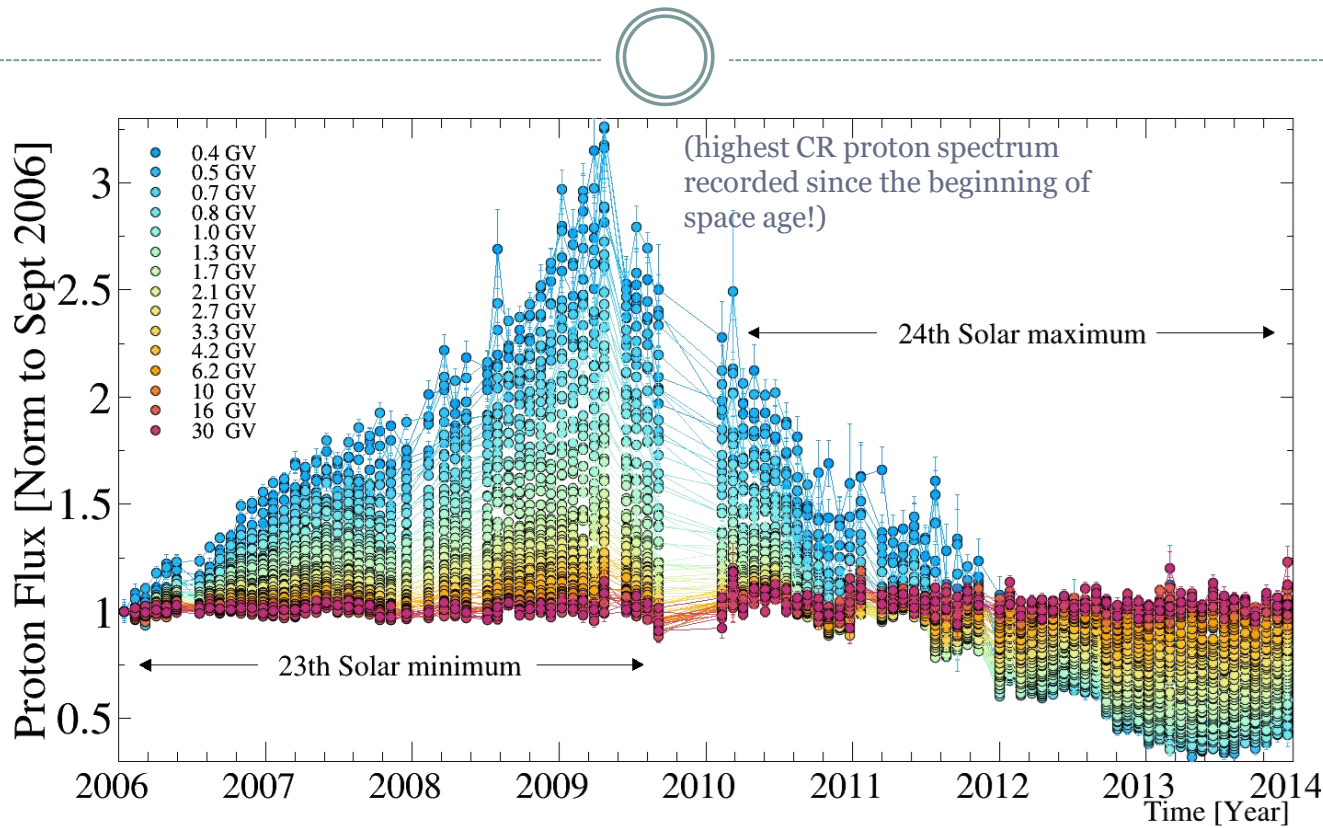
- Long-term CR-flux variations → **solar modulation** of various CR components
- **Solar-particle events (SEPs)**
- Short- and mid-term CR-flux variations (semi-periodic & transient phenomena)
- Geomagnetically trapped and re-entrant albedo particles



PAMELA observations during 23° and 24° solar cycles



Solar modulation



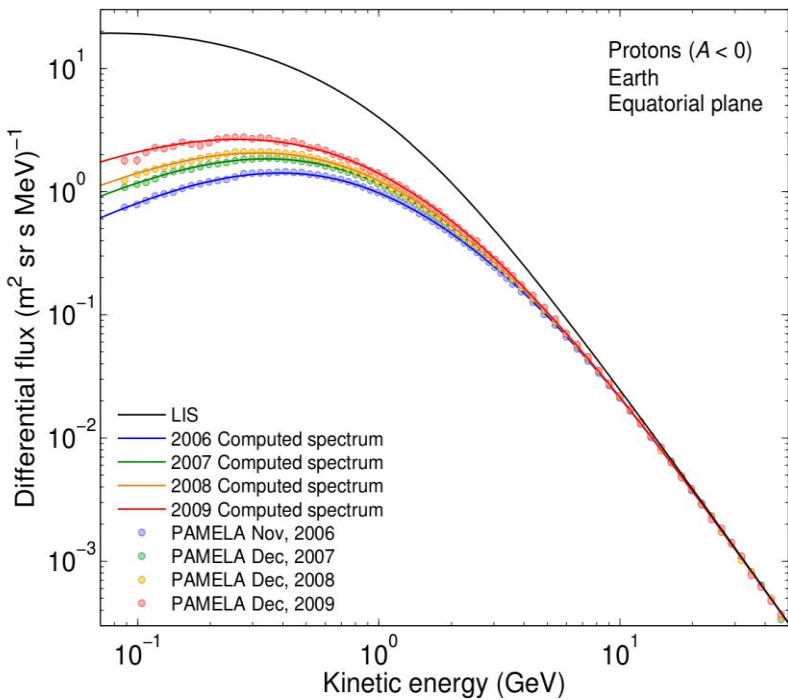
Adriani et al., Riv. N.Cim., 10, 473-522, 2017

- CRs at Earth strongly affected by Heliosphere below ~ 30 GV
- Heliosphere \rightarrow Ideal environment to test theory for propagation of charged particles under conditions which well approximate cosmic conditions

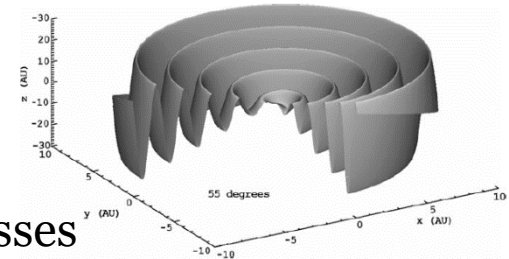
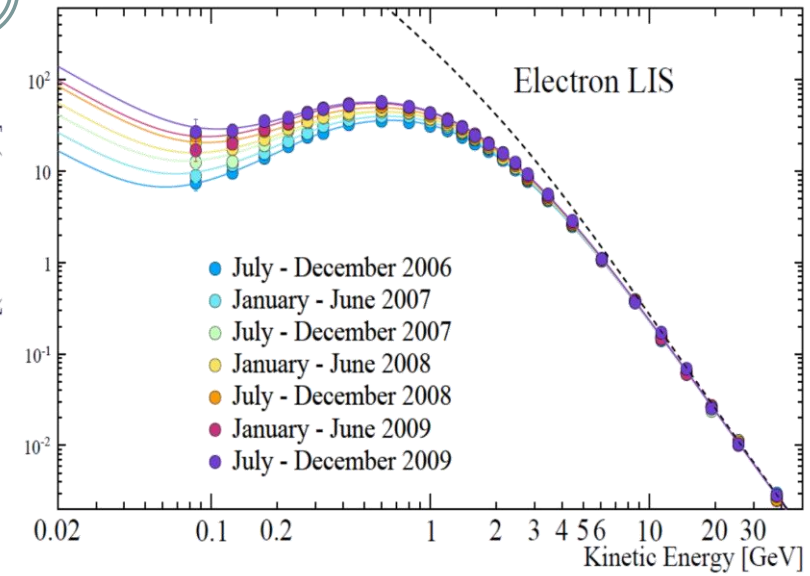
Heliospheric propagation modeling



Potgieter et al. ApJ 810 (2015) 141
 Adriani et al. ApJ 810(2015) 142



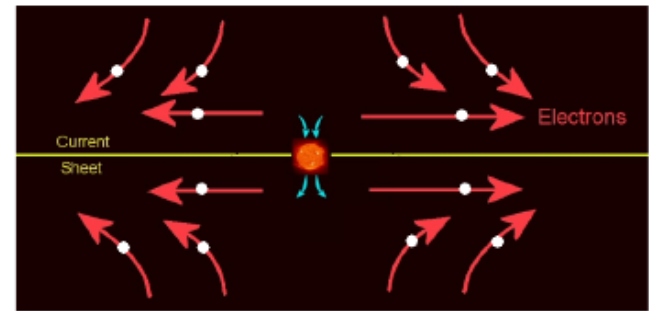
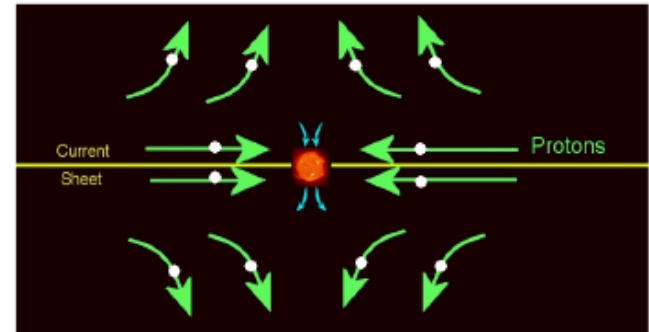
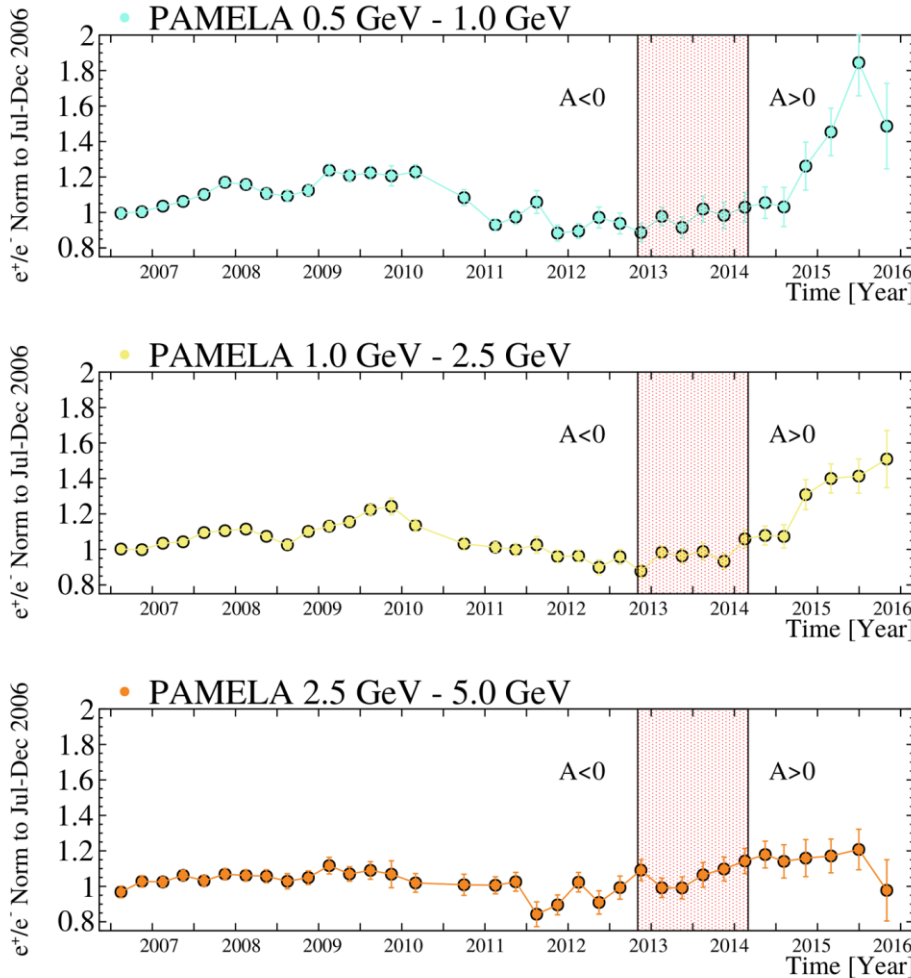
Adriani et al. ApJ 765 (2013) 91
 Potgieter et al. Solar Phys. 289 (2014) 391



- 3D heliospheric model
- Transport processes: convection, diffusion, drift, adiabatic losses
- Stationary approximation during minimum solar activity

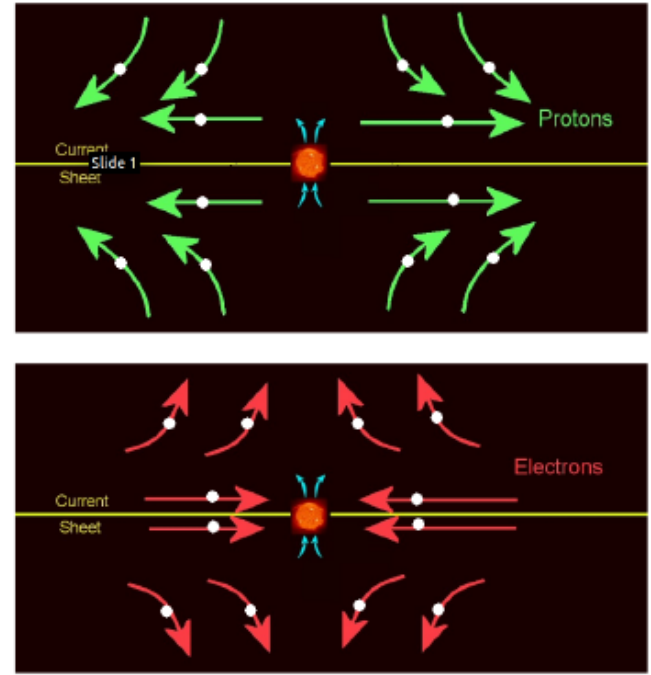
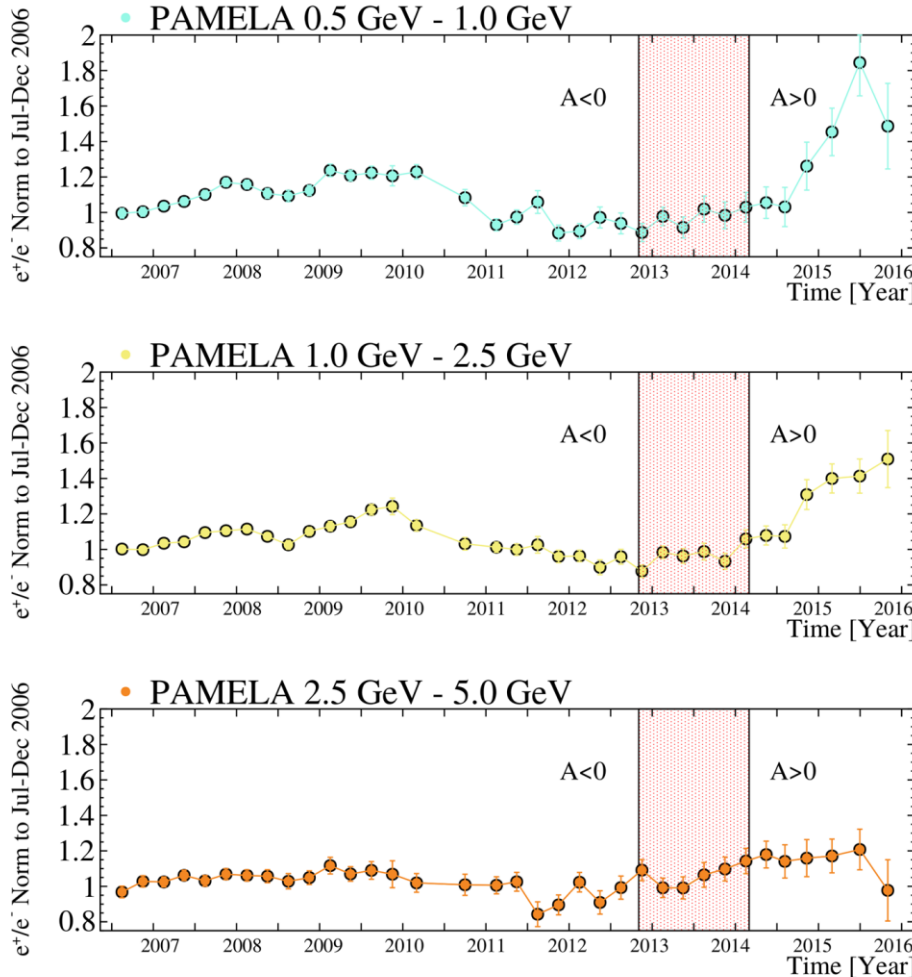
PAMELA multi-species low-energy time-dependent spectra used to constrain model parameters

Charge-dependent solar modulation



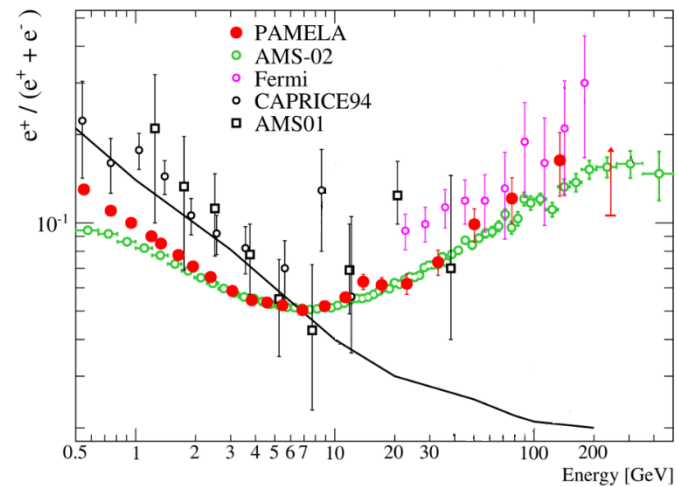
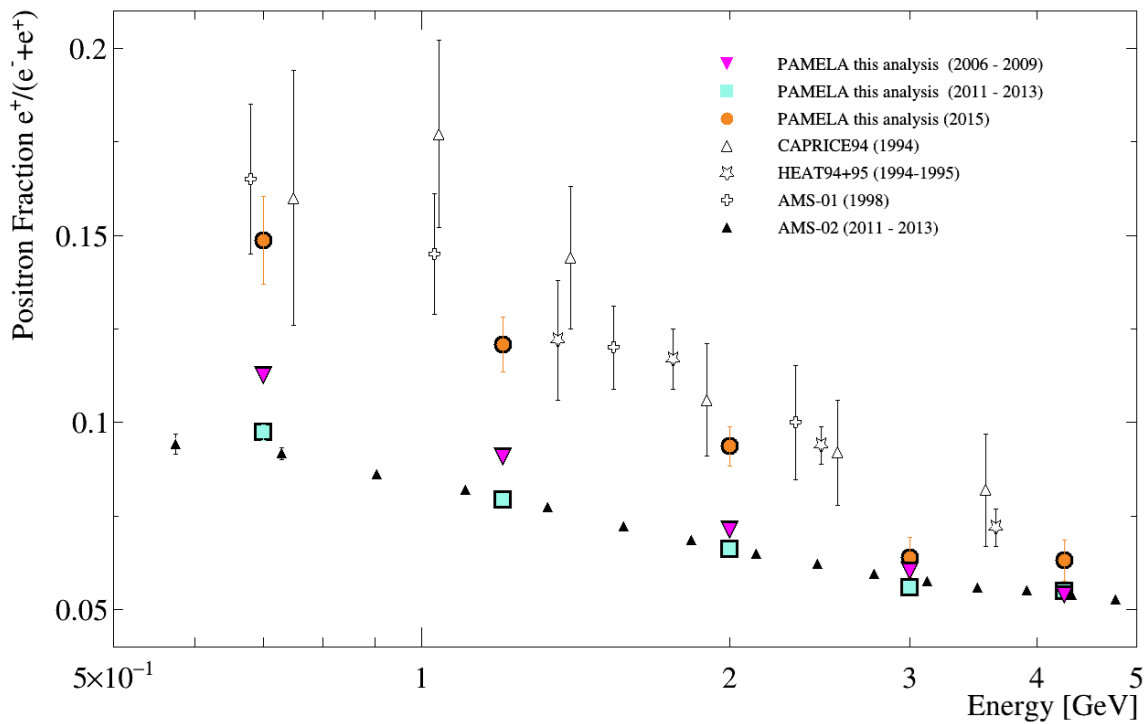
charge sign dependence introduced by drift motions experienced by the GCRs during their propagation through the heliosphere

Charge-dependent solar modulation



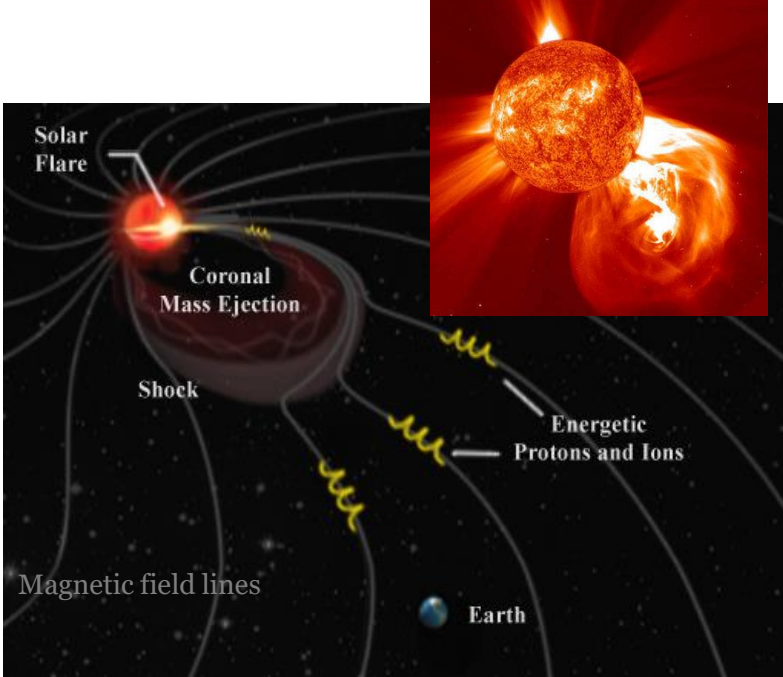
charge sign dependence introduced by drift motions experienced by the GCRs during their propagation through the heliosphere

Positron fraction



Charge-dependent solar-modulation effect accounts for discrepancies among PAMELA, AMS-02 and data collected during previous solar cycle

Solar energetic particles (SEPs)



SEP observation on Earth:

- Propagation of SEPs along IMF lines
⇒ Earth must be magnetically connected
- Anisotropic emission
⇒ flux observed on Earth depends depends on geomagnetic location



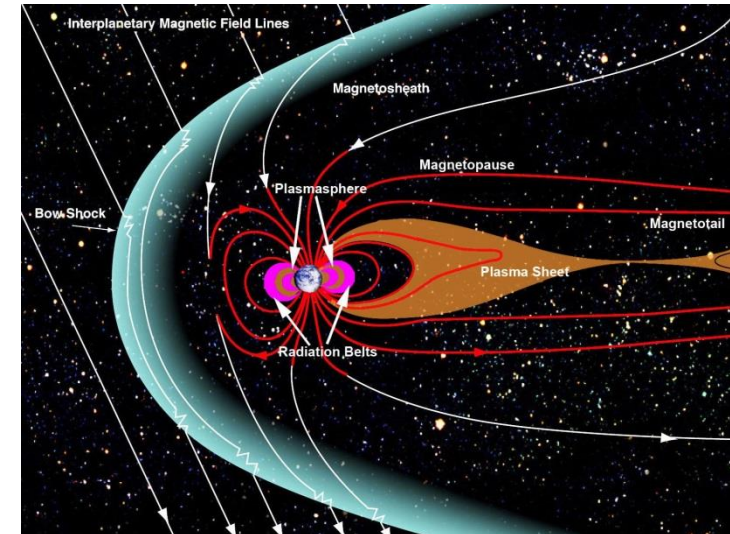
Sun can accelerate particles up to relativistic energies

- Magnetic reconnections
- CME-driven shock

SEPs can be observed in the interplanetary space

Often associated to other solar phenomena, eg:

- X and gamma-ray flares
- Coronal-mass ejections (CMEs)
- ...



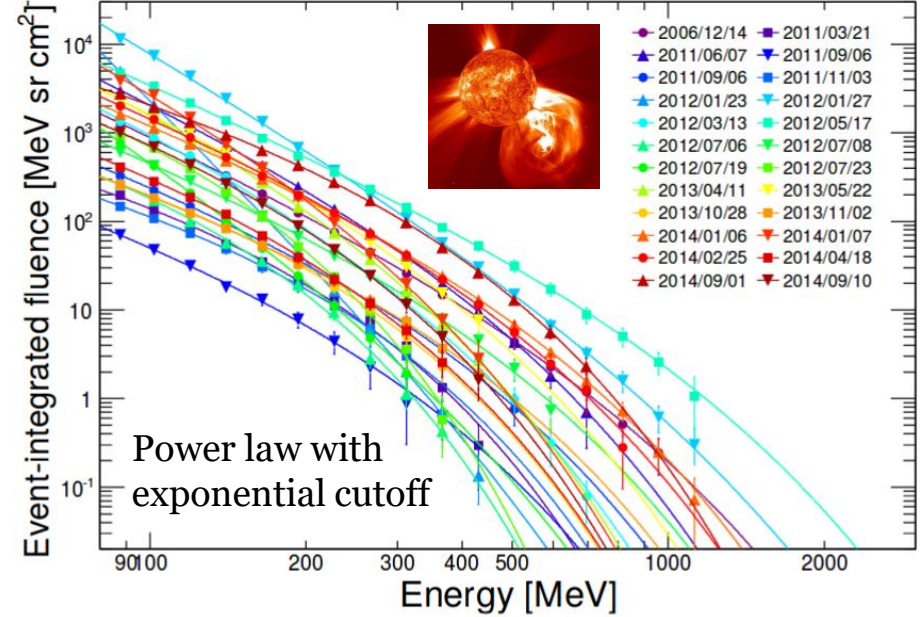
SEPs detected by PAMELA



| # | SEP Event | Flare | | | CME | | | m-type II | DH-type II | |
|----|-------------------|--------------|------------|---------|--------------|----------------------------|------------------|------------------|--------------|--------------|
| | | Date | Onset time | Class | Location | 1 st -app. time | V _{app} | V _{spa} | Width | Onset time |
| 1 | 2006 12/13, 02:55 | 12/13, 02:14 | X3.4 | S06W23 | 12/13, 02:54 | 1774 | 2184 | H | 12/13, 02:26 | 12/13, 02:45 |
| 2 | 2006 12/14, 22:55 | 12/14, 21:58 | X1.5 | S06W46 | 12/14, 22:30 | 1042 | 1139 | H | 12/14, 22:09 | 12/14, 22:30 |
| 3 | 2011 03/21, 04:10 | 03/21, 02:00 | -- | N23W129 | 03/21, 02:24 | 1341 | 1430 | H | -- | -- |
| 4 | 2011 06/07, 07:20 | 06/07, 06:16 | M2.5 | S21W54 | 06/07, 06:49 | 1255 | 1321 | H | 06/07, 06:25 | 06/07, 06:45 |
| 5 | 2011 09/06, 02:20 | 09/06, 01:35 | M5.3 | N14W07 | 09/06, 02:24 | 782 | 1232 | H | -- | 09/06, 02:00 |
| 6 | 2011 09/06, 23:00 | 09/06, 22:12 | X2.1 | N14W18 | 09/06, 23:05 | 575 | 830 | H | -- | 09/06, 22:30 |
| 7 | 2011 11/03, 23:00 | 11/03, 22:00 | -- | N09E154 | 11/03, 23:30 | 991 | 1188 | H | -- | -- |
| 8 | 2012 01/23, 04:45 | 01/23, 03:38 | M8.7 | N28W21 | 01/23, 04:00 | 2175 | 2511 | H | -- | 01/23, 04:00 |
| 9 | 2012 01/27, 18:55 | 01/27, 18:03 | X1.7 | N27W71 | 01/27, 18:27 | 2508 | 2541 | H | 01/27, 18:10 | 01/27, 18:30 |
| 10 | 2012 03/07, 02:50 | 03/07, 00:13 | X5.4 | N17E27 | 03/07, 00:24 | 2684 | 3146 | H | 03/07, 00:17 | 03/07, 01:00 |
| 11 | 2012 03/13, 18:05 | 03/13, 17:12 | M7.9 | N17W66 | 03/13, 17:36 | 1884 | 1931 | H | 03/13, 17:15 | 03/13, 17:35 |
| 12 | 2012 05/17, 01:55 | 05/17, 01:25 | M5.1 | N11W76 | 05/17, 01:48 | 1582 | 1596 | H | 05/17, 01:31 | 05/17, 01:40 |
| 13 | 2012 07/06, 23:30 | 07/06, 23:01 | X1.1 | S13W59 | 07/06, 23:24 | 1828 | 1907 | H | 07/06, 23:09 | 07/06, 23:10 |
| 14 | 2012 07/08, 18:10 | 07/08, 16:23 | M6.9 | S17W74 | 07/08, 16:54 | 1497 | -- | 157 | 07/08, 16:30 | 07/08, 16:35 |
| 15 | 2012 07/19, 06:40 | 07/19, 04:17 | M7.7 | S13W88 | 07/19, 05:24 | 1631 | 1631 | H | 07/19, 05:24 | 07/19, 05:30 |
| 16 | 2012 07/23, 08:00 | 07/23, 01:50 | -- | S17W132 | 07/23, 02:36 | 2003 | 2156 | H | -- | 07/23, 02:30 |
| 17 | 2013 04/11, 08:25 | 04/11, 06:56 | M6.5 | N09E12 | 04/11, 07:24 | 861 | 1369 | H | 04/11, 07:02 | 04/11, 07:10 |
| 18 | 2013 05/22, 14:20 | 05/22, 13:08 | M5.0 | N15W70 | 05/22, 13:25 | 1466 | 1491 | H | 05/22, 12:59 | 05/22, 13:10 |
| 19 | 2013 10/28, 16:30 | 10/28, 04:32 | M4.4 | S06E28 | 10/28, 15:36 | 812 | 1098 | H | -- | 10/28, 15:24 |
| 20 | 2013 11/02, 07:00 | 11/02, 04:00 | -- | N03W139 | 11/02, 04:48 | 828 | 998 | H | -- | -- |
| 21 | 2014 01/06, 08:15 | 01/06, 07:30 | X3.5 | S15W112 | 01/06, 08:00 | 1402 | 1431 | H | 01/06, 07:45 | 01/06, 07:58 |
| 22 | 2014 01/07, 19:55 | 01/07, 18:04 | X1.2 | S15W11 | 01/07, 18:24 | 1830 | 2246 | H | 01/07, 18:17 | 01/07, 18:27 |
| 23 | 2014 02/25, 03:50 | 02/25, 00:39 | X4.9 | S12E82 | 02/25, 01:25 | 2147 | 2153 | H | 02/25, 00:56 | 02/25, 00:56 |
| 24 | 2014 04/18, 13:40 | 04/18, 12:31 | M7.3 | S20W34 | 04/18, 13:25 | 1203 | 1359 | H | 04/18, 12:55 | 04/18, 13:06 |
| 25 | 2014 09/01, 17:20 | 09/01, 10:58 | X2.4 | N14E127 | 09/01, 11:12 | 1901 | 2017 | H | -- | 09/01, 11:12 |
| 26 | 2014 09/10, 21:35 | 09/10, 17:21 | X1.6 | N14E02 | 09/10, 18:00 | 1267 | 1652 | H | -- | 09/10, 17:45 |



Bruno et al., ApJ 862, 2018



- PAMELA bridges the gap between low-energy in-situ spacecrafts and ground-based NM network observations (GLEs)
- 26 SEPs observed within 2006-2014

SEPs detected by PAMELA



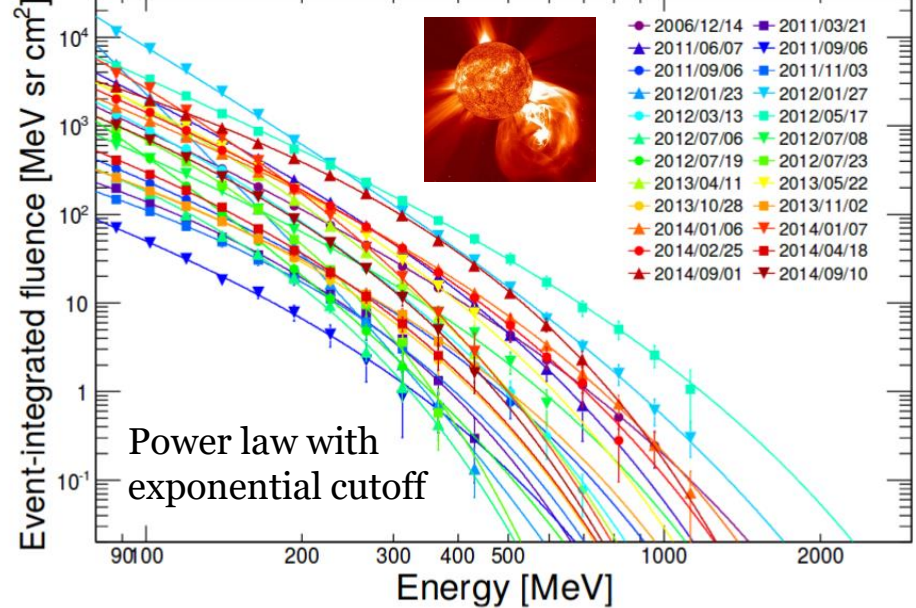
| # | SEP Event | Flare | | | CME | | | m-type II | DH-type II | |
|----|-------------------|--------------|------------|---------|--------------|----------------------------|------------------|------------------|--------------|--------------|
| | | Date | Onset time | Class | Location | 1 st -app. time | V _{app} | V _{spa} | Width | Onset time |
| 1 | 2006 12/13, 02:55 | 12/13, 02:14 | X3.4 | S06W23 | 12/13, 02:54 | 1774 | 2184 | H | 12/13, 02:26 | 12/13, 02:45 |
| 2 | 2006 12/14, 22:55 | 12/14, 21:58 | X1.5 | S06W46 | 12/14, 22:30 | 1042 | 1139 | H | 12/14, 22:09 | 12/14, 22:30 |
| 3 | 2011 03/21, 04:10 | 03/21, 02:00 | -- | N23W129 | 03/21, 02:24 | 1341 | 1430 | H | -- | -- |
| 4 | 2011 06/07, 07:20 | 06/07, 06:16 | M2.5 | S21W54 | 06/07, 06:49 | 1255 | 1321 | H | 06/07, 06:25 | 06/07, 06:45 |
| 5 | 2011 09/06, 02:20 | 09/06, 01:35 | M5.3 | N14W07 | 09/06, 02:24 | 782 | 1232 | H | -- | 09/06, 02:00 |
| 6 | 2011 09/06, 02:20 | | | | | | | | 06, 22:30 | |
| 7 | 2011 11/06, 02:20 | | | | | | | | -- | |
| 8 | 2012 01/06, 02:20 | | | | | | | | 23, 04:00 | |
| 9 | 2012 01/06, 02:20 | | | | | | | | 27, 18:30 | |
| 10 | 2012 01/06, 02:20 | | | | | | | | 07, 01:00 | |
| 11 | 2012 01/06, 02:20 | | | | | | | | 13, 17:35 | |
| 12 | 2012 01/06, 02:20 | | | | | | | | 17, 01:40 | |
| 13 | 2012 01/06, 02:20 | | | | | | | | 06, 23:10 | |
| 14 | 2012 01/06, 02:20 | | | | | | | | 08, 16:35 | |
| 15 | 2012 01/06, 02:20 | | | | | | | | 19, 05:30 | |
| 16 | 2012 01/06, 02:20 | | | | | | | | 23, 02:30 | |
| 17 | 2013 01/06, 02:20 | | | | | | | | 11, 07:10 | |
| 18 | 2013 01/06, 02:20 | | | | | | | | 22, 13:10 | |
| 19 | 2013 01/06, 02:20 | | | | | | | | 28, 15:24 | |
| 20 | 2013 01/06, 02:20 | | | | | | | | -- | |
| 21 | 2014 01/06, 02:20 | | | | | | | | 06, 07:58 | |
| 22 | 2014 01/06, 02:20 | | | | | | | | 07, 18:27 | |
| 23 | 2014 02/25, 03:50 | 02/25, 00:39 | A4.9 | S12E82 | 02/25, 01:25 | 2147 | 2153 | H | 02/25, 00:56 | 02/25, 00:56 |
| 24 | 2014 04/18, 13:40 | 04/18, 12:31 | M7.3 | S20W34 | 04/18, 13:25 | 1203 | 1359 | H | 04/18, 12:55 | 04/18, 13:06 |
| 25 | 2014 09/01, 17:20 | 09/01, 10:58 | X2.4 | N14E127 | 09/01, 11:12 | 1901 | 2017 | H | -- | 09/01, 11:12 |
| 26 | 2014 09/10, 21:35 | 09/10, 17:21 | X1.6 | N14E02 | 09/10, 18:00 | 1267 | 1652 | H | -- | 09/10, 17:45 |

SEP-analysis issues:

- Source identification & classification
 - Association to flares, CMEs...
- GLEs
 - different class of events?
- Spectra evolution
 - Intensity, time profile , spectral signatures...
- Composition
 - p/He, ³He content...
- Magnetospheric effects



Bruno et al., ApJ 862, 2018



- PAMELA bridges the gap between low-energy in-situ spacecrafts and ground-based NM network observations (GLEs)
- 26 SEPs observed within 2006-2014

- Spectra consistent with CME-driven shock acceleration (finite escape time)
- No qualitative distinction between SEPs observed as GLEs and those that are not



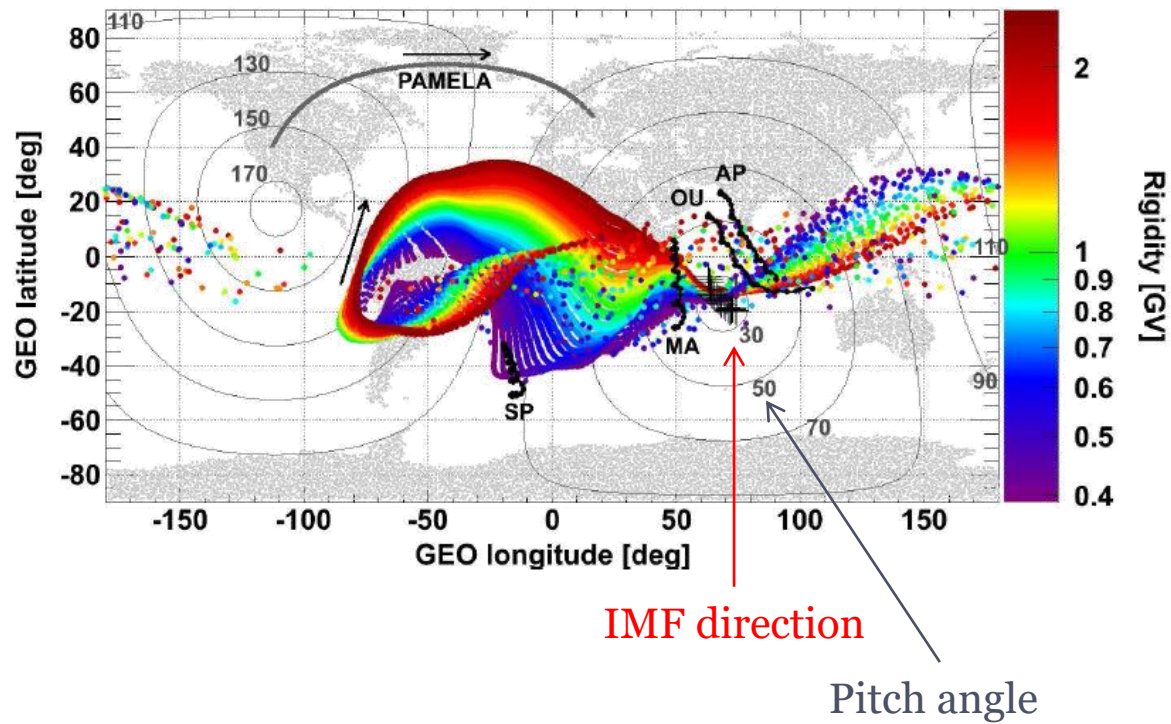
May 17°, 2012 SEP event

- First observed GLE of 24° solar cycle
- Earth magnetically connected to the Sun
- Associated to M1.5-class X-ray flare
- Extended emission ($>100\text{MeV}$) seen by Fermi-LAT

Unique possibility to measure pitch angle distribution over broad energy range, to disentangle interplanetary **transport** process

Asymptotic direction during first polar pass after the event onset

May 17, 2012, 01:57:00 - 02:20:00 UT



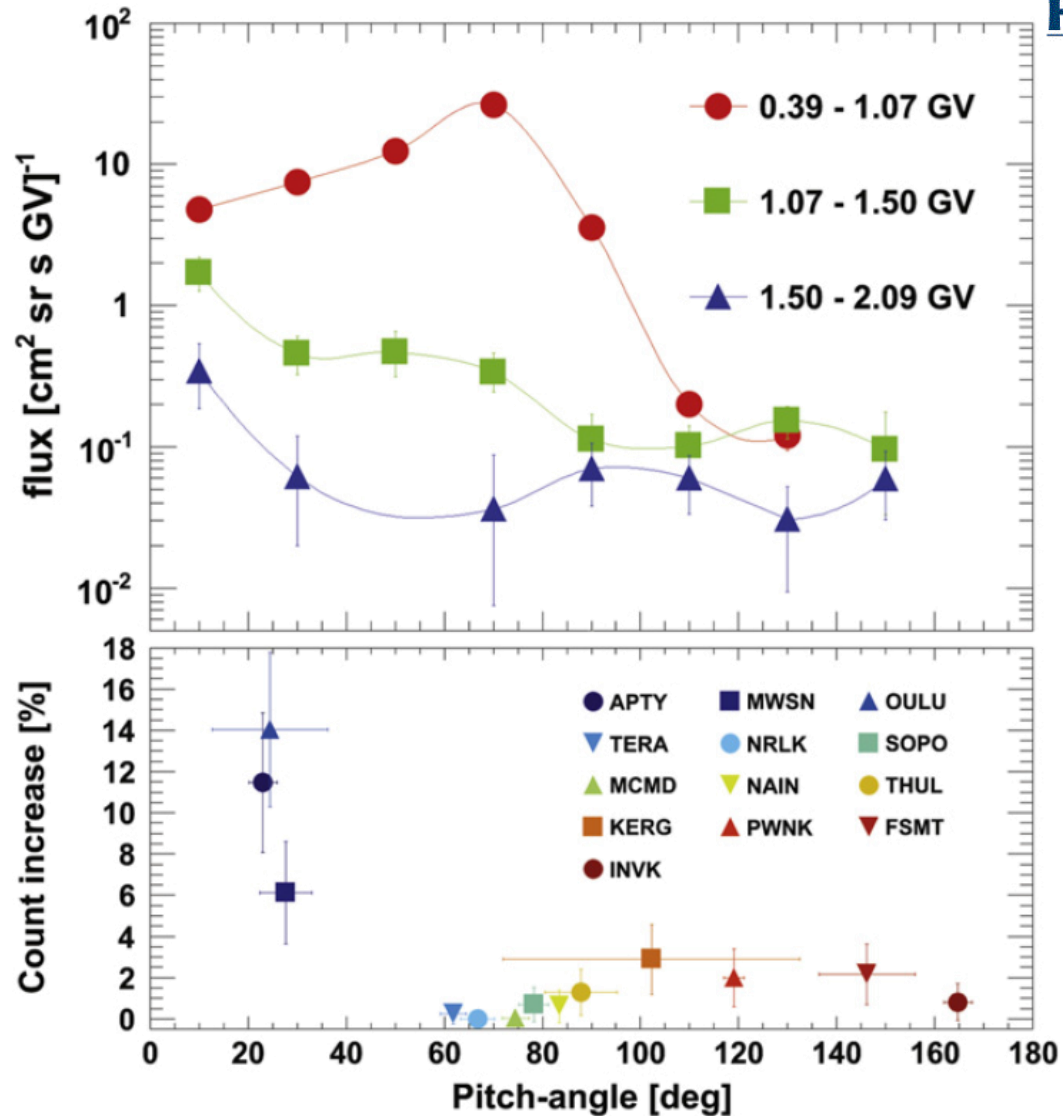
Adriani et al. - ApJL - 801 (2015) L3

May 17°, 2012 SEP event

First evidence of two simultaneous particle populations:

- High rigidity component consistent with NM where particles are field aligned → Beam width \sim 40-60° (not scattered)
- Low rigidity component shows significant scattering for pitch angles \sim 90°

Adriani et al. - ApJL - 801 (2015) L3

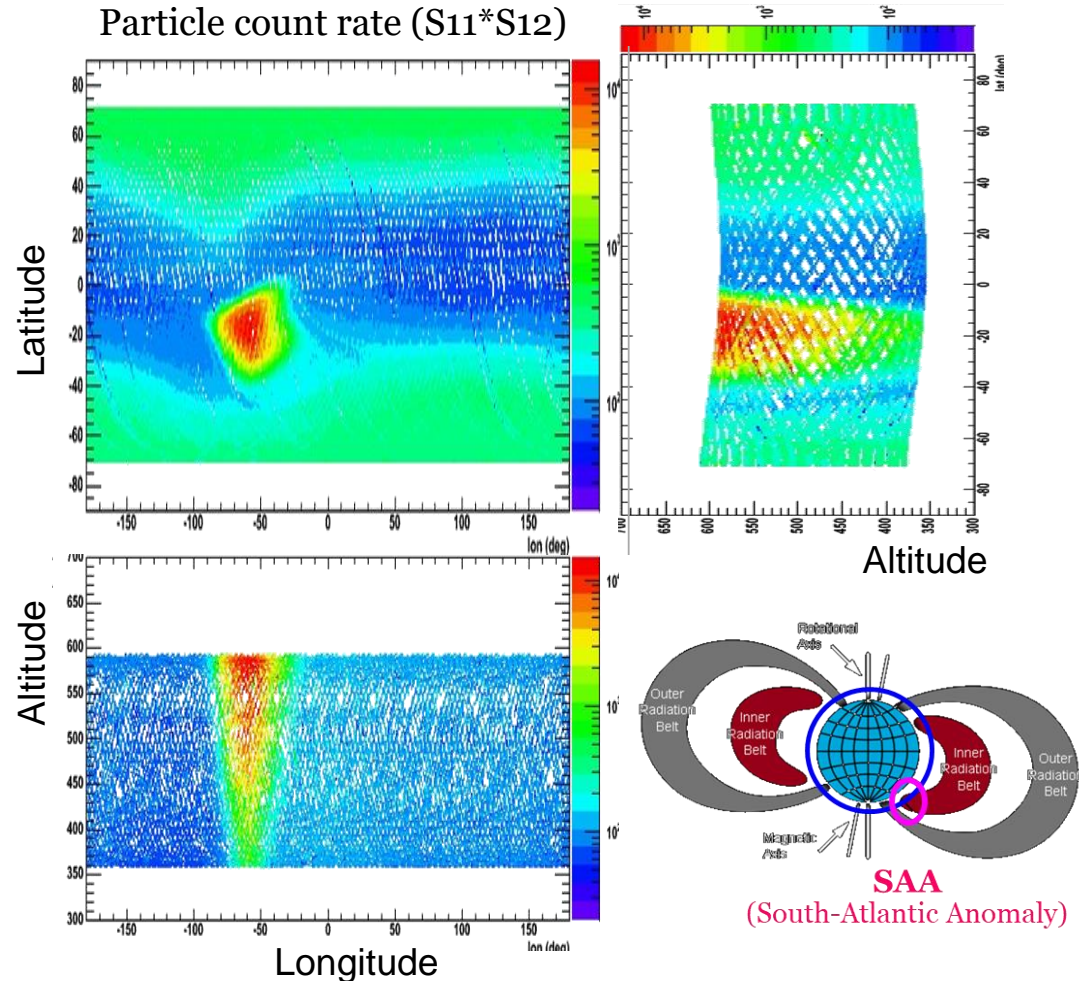


The PAMELA orbital environment



PAMELA sweep through the magnetosphere along a near-Earth semipolar orbit

- Observation of trapped radiation
 - Characterization of high-energy albedo population
- Improvement in low-altitude radiation-environment description

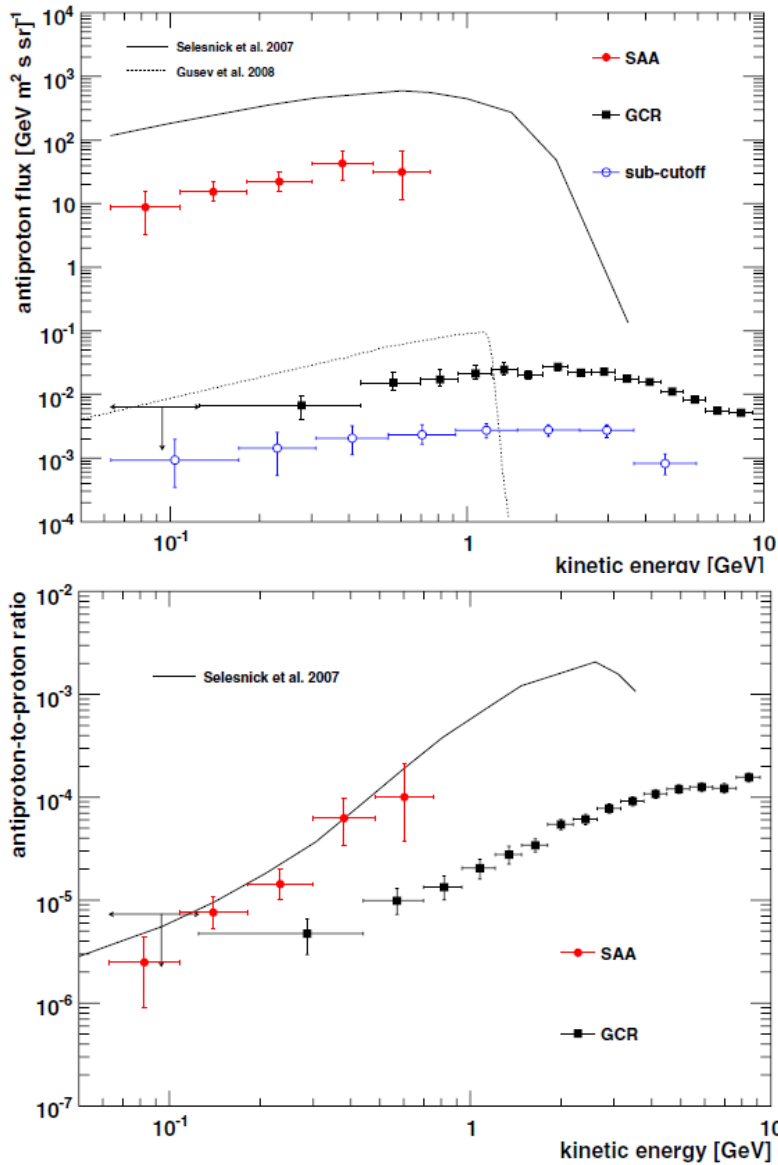


Trapped antiprotons

First observation of
geomagnetically trapped
 $p\bar{p}$

Produced by CR
interaction with
atmosphere and trapped
by the magnetosphere

Most abundant $p\bar{p}$
source near the Earth!



Adriani et al. - ApJ Lett. - 737 (2011) L29



Conclusions



Before PAMELA

- Standard paradigm
 - GCRs originates from uniformly distributed SNRs via shock-driven 2^o-order Fermi acceleration (**single power-law spectra**)
 - **Antiparticles** are produced by nuclear interactions with uniformly distributed matter within the Galaxy
 - Absolute fluxes of GCRs altered while penetrating the heliosphere, modulation described by **spherical potential**

Conclusions



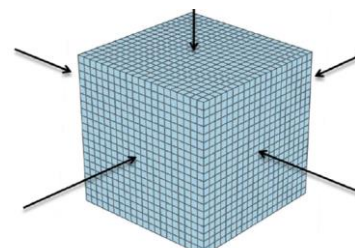
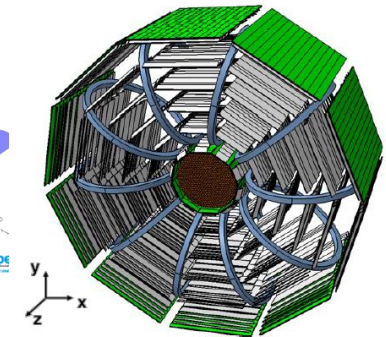
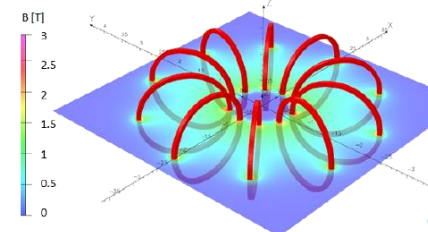
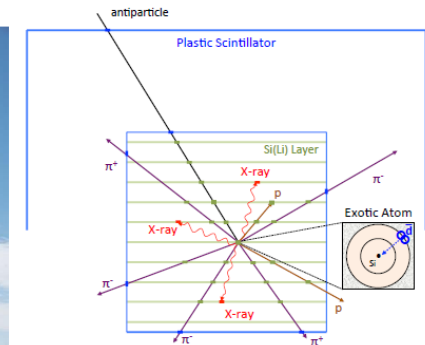
After PAMELA

- Measurement of GCR particles and antiparticles over a wide energy range:
 - Spectral hardening of H and He at about 200GV and different slope for H and He indicate a more complex scenario of nuclear GCR origin and/or propagation
 - Evidence of a positron excess above 10GeV indicates new phenomena (dark matter? astrophysical e+- sources?)
 - p-bar consistent with secondary production hypothesis up to 200 GeV puts further constraints to possible sources
 - Precise measurements of light particle spectra provides improvement to propagation models
- Measurement of long- and short- time variation of low-energy particles:
 - Tuning of fluid-dynamic model of heliosphere
 - Study of solar phenomena, bridging the information provided by low-energy in-situ observations and high-energy surface observations
- Measurement of trapped and quasi-trapped particles:
 - Significant improvement in magnetosphere modeling (radiation-environment)

Continuità con l'attività Wizard



- Cosmic-antimatter search
 - Independent approach to anti-nuclei search
 - GAPS experiment
 - Next generation spectrometers → must rely on superconducting magnets
 - LAPUTA r&d, ALADINO proposal
- High-energy CRs
 - Calorimetric measurements
 - CALET experiment
 - CaloCube r&d
 - HERD experiment



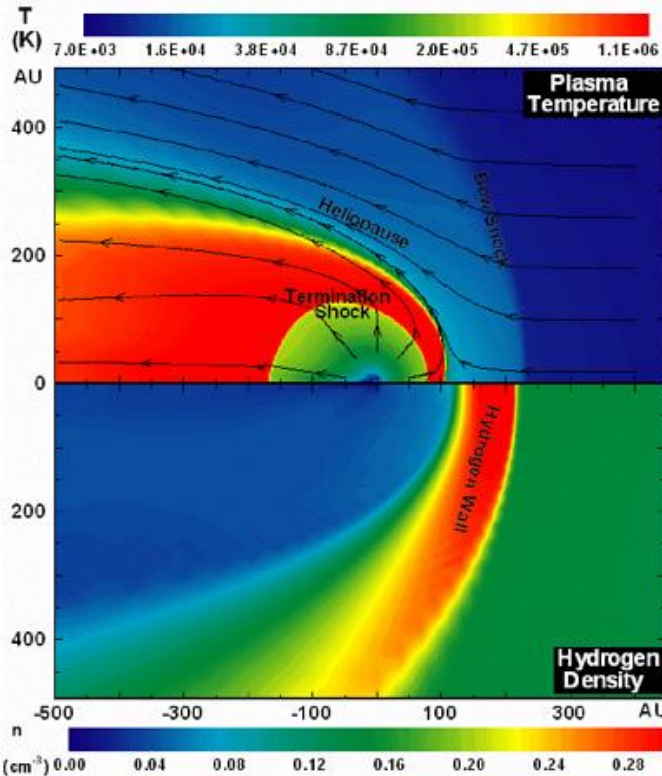
Spares



Heliospheric transport equation



$$\underbrace{\frac{\partial f}{\partial t}}_a = - \underbrace{\mathbf{V} \cdot \nabla f}_b + \underbrace{\nabla \cdot (\mathbf{K}_s \cdot \nabla f)}_c - \underbrace{\langle \mathbf{v}_D \rangle \cdot \nabla f}_d + \underbrace{\frac{1}{3} (\nabla \cdot \mathbf{V}) \frac{\partial f}{\partial \ln p}}_e$$

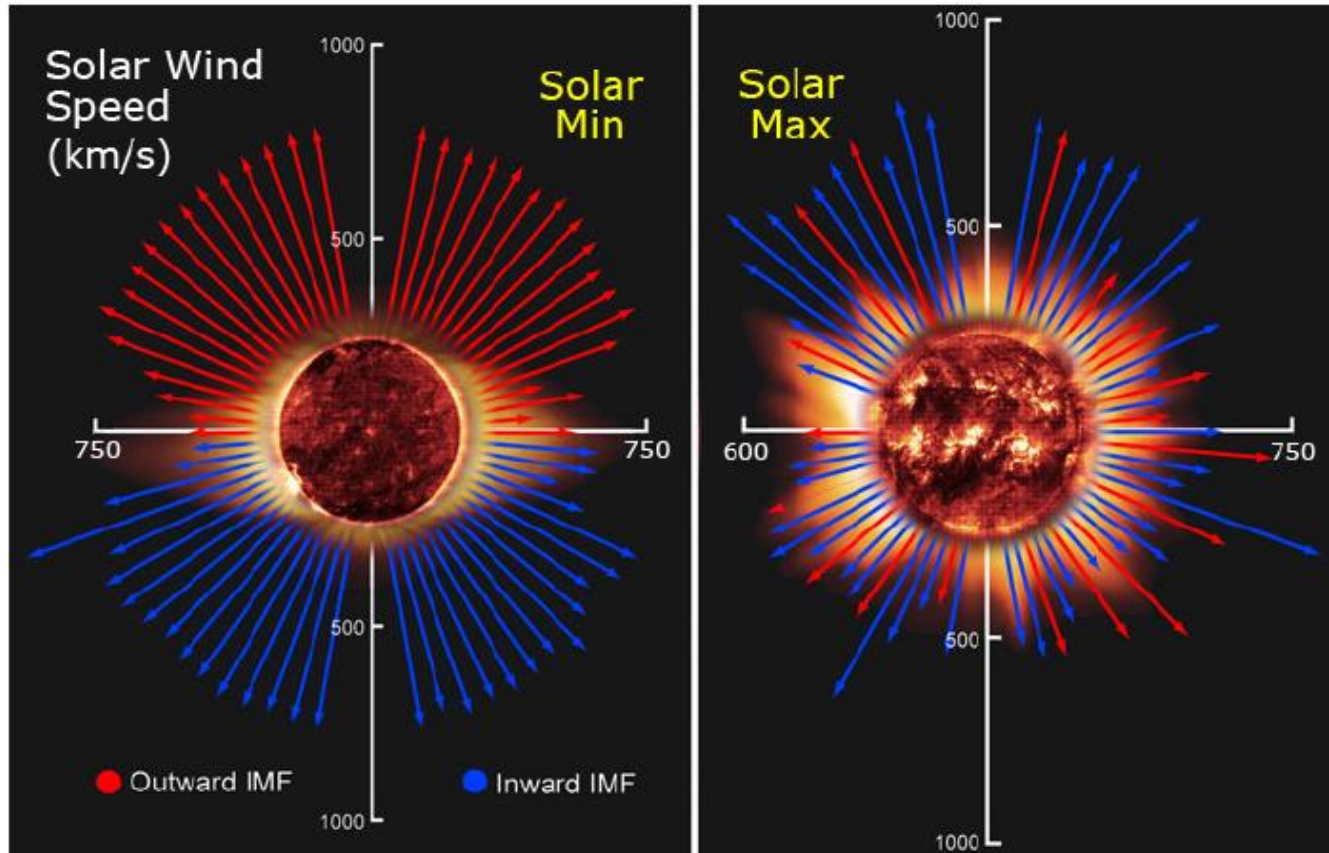


(Parker 1965)

- a: $f(\mathbf{x}, p, t)$, omnidirectional function distribution of CRs;
- b: convection with solar wind \mathbf{V} ;
- c: diffusion by magnetic field irregularities;
- d: drift, curvature and gradient in magnetic field;
- e: adiabatic energy losses;

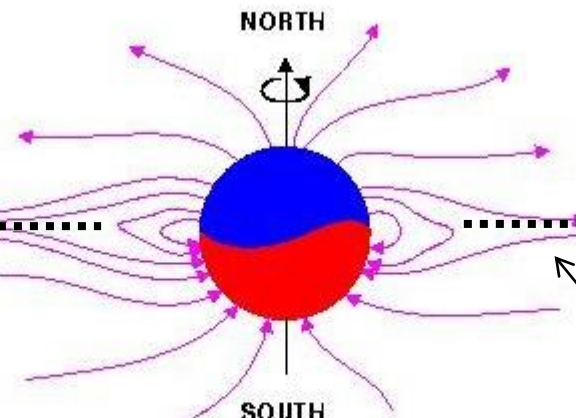
Stationary approximation during minimum solar activity

The solar wind

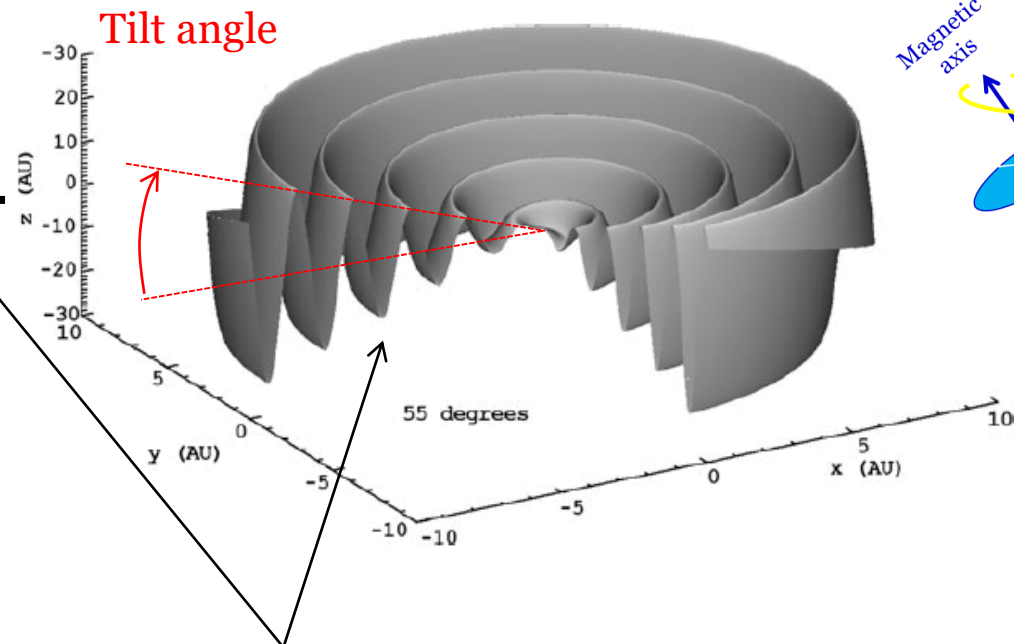


- **Convection** with solar-wind velocity \mathbf{V}
- Adiabatic energy changes ($\propto \nabla \cdot \mathbf{V}$)

Heliospheric magnetic field (HMF)

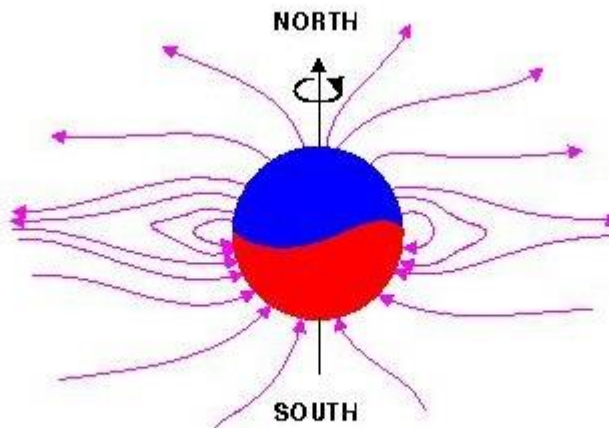


CORONAL MAGNETIC FIELD LINES AT
SOLAR MINIMUM ACTIVITY

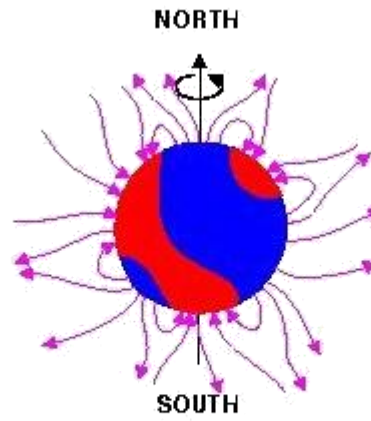


Heliospheric Current Sheet (HCS)

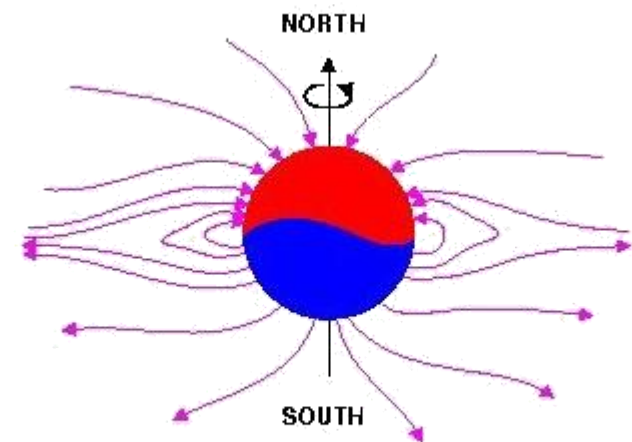
Heliospheric magnetic field (HMF)



CORONAL MAGNETIC FIELD LINES AT
SOLAR MINIMUM ACTIVITY



CORONAL MAGNETIC FIELD LINES AT
SOLAR MAXIMUM ACTIVITY



CORONAL MAGNETIC FIELD LINES AT
NEXT SOLAR MINIMUM

A>0



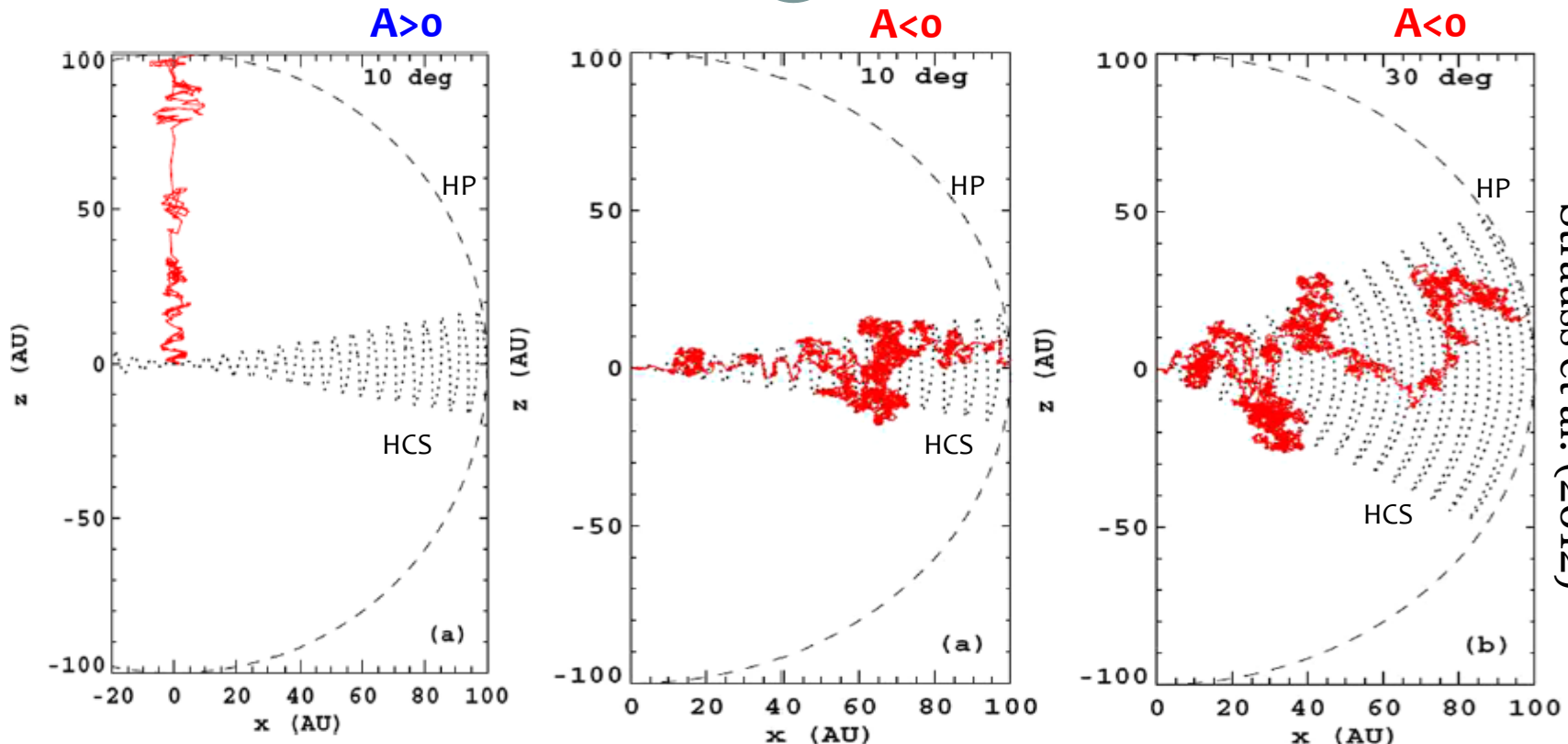
magnetic-field reversal

A<0



~22-year cycle

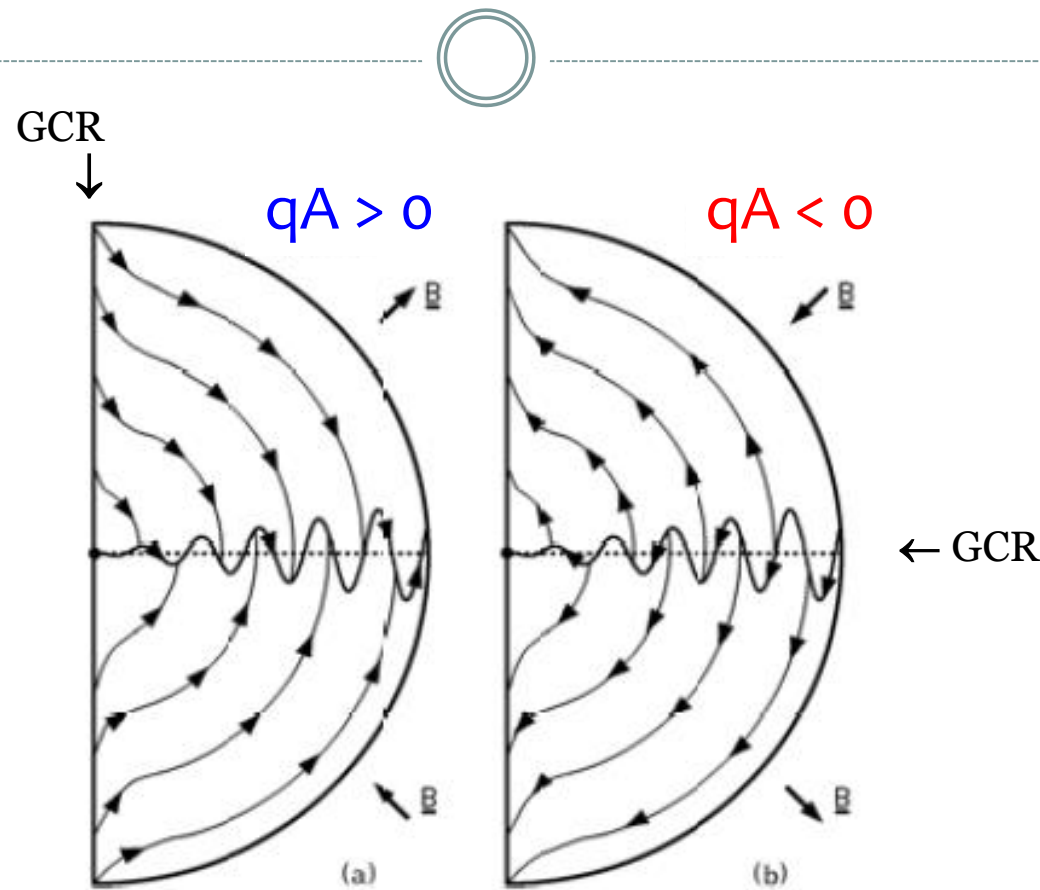
Drift & diffusion



Strauss et al. (2012)

- **Diffusion**, driven by small-scale HMF irregularities
- **Drift** caused by gradients and curvature in the global HMF

Drift path



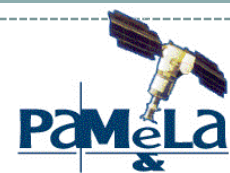
- Drift path changes at each field reversal $\rightarrow \sim 22\text{-year cycle}$
- Asymmetry between particle of opposite charge \rightarrow charge dependent solar modulation



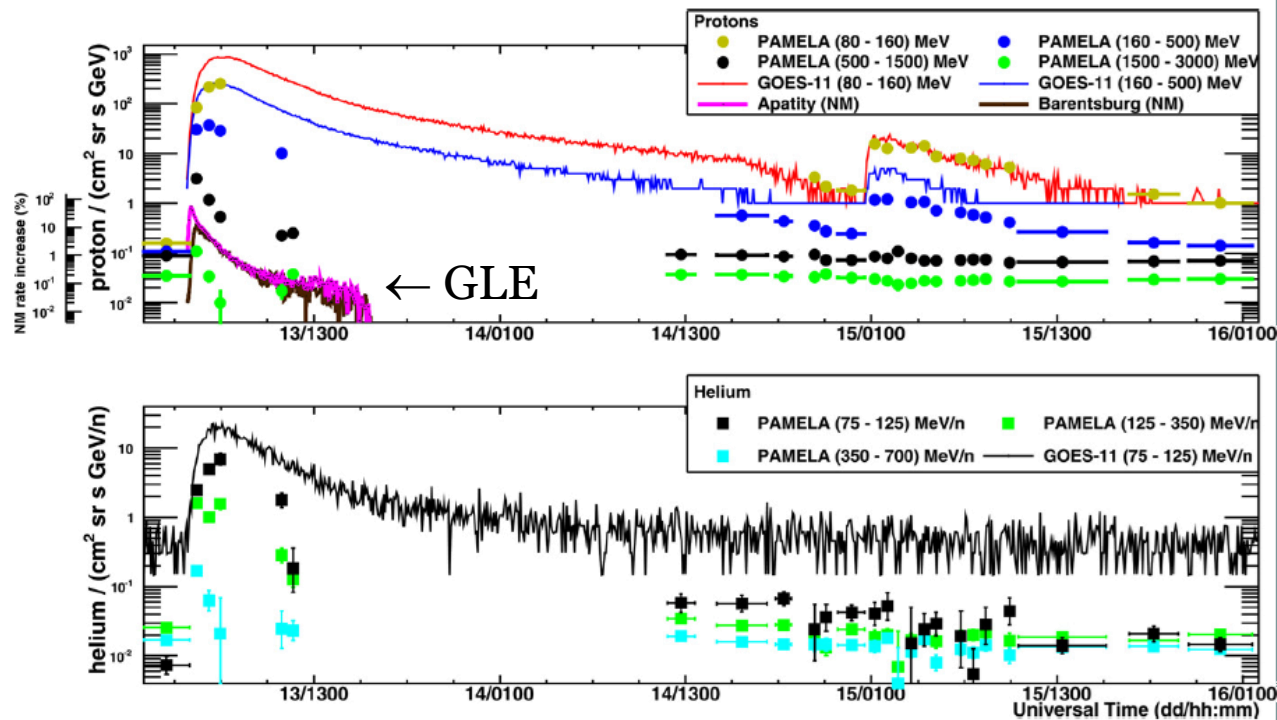
Dec 13°-14° 2006 SEP event

First instrument to directly measure relativistic SEPs in near-Earth space.

It bridges the gap between low-energy direct space-based observations (GOES) with high-energy indirect ground-based measurements (NM GLEs)



Adriani et al. - ApJ - 742 (2011) 102



PAMELA observation done during passages over high-latitude regions

The apparatus



The Time-of-Flight system

- 3 double-layer scintillator paddles
- X/Y segmentation
- Total: 48 Channels

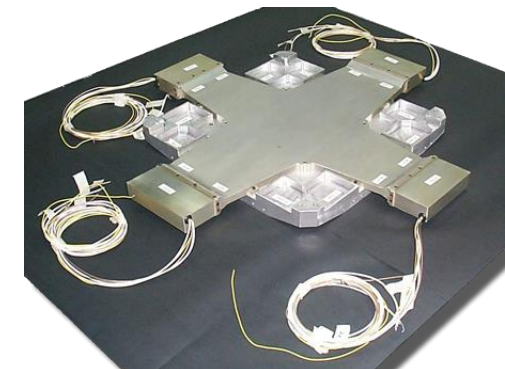
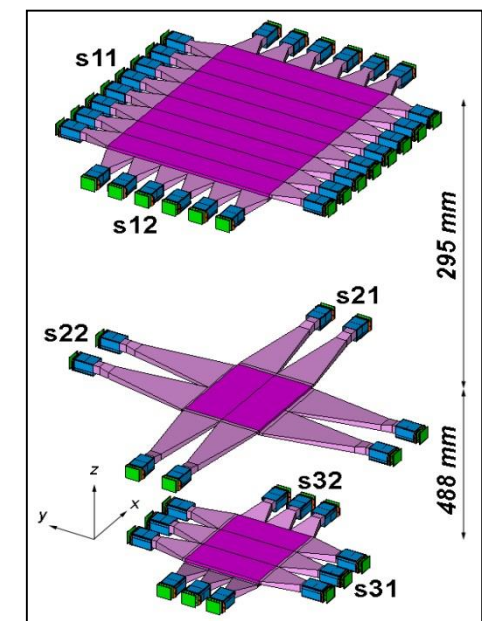
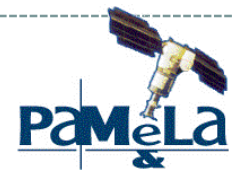


Main tasks:

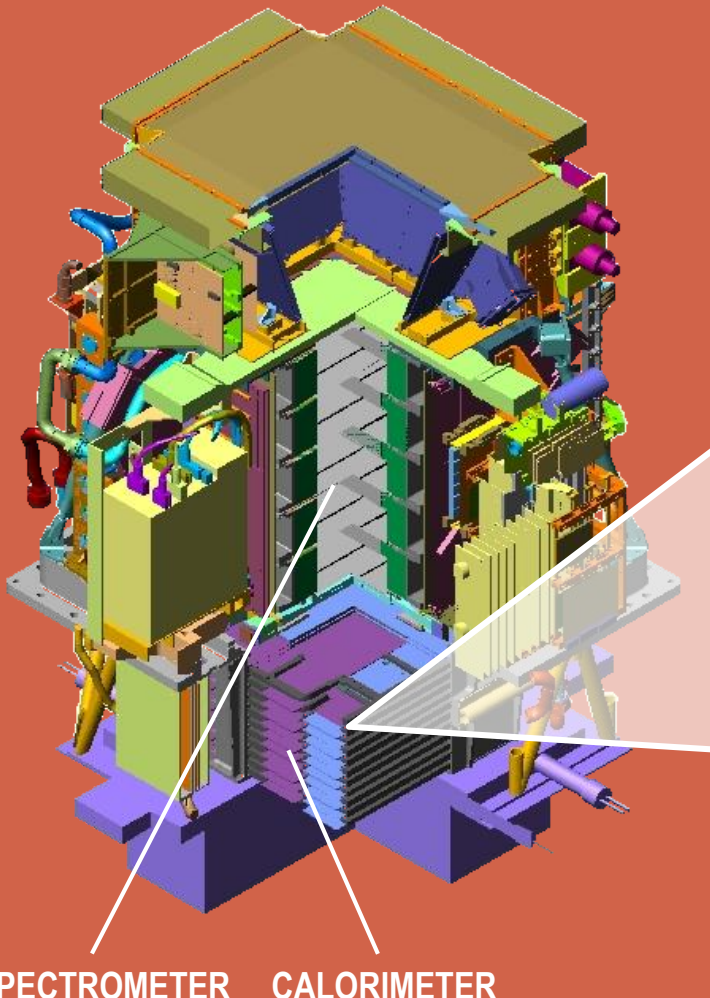
- First-level trigger
- Albedo rejection
- dE/dx
- Particle identification ($<1\text{GeV}/c$)

Performances:

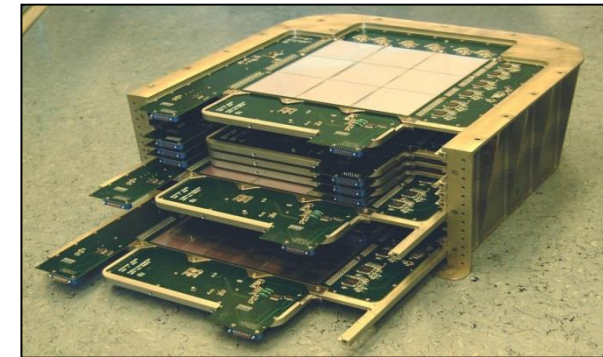
- $\sigma_{\text{paddle}} \sim 110\text{ps}$
- $\sigma_{\text{TOF}} \sim 330\text{ps}$ (for MIPs)



The apparatus



The em calorimeter



- 44 Si layers (X/Y)
+22 W planes
- $16.3 X_0 / 0.6 l_0$
- 4224 channels
- Dynamic range 1400 mip
- Self-trigger mode ($> 300 \text{ GeV } GF \sim 600 \text{ cm}^2 \text{ sr}$)

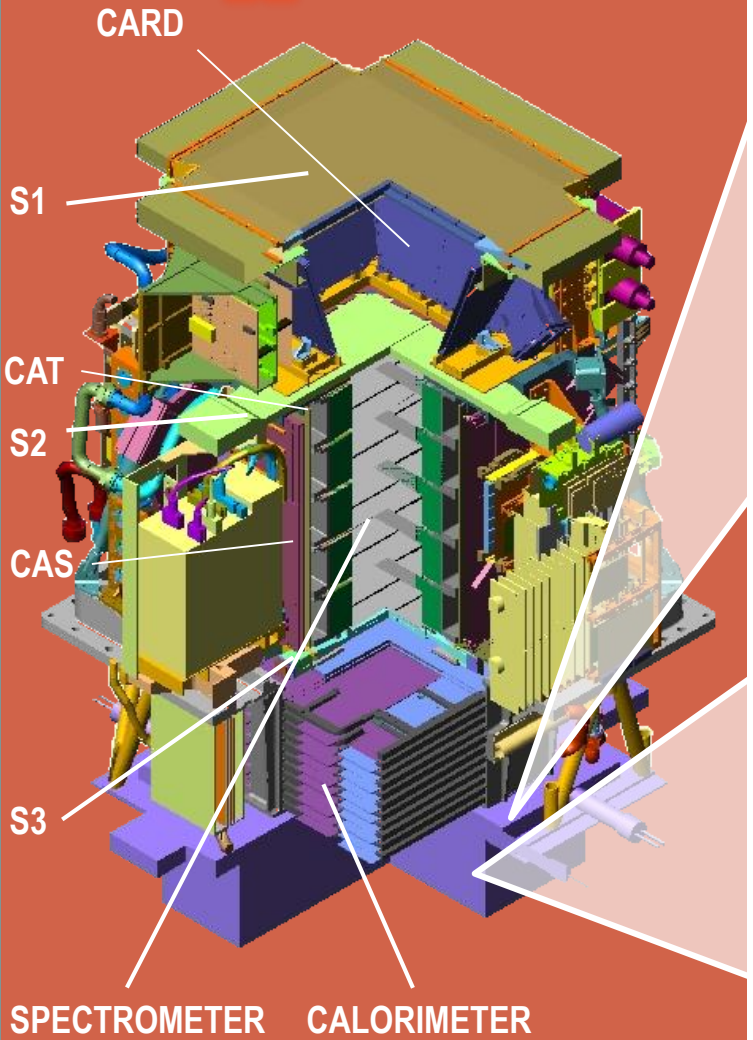
Main tasks:

- e/h discrimination
- $e^{+/-}$ energy measurement

Performances:

- p/e⁺ selection efficiency $\sim 90\%$
- p rejection factor 10^6
- e rejection factor $> 10^4$
- Energy resolution $\sim 5\% @ 200 \text{ GeV}$

The apparatus

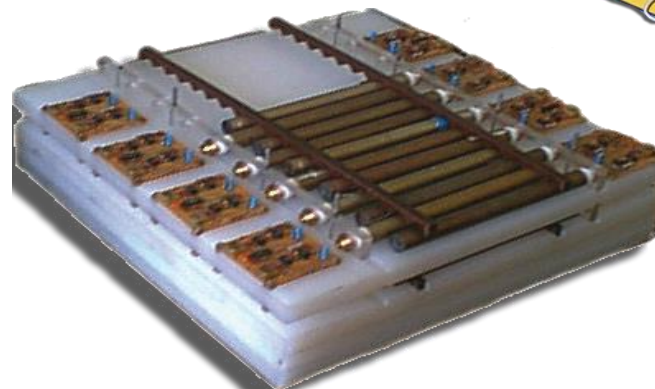
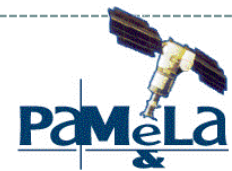


Shower-tail catcher (S4)

- 1 scintillator paddle 10mm thick

Main tasks:

- ND trigger



Neutron detector

- 36 ^3He counters: $^3\text{He}(n,p)\text{T} \rightarrow E_p = 780 \text{ keV}$
- 1cm thick polyethylene moderators
- n collected within 200 μs time-window

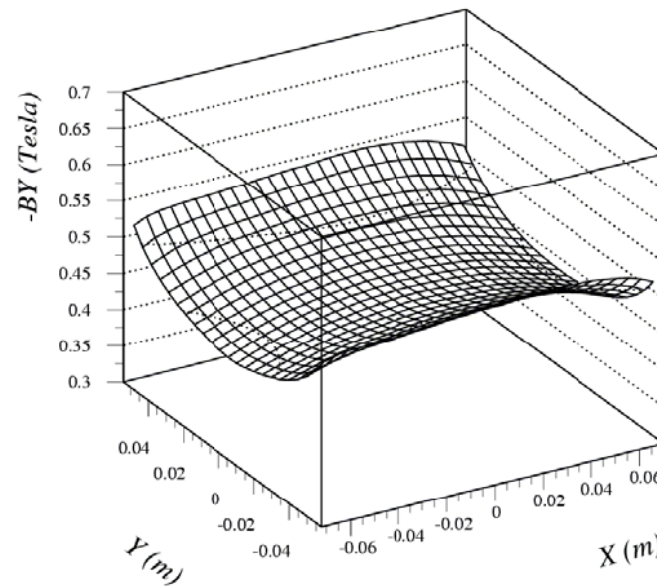
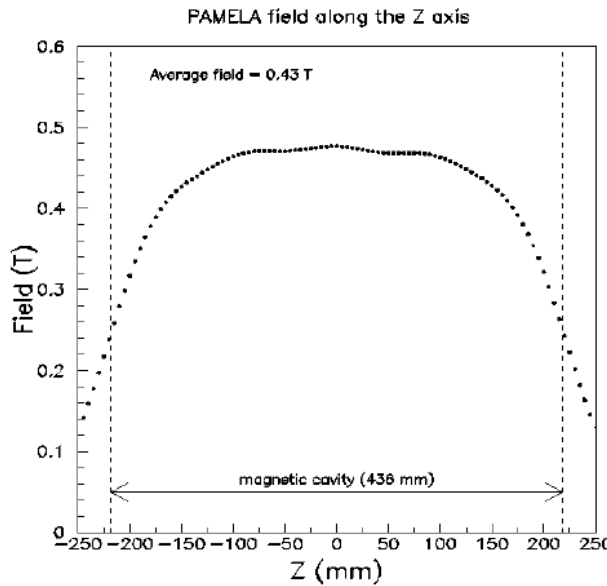
Main tasks:

- e/h discrimination @high-energy

The magnetic field

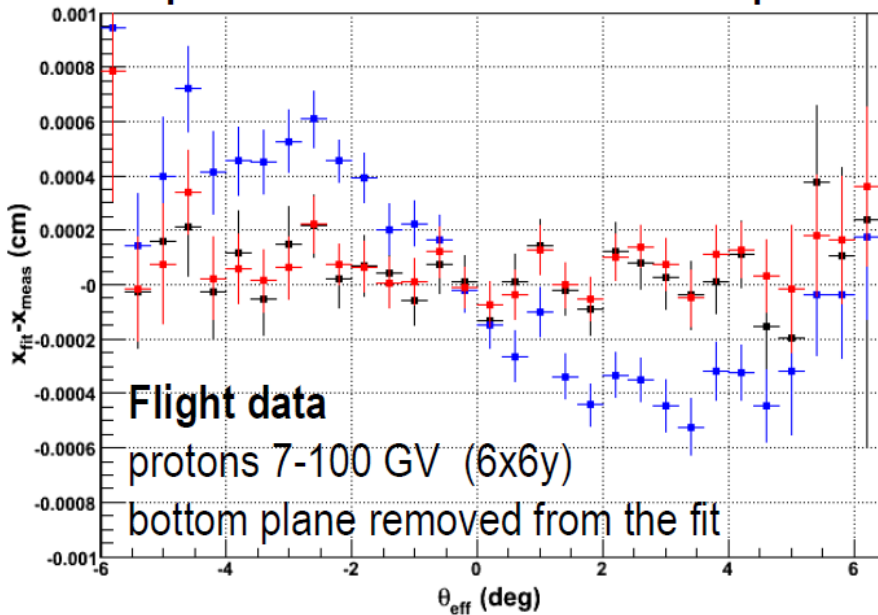
MAGNETIC FIELD MEASUREMENTS

- Gaussmeter (F.W. Bell) equipped with 3-axis probe mounted on a motorized positioning device (0.1mm precision)
- Measurement of the three components in 67367 points 5mm apart from each other
- Field inside the cavity:
 - **0.48 T @ center**
 - Average field along the axis: **0.43 T**
- **Good uniformity**
- External magnetic field: magnetic momentum < 90 Am²

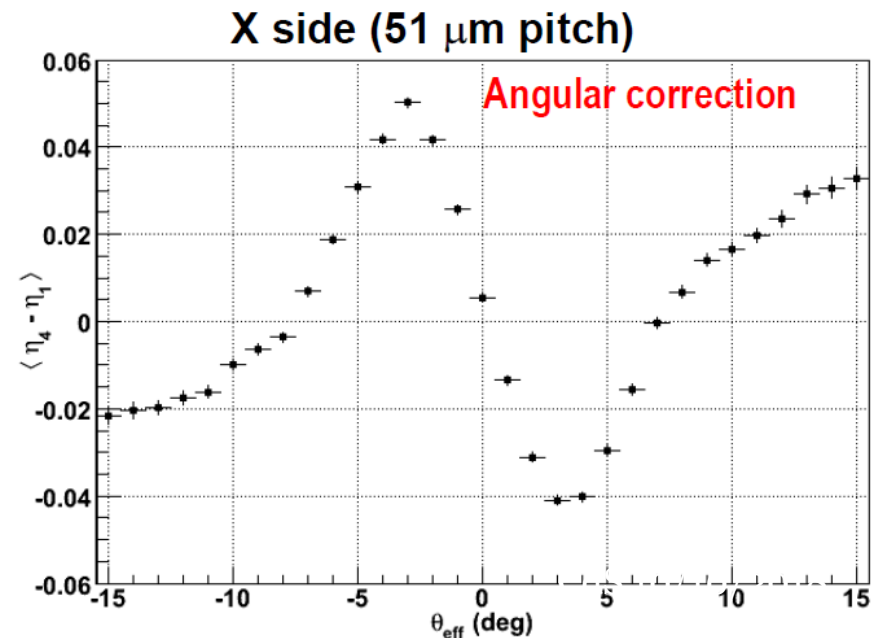
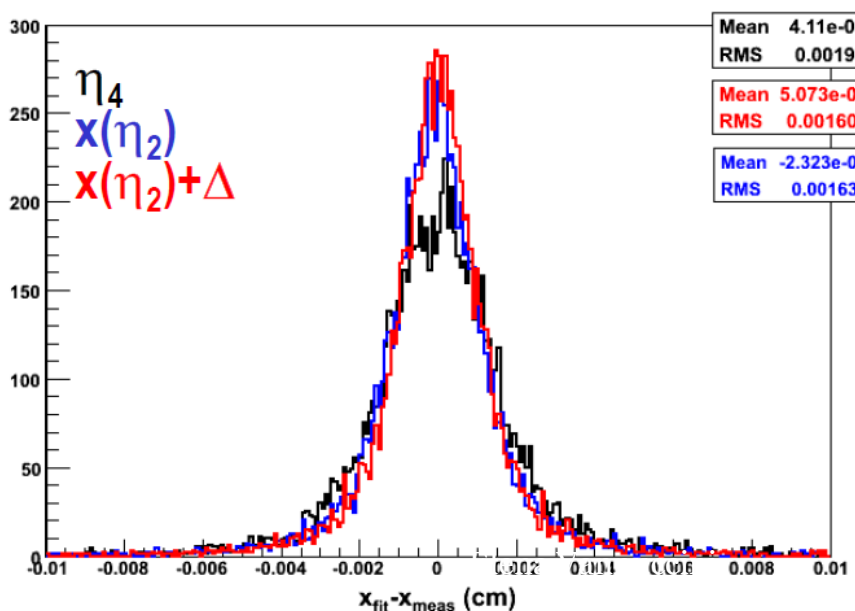
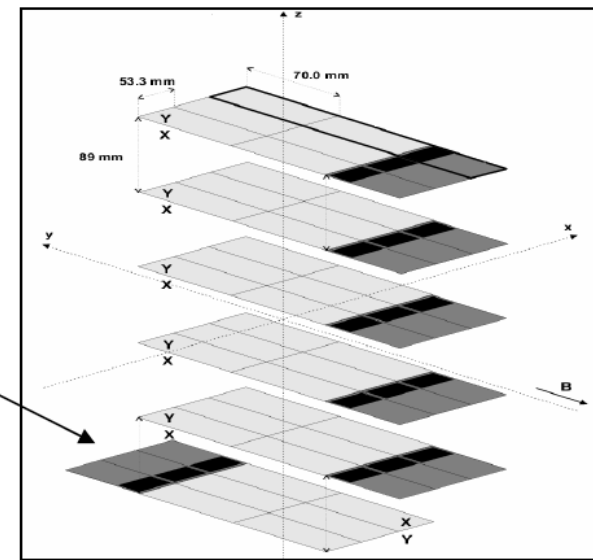


Angular systematic (flight data)

Spatial x-residual on the bottom plane

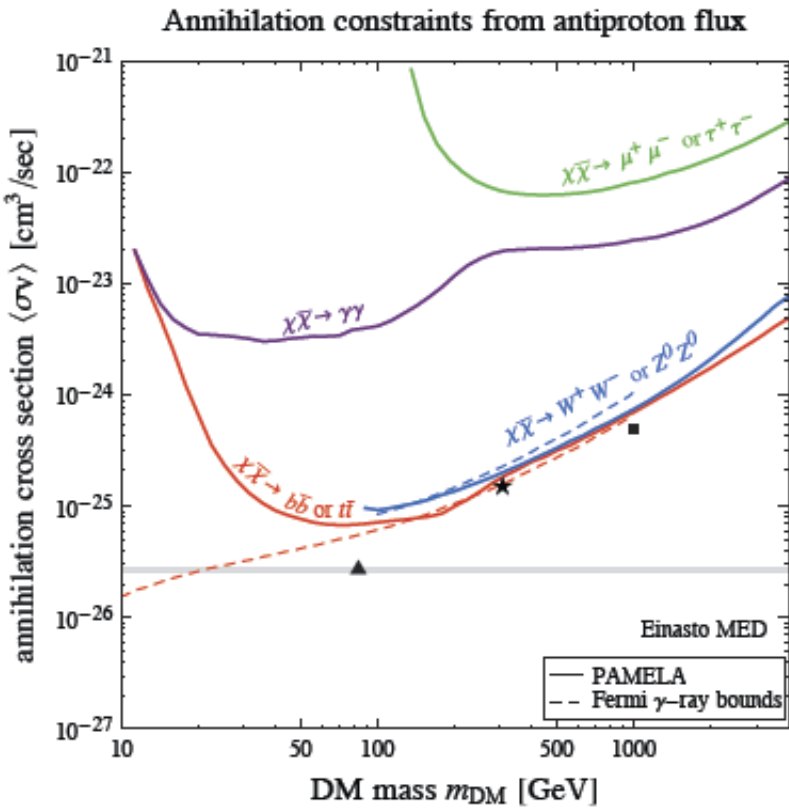


Angular systematic has opposite sign on the x view of the last plane

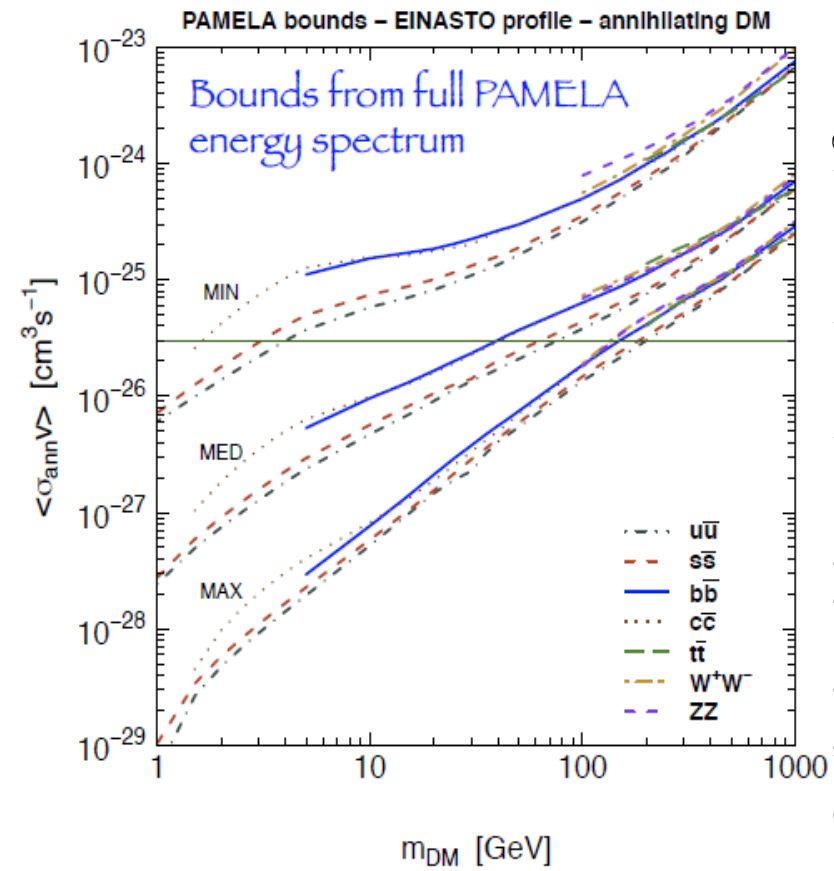




PAMELA antiproton DM limits



M. Cirelli & G. Giesen, JCAP 1304 (2013) 015



Fornengo, Maccione, Vittino, JCAP 1404 (2014) 04, 003

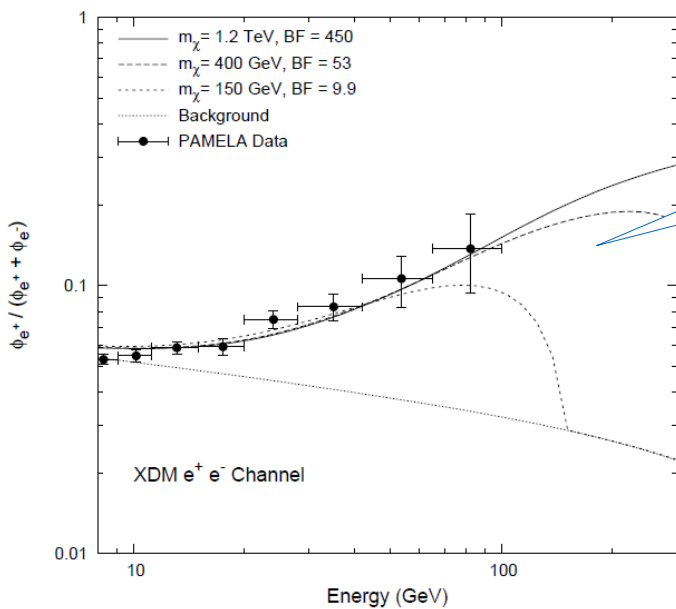
Positron-excess interpretations

Dark matter

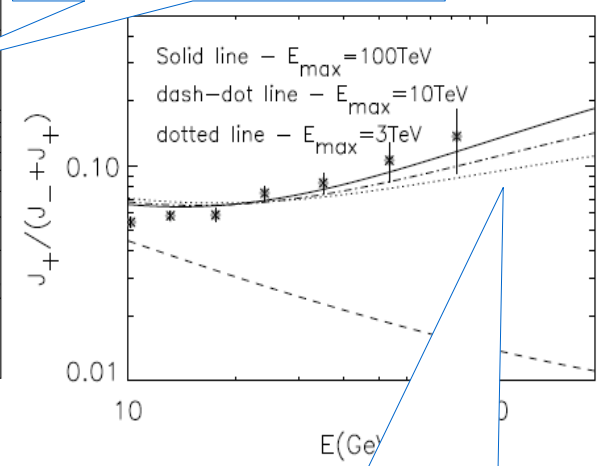
- boost factor required
- lepton vs hadron yield must be consistent with p-bar observation

Astrophysical processes

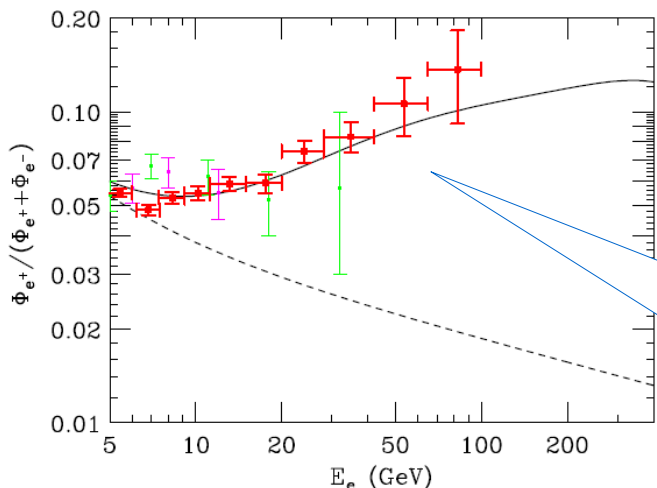
- known processes
- large uncertainties on environmental parameters



(Cholis et al. 2009)
Contribution from **DM annihilation**.



(Blasi 2009)
 e^+ (and e^-) produced as **secondaries** in the CR acceleration sites (e.g. SNR)

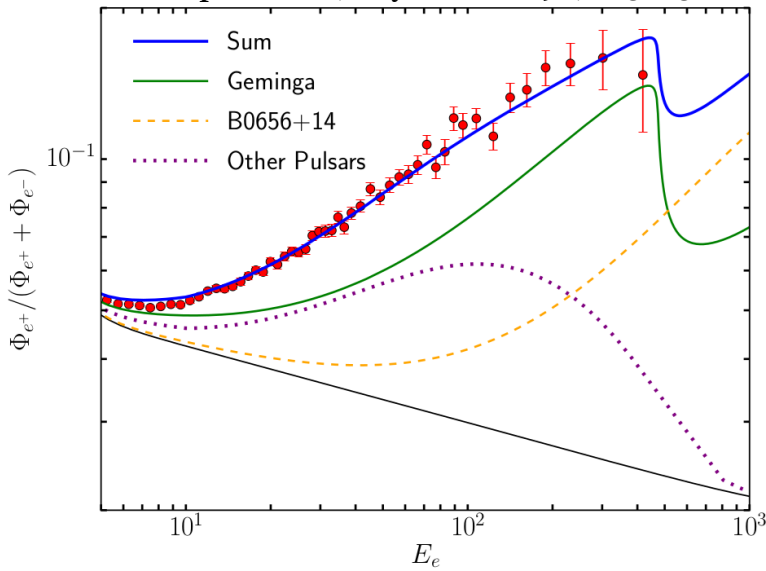


(Hooper, Blasi and Serpico, 2009)
contribution from diffuse mature & nearby young **pulsars**.

Positrons from Geminga and PSR B0656+14

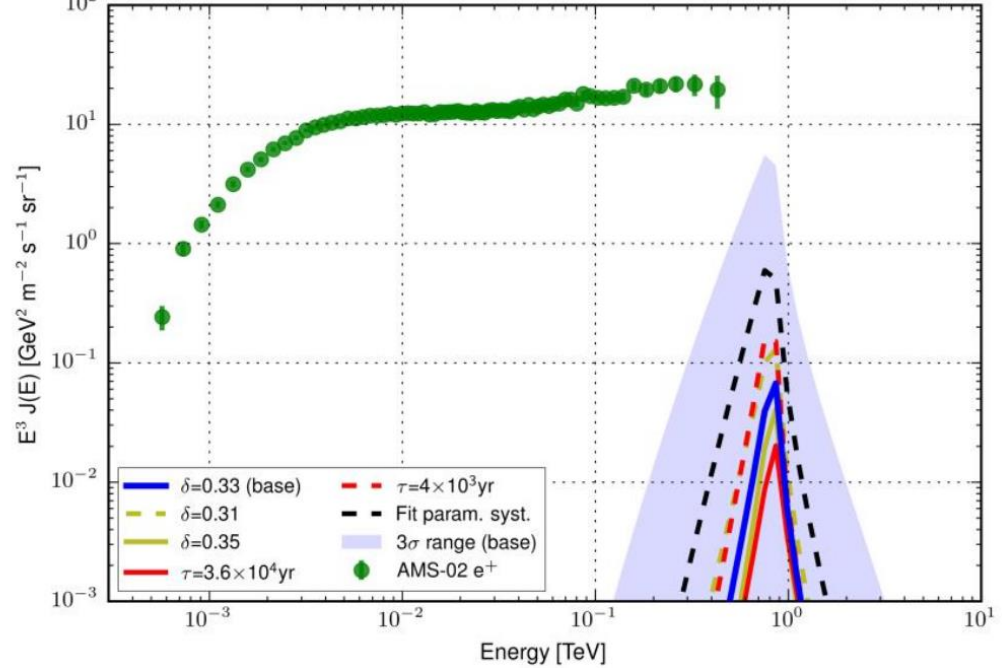


Dan Hooper et. al., Phys. Rev. D 96, 103013 (2017)



“HAWC observations strongly favor pulsar interpretations of the cosmic-ray positron excess”

Abeysekara et. al., Science, 358 (2017) 911



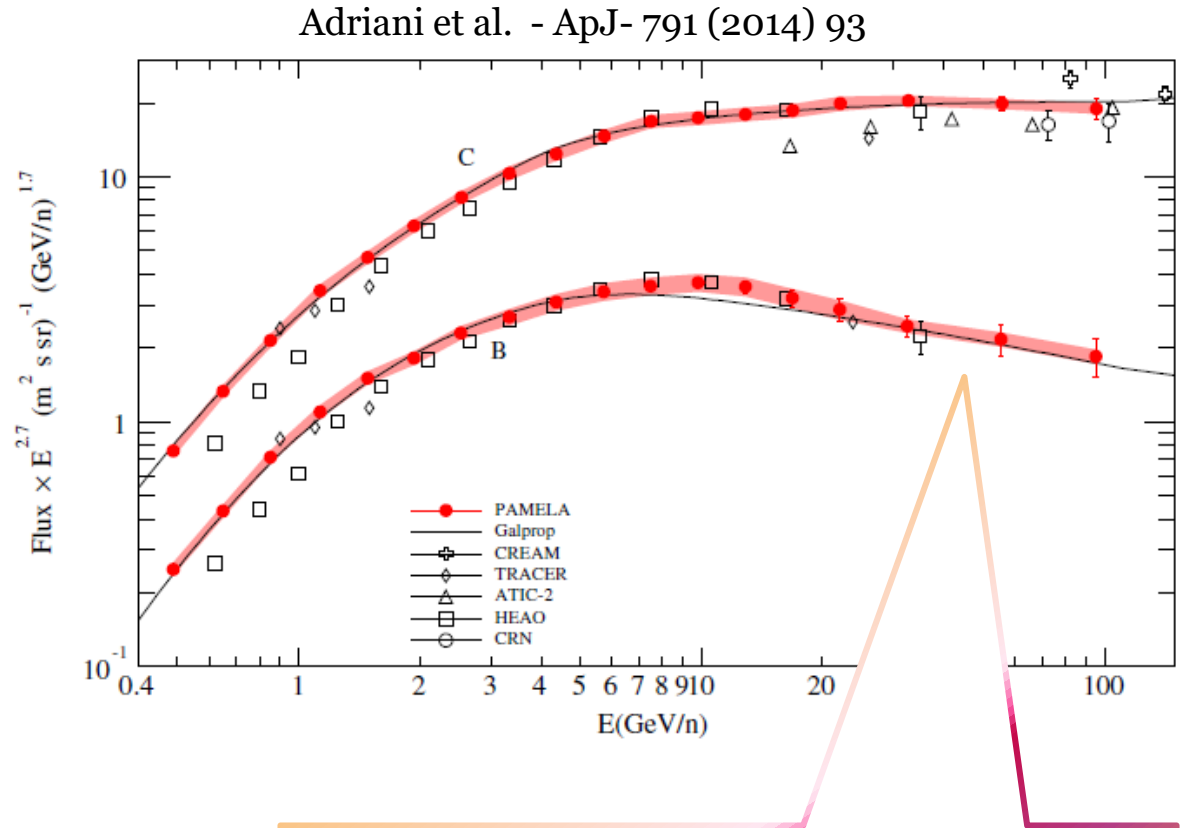
“...leptons emitted by these objects are therefore unlikely to be the origin of the excess positrons, which may have a more exotic origin”

B and C absolute fluxes

Widest energy range covered so far

Reduced tracking performance, due to detector saturation:

- $\sigma_x = 14 \mu\text{m}$, $\sigma_y = 19 \mu\text{m}$
- MDR = 250 GV



GALPROP code tuned to PAMELA B&C data

- Plain diffusion model (Vladimirov et al. 2012)
- Solar modulation: spherical model ($\phi=400\text{MV}$)

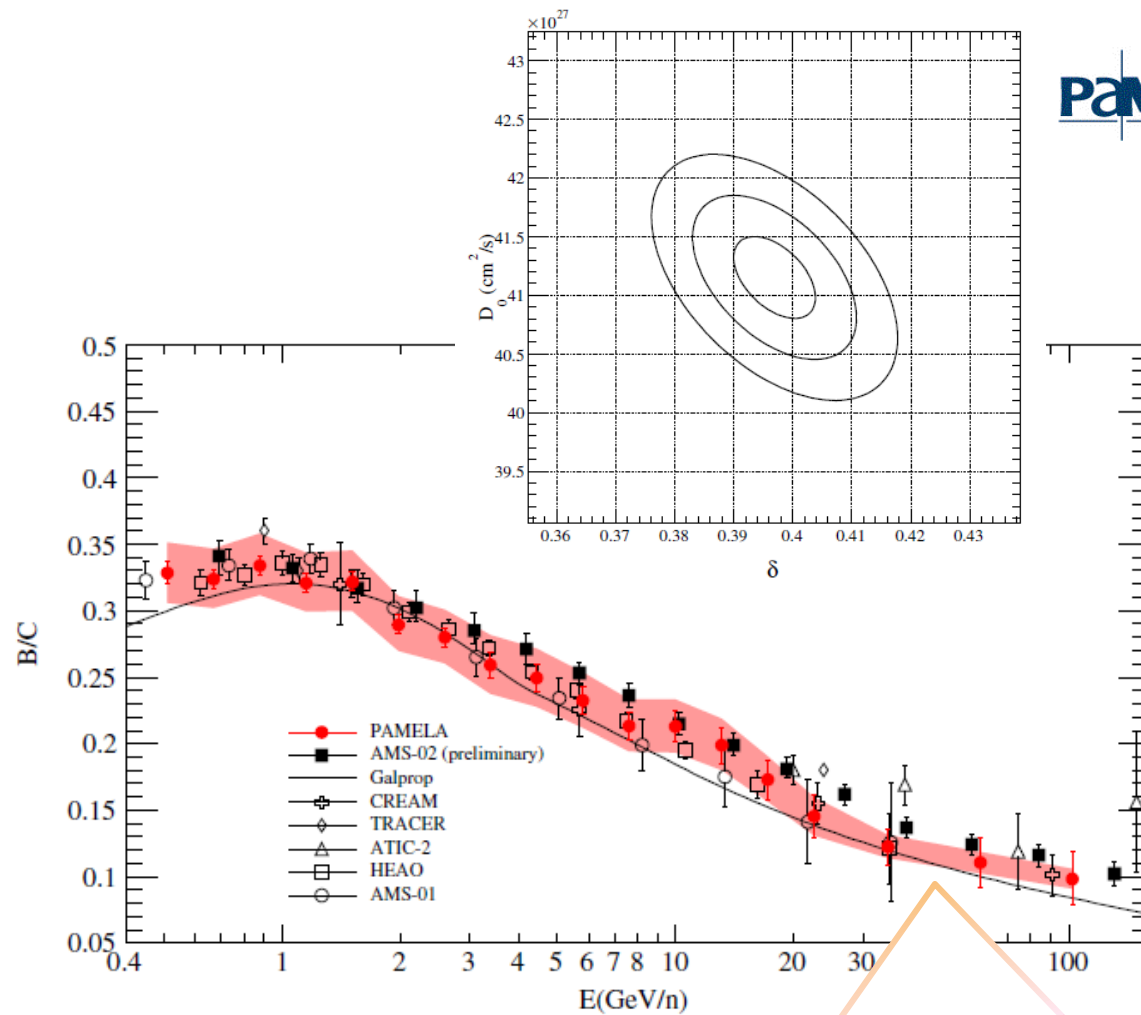
B/C ratio

B nuclei are of ~pure **secondary** origin

C,N,O + ISM \rightarrow B + ...

\rightarrow B/C provides the strongest constraint to propagation parameters so far

PAMELA data consistent with previous measurements and with a standard scenario

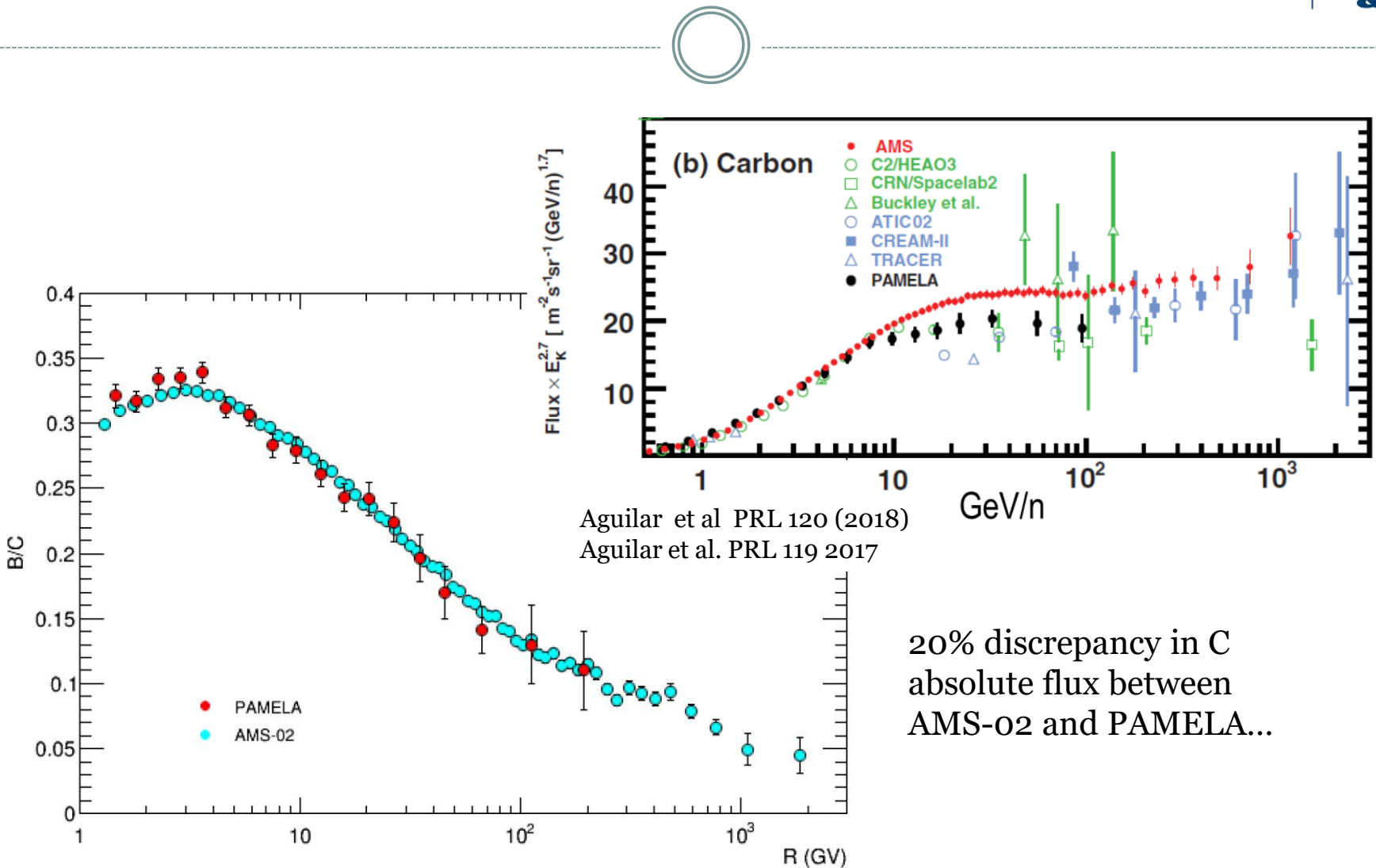


GALPROP code tuned to PAMELA B&C data

- Plain diffusion model (Vladimirov et al. 2012)
- Solar modulation: spherical model ($\phi=400\text{MV}$)



B and C abundances



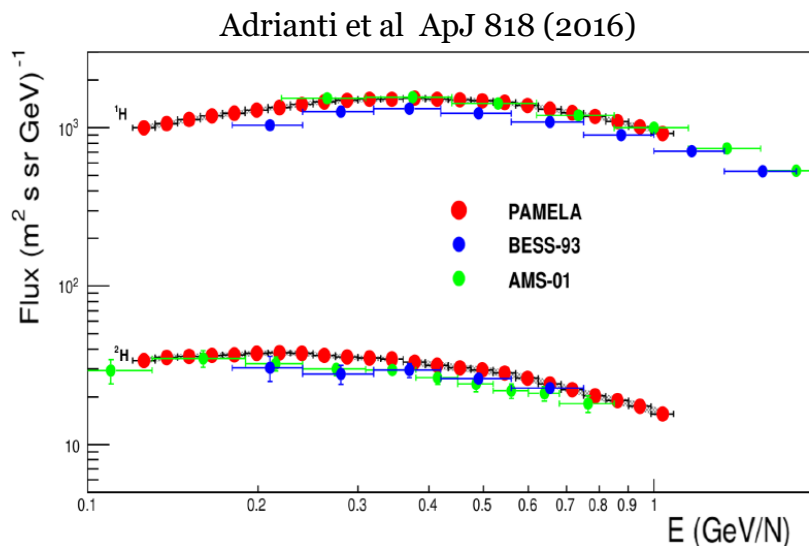
H isotopes

Parameter constraint
competitive/complementary to B/C measurement
with current instrument precision

Probe different Z/A
regime

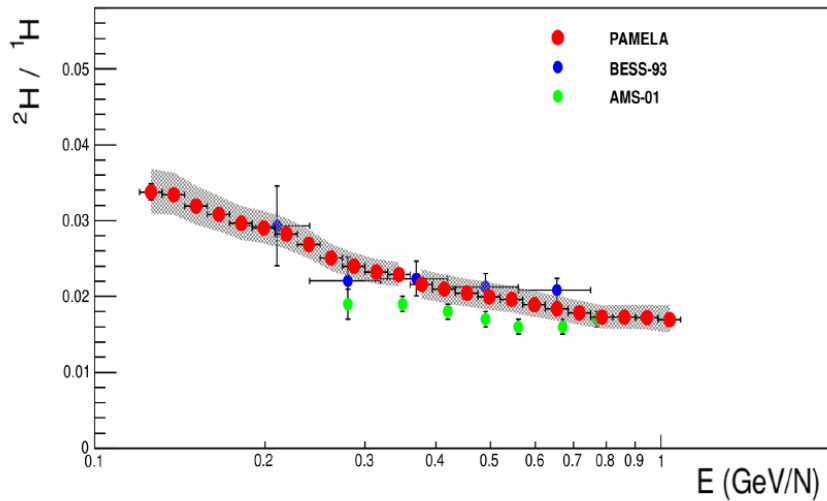
Test «universality» of
propagation

(Coste et al. 2012)



${}^1\text{H} \rightarrow \text{primary}$

${}^2\text{H} \rightarrow \text{secondary}$
90% from ${}^4\text{He} + {}^1\text{H}$
(40%@1GeV/n)



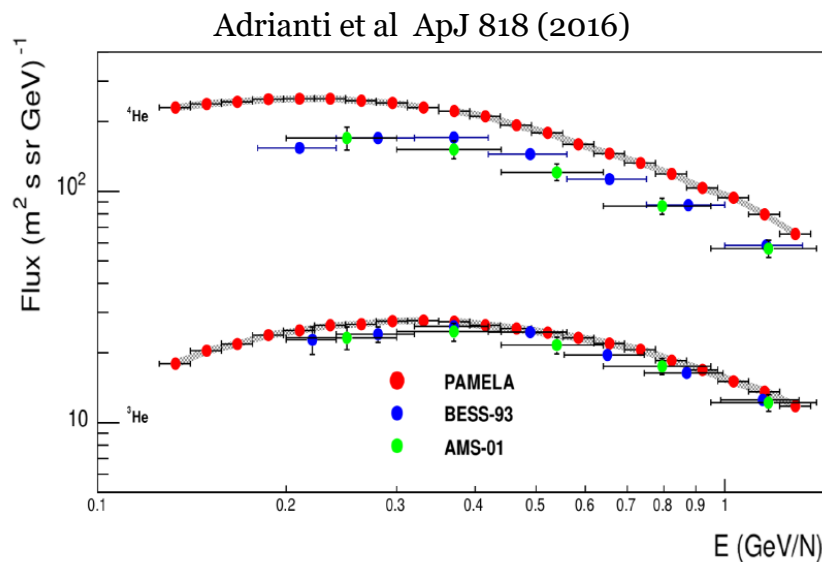
He isotopes

Parameter constraint
competitive/complementary
to B/C measurement
with current instrument
precision

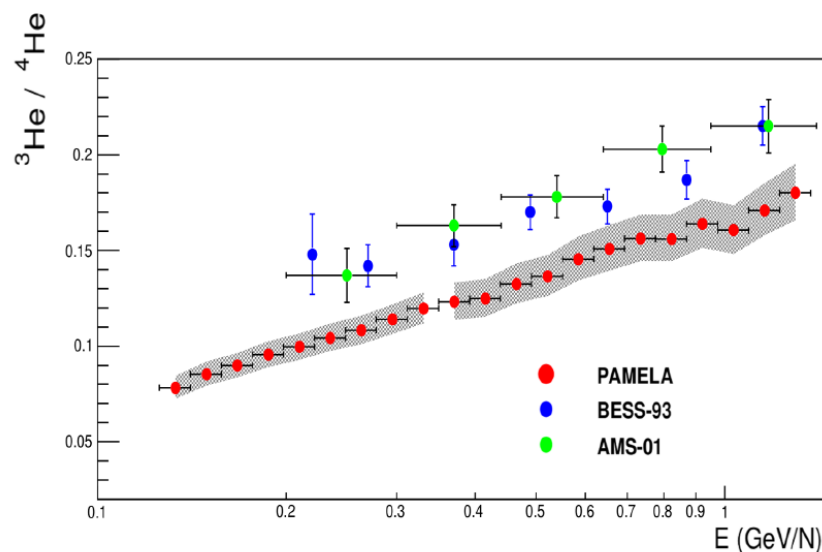
Probe different Z/A
regime

Test «universality» of
propagation

(Coste et al. 2012)



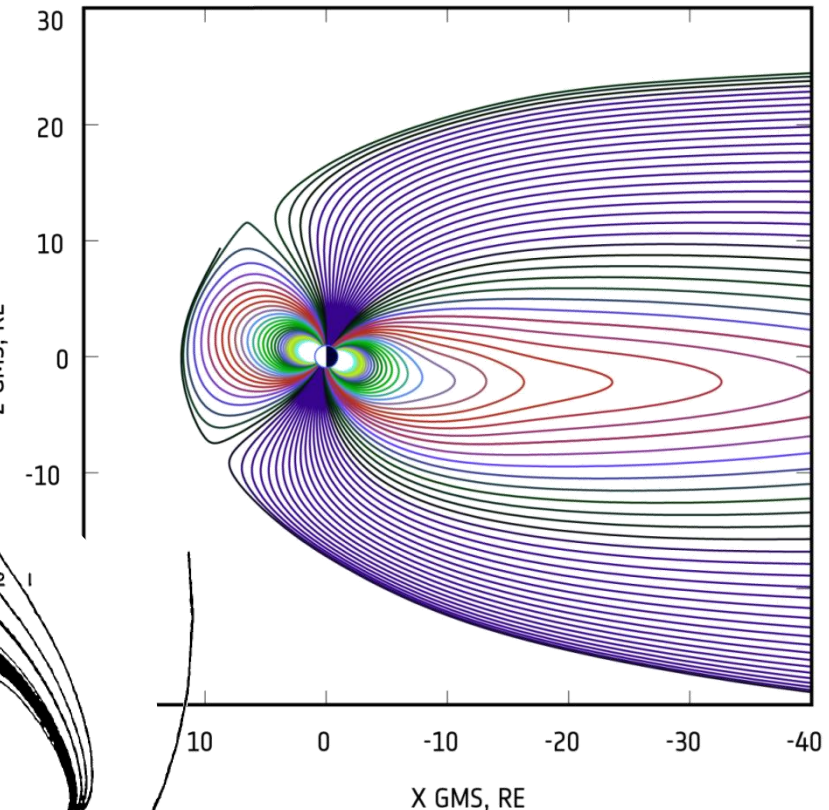
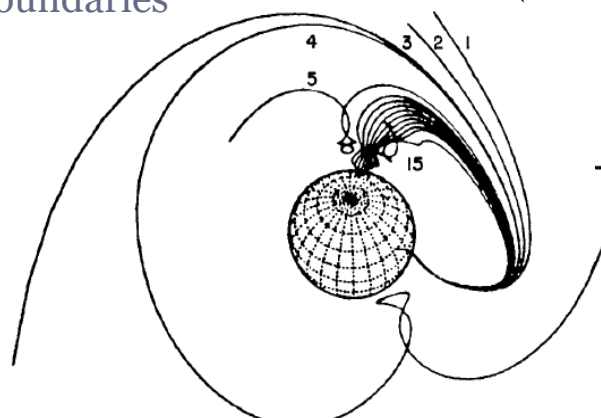
$4\text{He} \rightarrow \text{primary + secondary}$
 $\sim 10\% @ 2\text{GeV/n}$
from CNO



$3\text{He} \rightarrow \text{secondary}$
95% from 4He

Trajectory analysis

- Trajectories propagated back and forth the measurement location
- Particles classified according to trajectory behaviour
 - Reach magnetosphere boundary
 - ✖ Interplanetary origin
 - Intersect atmosphere boundary
 - ✖ Albedo
 - Do not intersect the boundaries
 - ✖ Stably trapped

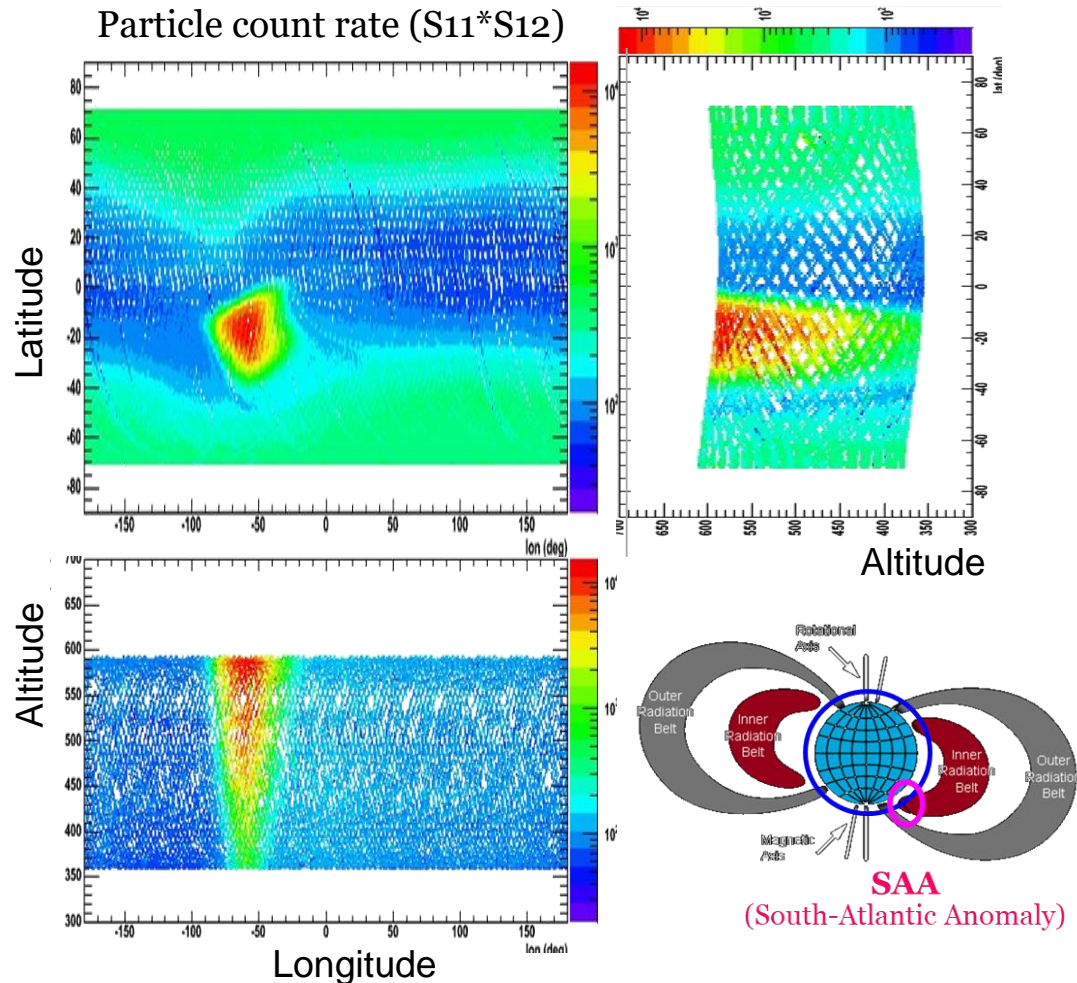


The PAMELA orbital environment



PAMELA sweep through the magnetosphere along a near-Earth semipolar orbit

- Observation of trapped radiation
 - Characterization of high-energy albedo population
- Improvement in low-altitude radiation-environment description

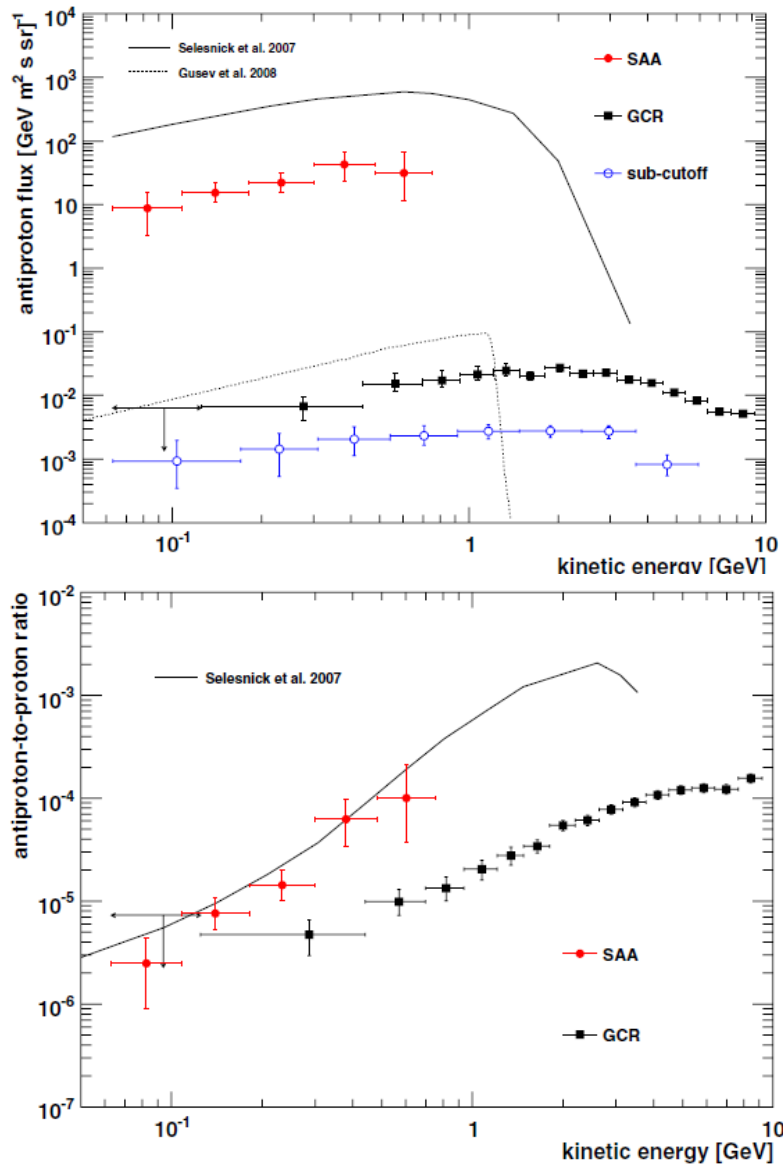


Trapped antiprotons

First observation of
geomagnetically trapped
 $p\bar{p}$

Produced by CR
interaction with
atmosphere and trapped
by the magnetosphere

Most abundant $p\bar{p}$
source near the Earth!



Adriani et al. - ApJ Lett. - 737 (2011) L29

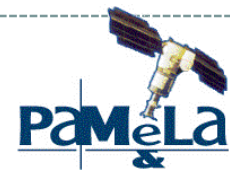
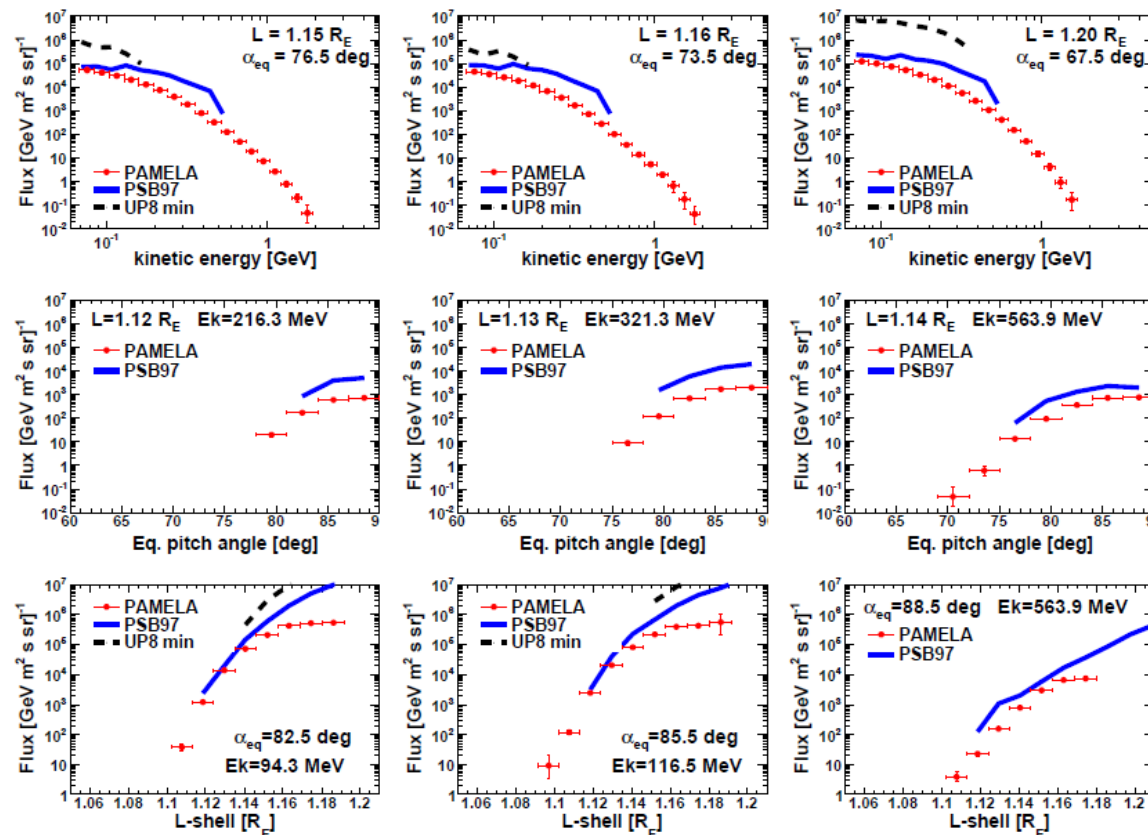
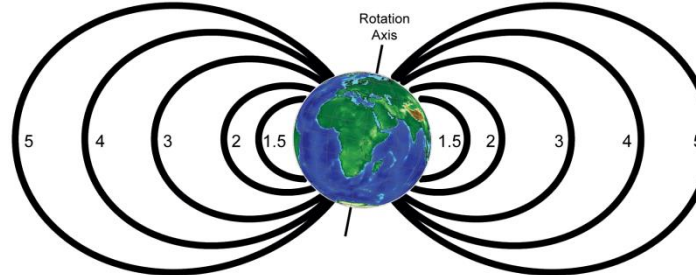


Trapped protons

Observation of trapped radiation performed down to $L_{\text{shell}} \sim 1.1 R_E$ and up to 4 GeV

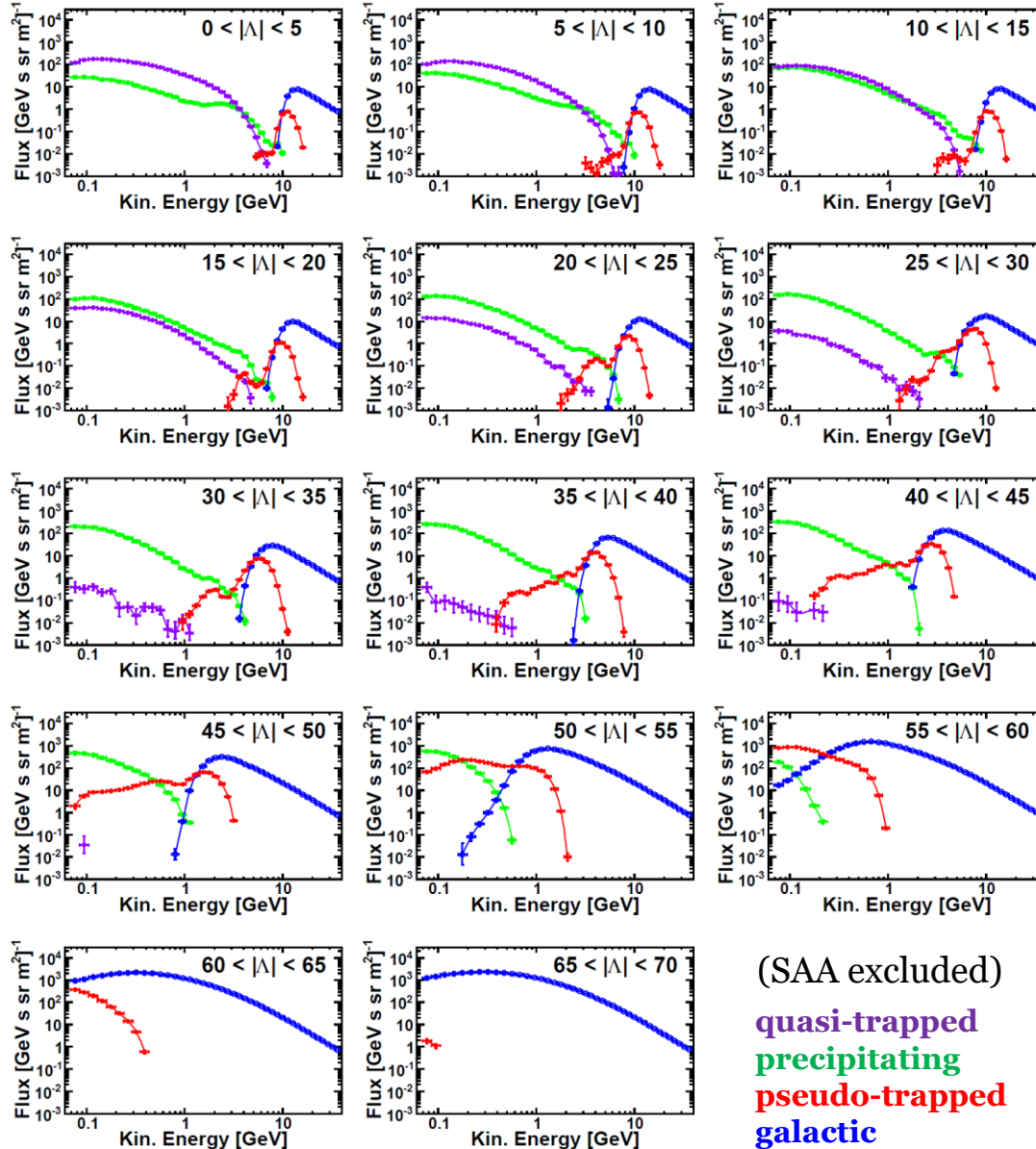
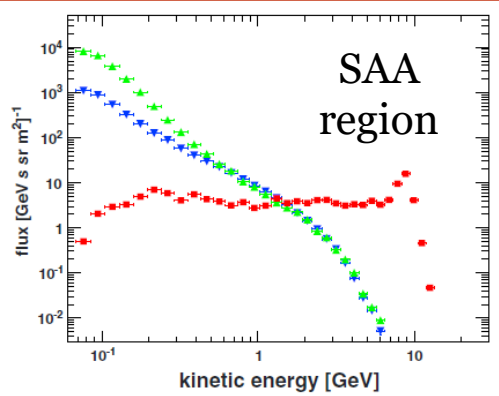
Comparison with empirical model

Improvement in low-altitude radiation-environment description



Re-entrant albedo protons

Caracterization of high-energy albedo population





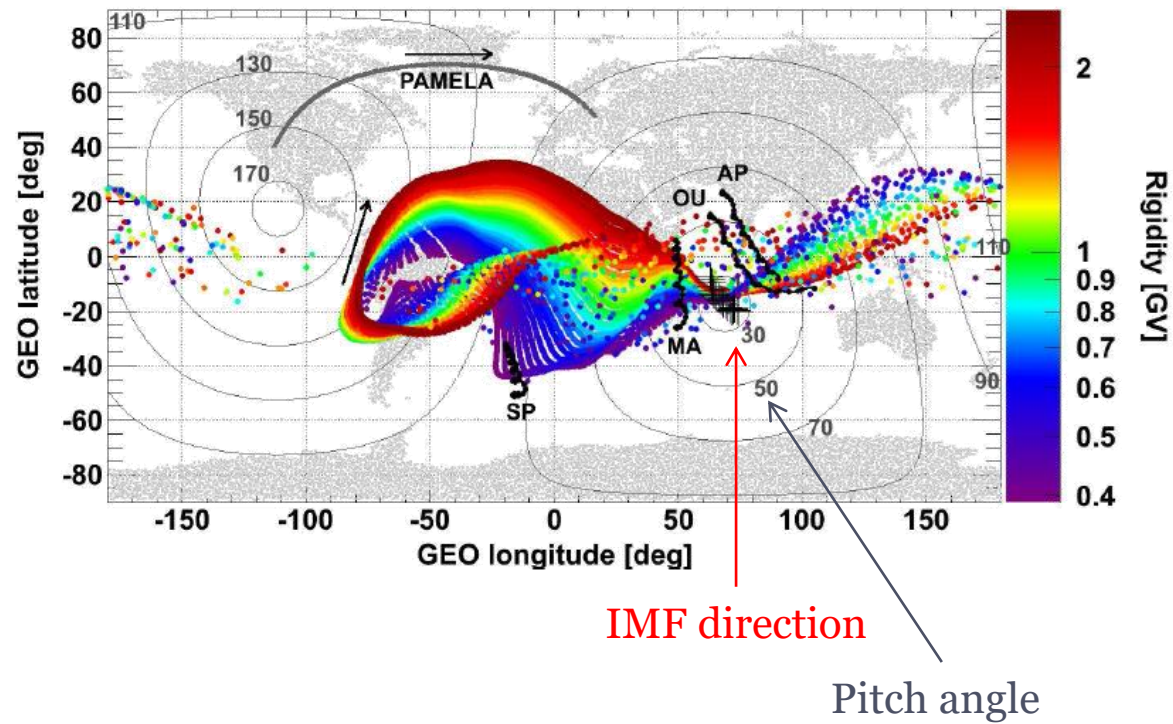
May 17°, 2012 SEP event

- First observed GLE of 24° solar cycle
- Earth magnetically connected to the Sun
- Associated to M1.5-class X-ray flare
- Extended emission ($>100\text{MeV}$) seen by Fermi-LAT

Unique possibility to measure pitch angle distribution over broad energy range, to disentangle interplanetary **transport** process

Asymptotic direction during first polar pass after the event onset

May 17, 2012, 01:57:00 - 02:20:00 UT



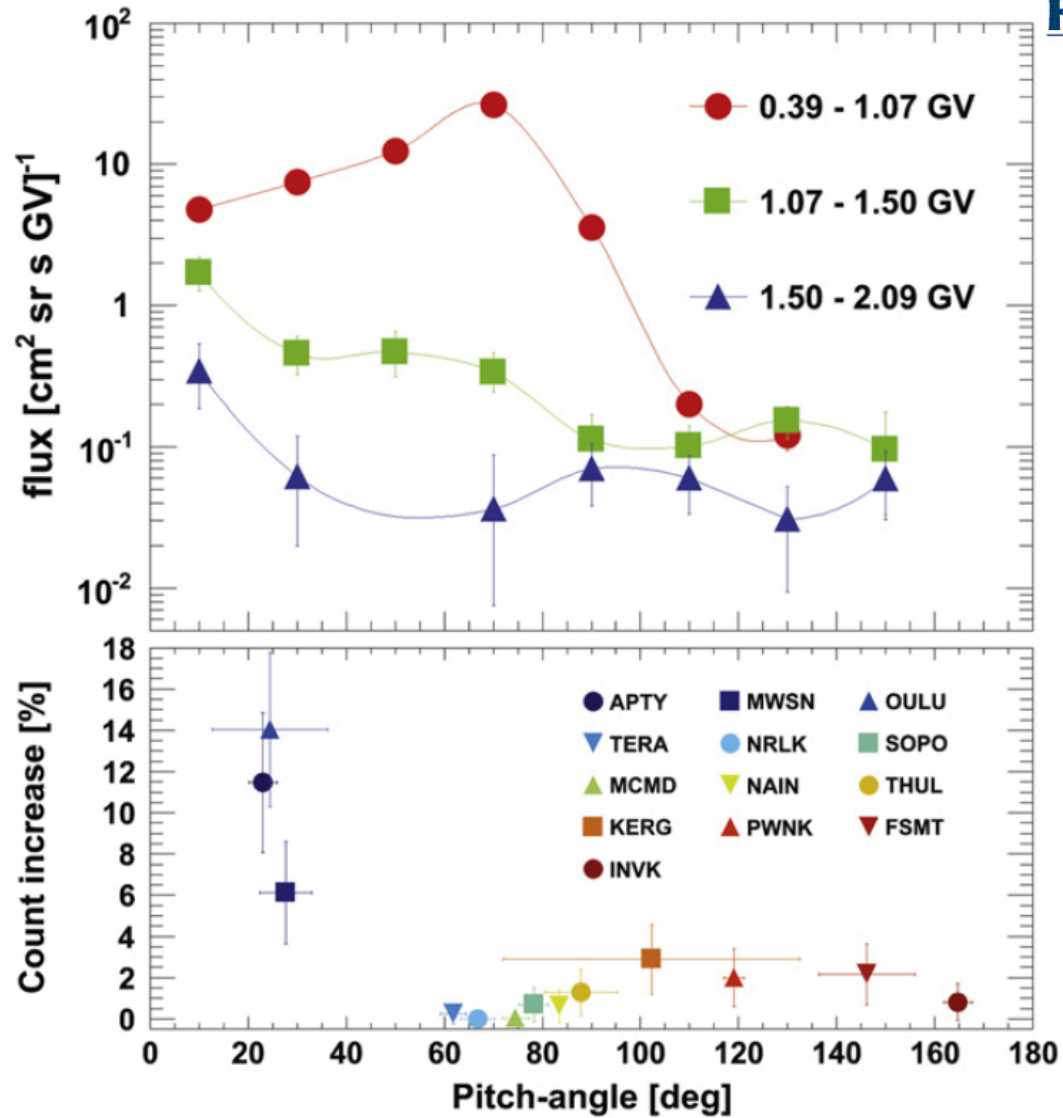
Adriani et al. - ApJL - 801 (2015) L3

May 17°, 2012 SEP event

First evidence of two simultaneous particle populations:

- High rigidity component consistent with NM where particles are field aligned → Beam width \sim 40-60° (not scattered)
- Low rigidity component shows significant scattering for pitch angles \sim 90°

Adriani et al. - ApJL - 801 (2015) L3



Electron inclusive spectrum

